UNIV. OF MICHIGAN
APR 6 1953
EAST ENGINEERING

Electrochemical Society

Vol. 100, No. [illegible] April, 195[illegible]

ELECTROCHEMICAL INDUSTRY

Phosphate-Smelting Electric Furnaces

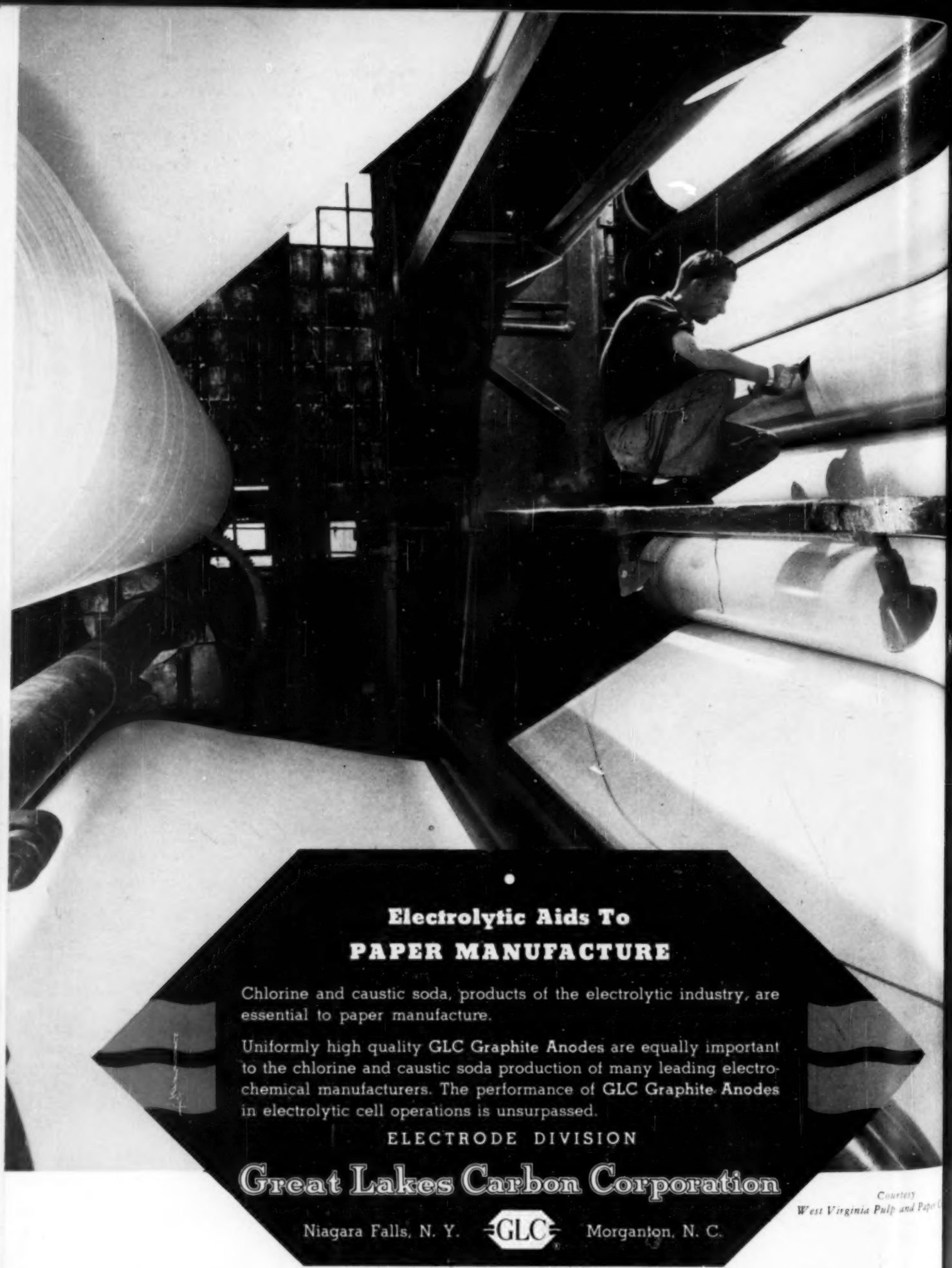

Electrolytic Aids To
PAPER MANUFACTURE

Chlorine and caustic soda, products of the electrolytic industry, are essential to paper manufacture.

Uniformly high quality **GLC Graphite Anodes** are equally important to the chlorine and caustic soda production of many leading electrochemical manufacturers. The performance of **GLC Graphite Anodes** in electrolytic cell operations is unsurpassed.

ELECTRODE DIVISION

Great Lakes Carbon Corporation

Niagara Falls, N. Y. GLC Morganton, N. C.

Courtesy West Virginia Pulp and Paper C

Graphite Anodes, Electrodes and Specialties

Sales office: Niagara Falls, N. Y. **Other offices:** New York, N. Y., Chicago, Ill., Pittsburgh, Pa.

Sales Agents: J. B. Hayes, Birmingham, Ala., George O'Hara, Long Beach, Cal., Great Northern Carbon & Chemical Co. Ltd., Mon eal, Cana

EDITORIAL STAFF

R. M. Burns, *Chairman*
Norman Hackerman, *Technical Editor*
Ruth G. Sterns, *Managing Editor*
Cecil V. King, *Associate Editor*
U. B. Thomas, *News Editor*
Mary F. Murray, *Assistant Editor*

DIVISIONAL EDITORS

M. A. Streicher, *Corrosion*
Abner Brenner, *Electrodeposition*
N. C. Cahoon, *Battery*
H. C. Froelich, *Electronics*
W. C. Gardiner, *Industrial Electrolytic*
S. J. Sindeband, *Electrothermic*
John J. Chapman, *Electric Insulation*
L. B. Rogers, *Theoretical*
Sherlock Swann, Jr., *Electro-Organic*

REGIONAL EDITORS

Joseph Schulein, *Pacific Northwest*
J. C. Schumacher, *Los Angeles*
O. W. Storey, *Chicago*
G. W. Heise, *Cleveland*
Paul S. Brallier, *Niagara Falls*
Oliver Osborn, *Houston*
Earl A. Gulbransen, *Pittsburgh*
A. C. Holm, *Canada*
J. W. Cuthbertson, *Great Britain*
T. L. Rama Char, *India*

ADVERTISING OFFICE

Jack Bain
Advertising Manager
345 Fifth Avenue
New York 17, N. Y.
PHONE—*Murray Hill 2-3345*

Journal of the
Electrochemical Society

APRIL, 1953 VOL. 100 • NO. 4

CONTENTS

Editorial

Educate the Gifted 79C

Technical Papers

Electrical Properties of Pentachlordiphenyl Impregnated Glass Fiber Paper. *Thomas D. Callinan* 141

Cathodic Lead Disintegration and Hydride Formation. *Hugh W. Salzberg* 146

A Preliminary Study of the Ductility of Chromium. *H. B. Goodwin, R. A. Gilbert, C. M. Schwartz, and C. T. Greenidge* 152

Effect of Germanium on the Transformation of White to Gray Tin, at Comparatively Low Temperature. *R. R. Rogers and J. F. Fydell* 161

The Caustic Electrolytic-Zinc Process. *Charles T. Baroch, R. V. Hilliard, and R. S. Lang* 165

Effect of Local Action Currents on the EMF of the Weston Standard Cell. *Herbert H. Uhlig* 173

Some Electrochemical Properties of New Synthetic Ion Exchange Membranes. *Alvin G. Winger, George W. Bodamer, and Robert Kunin* 178

Acid Strengths of the Phenylacetic Acids. *Mary L. Kilpatrick and Edward Fackenthal* 185

The Capacity of Polarized Platinum Electrodes in Hydrochloric Acid. *W. D. Robertson* 194

Feature Section

The Electric Furnace as a Producer of Elemental Phosphorus. *Harry A. Curtis* 81C

Science and Scientists in Telecommunications. *R. M. Burns* .. 90C

Current Affairs

Officers to Start New Terms at New York Meeting 95C

New York Technical Program 95C

News Notes 100C
Section News 102C
Division News 104C
Personals 104C
New Members 105C
Letter to the Editor 106C
Book Reviews 107C
Literature from Industry 109C

Published monthly by The Electrochemical Society, Inc., Mount Royal and Guilford Aves., Baltimore 2, Md., combining the JOURNAL and TRANSACTIONS OF THE ELECTROCHEMICAL SOCIETY. Editorial offices: 235 West 102nd Street, New York 25, N. Y. Statements and opinions given in articles and papers in the JOURNAL OF THE ELECTROCHEMICAL SOCIETY are those of the contributors, and The Electrochemical Society assumes no responsibility for them. Subscription $11.25 to members, $15.00 to nonmembers. Single copies $1.25 to members, $1.50 to nonmembers. Copyright 1953 by The Electrochemical Society, Inc. Entered as second-class matter November 15, 1947, at the Post Office at Baltimore, Md., under the act of August 24, 1912.

You change ranges this simple way

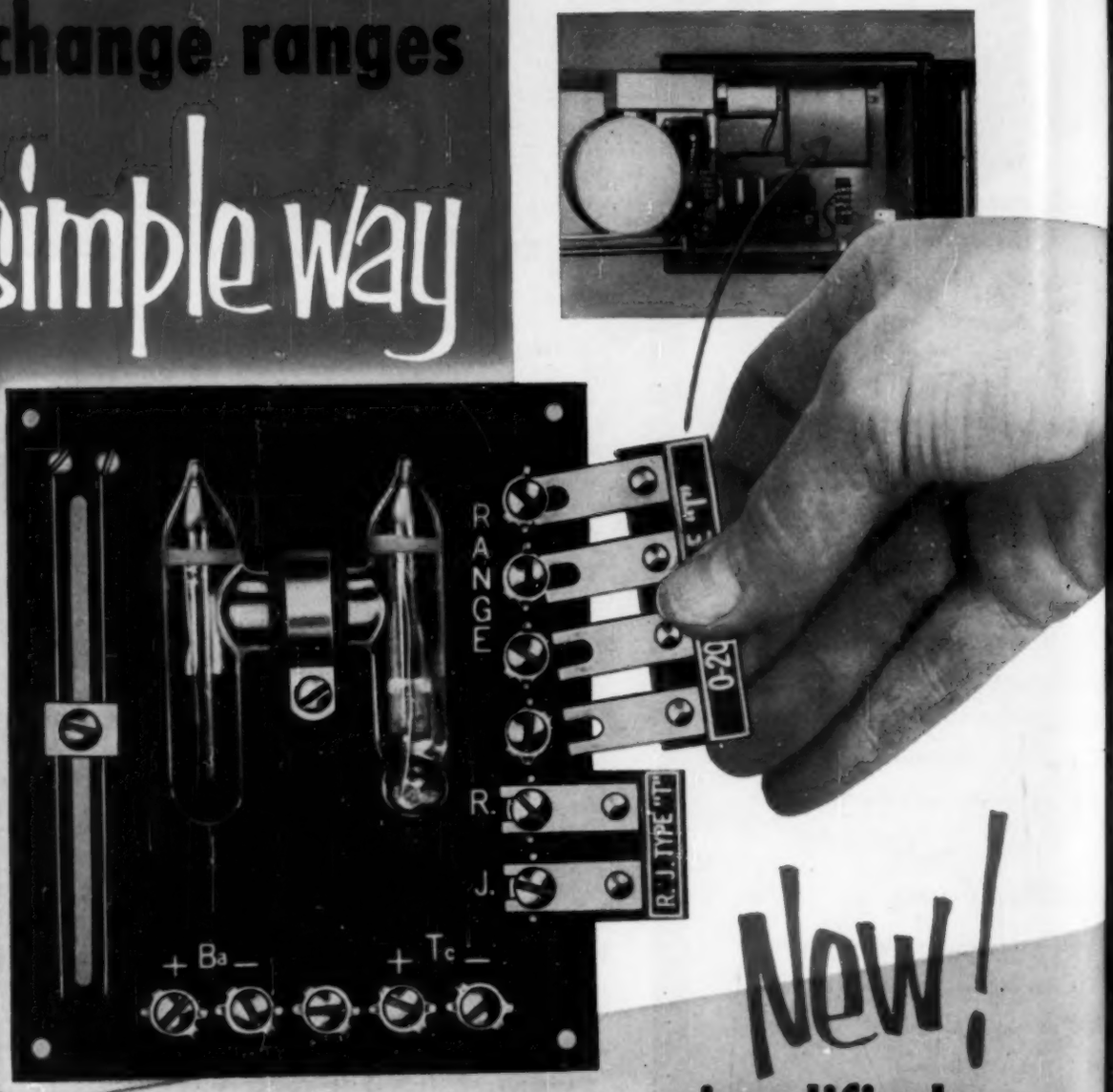

New! simplified...

Recording Potentiometer by WESTON

The question probably occurs to you, as it has to many other instrument users who have examined the new WESTON Recording Potentiometer, "Why haven't such improvements been offered before?"

Take range changing, just as an example. *You* make the change, simply by inserting the desired range standard, as illustrated above. Not even a soldered connection to break. No change in the universal slide-wire necessary. And reference junction compensation is changed in like manner, when changing type of sensing element.

And there are many more features, electrical and mechanical, that remove the complexities from instrument operations and maintenance. They're all found in this new WESTON Recorder. Ask us to send you all the facts . . . WESTON Electrical Instrument Corporation, 617 Frelinghuysen Avenue, Newark 5, New Jersey . . . *manufacturers of Weston and Tag Instruments.*

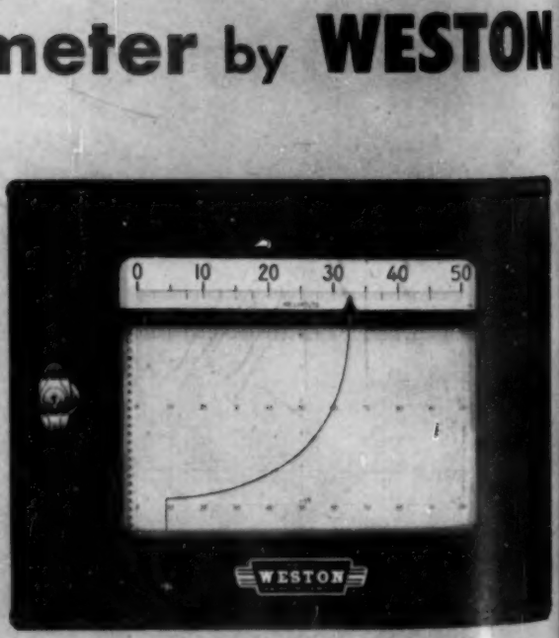

WESTON TAG **WESTON** *Instruments* . . . INDICATE — RECORD — CONTROL

Electrical Properties of Pentachlordiphenyl Impregnated Glass Fiber Paper[1]

THOMAS D. CALLINAN

Naval Research Laboratory, Washington, D. C.

ABSTRACT

In an effort to determine the effectiveness of glass fiber paper when used as a thermally stable dielectric in capacitors, a study was made of the electrical properties of the glass, the impregnant, the glass fiber paper, and impregnated paper.

The dielectric constant of Pyrex-E glass was found to be 6.1 to 6.5 over the temperature range −60° to 120°C at 60, 1000, and 10,000 cycles. The loss factor under similar conditions was 0.01 to 0.3. Glass fiber paper has a dielectric constant of 1.07 and a loss factor of 0.0001 to 0.0005. These values are in agreement with Endicott's equations. When impregnated with pentachlordiphenyl (dielectric constant 3.0 to 5.5; loss factor 0.05 to 1.0), the electrical losses of the glass fiber paper are lower than those predicted by the equations. It would seem that these equations may be employed to predict the upper limit to be expected in loss factor from a combination of impregnants.

INTRODUCTION

The preparation of paper from glass fibers (1) permits thorough evaluation of the classical equations (2) relating the dielectric constant and power factor of a substance under investigation to the dielectric constant and power factor of an impregnated paper made from such a substance. The employment of cellulose fibers to establish the applicability of the equations is undesirable since the values of dielectric constant and power factor of the cellulose *per se* are questionable.

The chemical and electrical properties of the glass, the qualities of the impregnant, the characteristics of the glass fiber paper, and the electrical qualities of the impregnated paper were studied in detail. The values predicted by the classical equations and those obtained when possible over the temperature range −60° to 120°C are tabulated and compared.

Due to the thickness of the glass fiber paper available for test, measurements at the gradients employed by Endicott (3) were precluded; consequently measurements throughout this work were made at the relatively low stresses of 150–200 volt/cm.

EXPERIMENTAL

Chemical and Physical Properties of the Glass Used

The glass fibers employed in these studies were produced for the Naval Research Laboratory by Glass Fibers, Incorporated, Waterville, Ohio (4).

Analysis indicated the following chemical composition: density, 2.54 g/cc; index of refraction, 1.52; deformation temperature, 690°C; softening temperature 855°C; coefficient of expansion, 49.10^{-7} cm/°C; modulus of elasticity, 7500 kg/mm^2; tensile strength, 100,000 psi.

The fiber was found to be a soft white material which felt like suede. It was free from shot, slubs, or other inclusions. A sample of the glass was melted in a platinum dish and the product cut and polished to yield a disk 1.992 cm in diameter and 0.050 cm in thickness. Onto this disk silver electrodes were painted (5) and the dielectric loss factor determined in an Elliott cell (6) over the temperature range −60° to 120°C. A General Radio 716-C Bridge was employed. Some of the data obtained are presented graphically in Fig. 1. The presentation of the power factor data as well as the dielectric loss factor data is based on the widespread use of the former among engineers as a measure of the energy dissipated in a dielectric.

The dielectric constant is seen to fall with rising frequency and to rise with increasing temperature. The dielectric loss factor vs. frequency curve at elevated temperatures apparently passes through a minimum (7), fulfilling some of Hopkinson's predictions on the characteristics of this curve (8). Again the runaway characteristics of the dielectric loss factor vs. temperature over the frequency range studied are in agreement with Kraus (9) and Yager and Morgan (10). While the classic relationship, $\epsilon' = 2.2\ \rho$ predicting a dielectric constant of 5.58 for the glass of density ρ, employed does not hold, extrapolation indicates the equation may be applicable at frequencies higher than 10^9 cps. It is probably also true at a temperature of −240°C. Since the glass has an Index of Refraction of 1.52, it would appear that the dielectric constant is the sum of possibly three effects amounting to 30 per cent electronic polariza-

[1] Manuscript received September 24, 1952. This paper was prepared for delivery before the Washington Meeting, April 8 to 12, 1951.

tion, 60 per cent ionic polarization, and 10 per cent ionic conductivity in the audio frequency range.

Impregnant

The impregnant employed in these studies was commercial[2] grade of pentachlordiphenyl. It is a clear, viscous, slightly yellow liquid with an irritating odor. The material was warmed to 110°C, infusorial earth was added, (1% by weight), and filtered through #52 S & S paper on a Buchner funnel. The

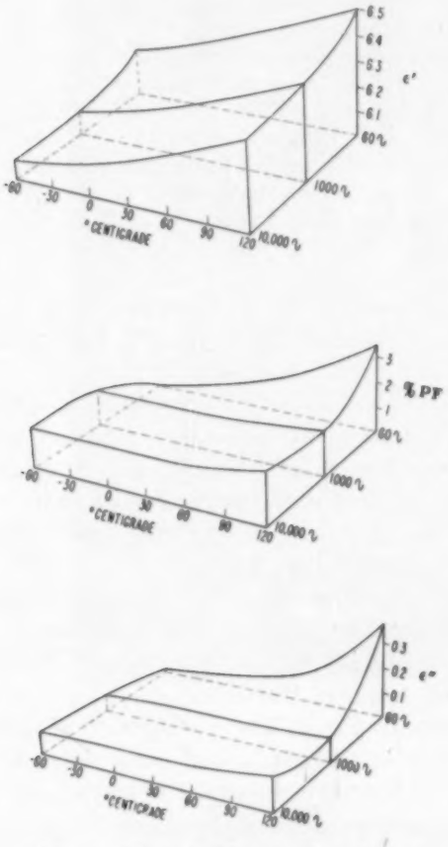

FIG. 1. Electrical properties of glass

filtration was carried out just before each test or impregnation.

The dielectric constant, power factor, and dielectric loss factor were determined also on a General Radio 716-C Bridge over the temperature range −60° to 120°C as presented in Fig. 2. The interpretation of these data has been discussed exhaustively by White and Morgan (11). Suffice it to say, the constants are presented here for use in quantitatively interpreting the role played by the impregnant at the voltage gradients available on the electrical characteristics of the assembled capacitor, as well as to indicate the condition and high quality of the impregnant.

[2] Aroclor-1254, Monsanto Chemical Company, St. Louis, Missouri.

Physical Properties of Glass Fibers

Physically, the fibers were found to be smooth, cylindrical rods as shown in the accompanying micrograph (Fig. 3).

The distribution of fibers is plotted in Fig. 4 and seen to be surprisingly sharp. A cumulative frequency plot of these data is presented graphically also showing the median value to be 0.16 μ. This value is not to be confused with the average fiber diameter of 0.24 μ, nor the root-mean-square value of 0.28 μ. All three values indicate these fibers to be well within the colloidal range. It is thought that this has a bearing on the results obtained.

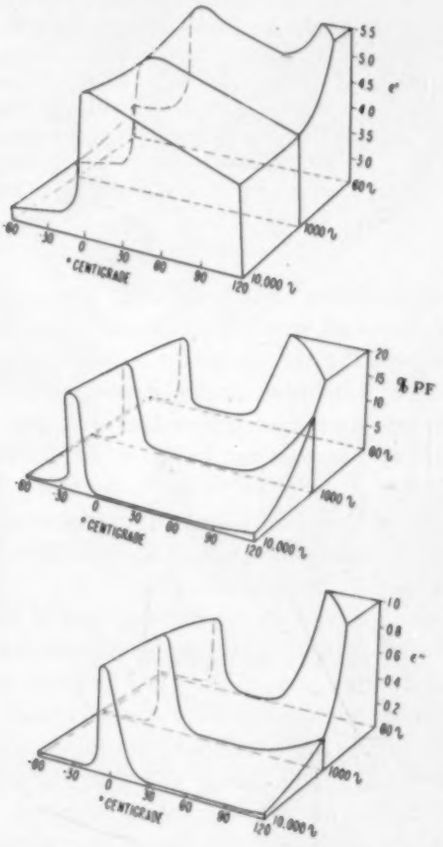

FIG. 2. Electrical properties of pentachlordiphenyl

Glass Fiber Paper

That paper could be made from glass fibers without the use of extraneous binders or contiguous fibers was announced by the Naval Research Laboratory in December 1950 after the successful completion of a series of machine runs on the Fourdrinier at the National Bureau of Standards. Among the many runs made at National Bureau of Standards, the results listed in Table I are typical of the quality of paper produced.

The electrical properties of the paper were determined using the procedure developed by Endicott (3), consisting of subjecting the paper simultaneously

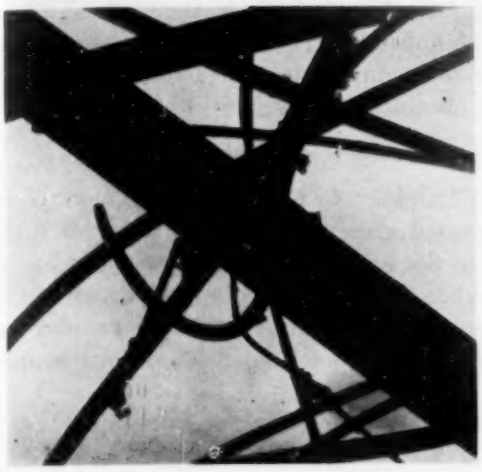

FIG. 3. Photomicrograph of glass fibers

TABLE I. *Physical properties of glass fiber paper*

Appearance	Soft, suede-like, porous paper
Color	White
Thickness, in.	0.0075
Density, g/cc	0.220
Tensile strength, psi	177
Elmendorff tear No.	24
Mullen burst, psi	2
Basis weight (25 × 40 − 500)	29.8
Uniformity	Excellent
Dirt count	0
Wet strength, (50% water) psi	235
Absorptivity	Very high
Porosity (Gurley-sec)	3.4
Air resistance mm/mil	14.7

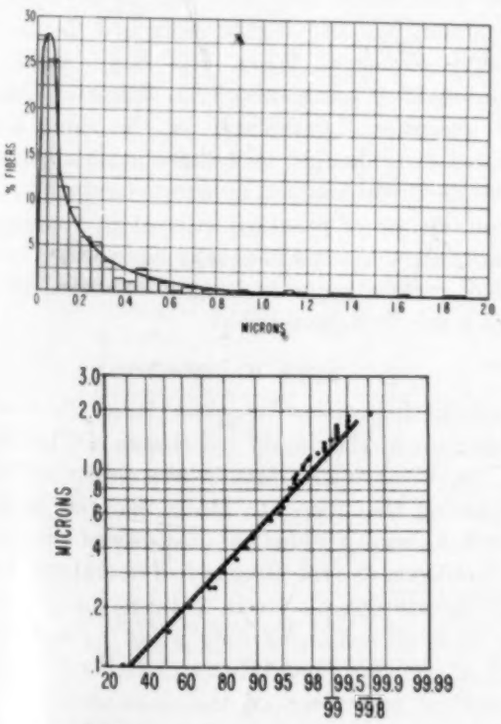

FIG. 4. Distribution of fiber diameters in glass fiber

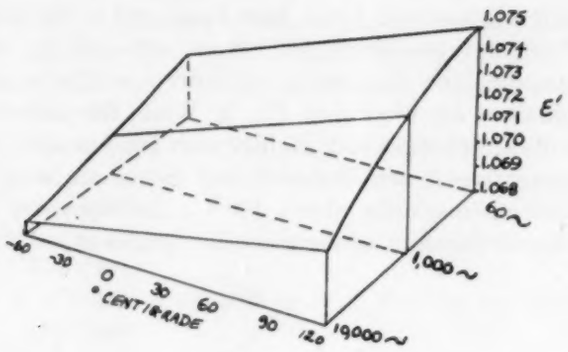

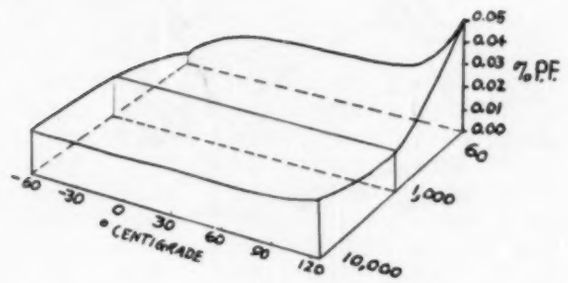

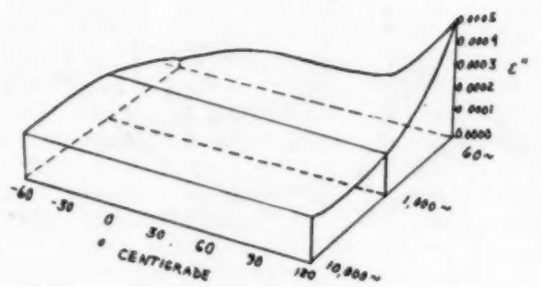

FIG. 5. Electrical properties of glass fiber paper

DIELECTRICS IN SERIES

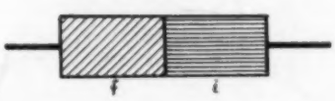

Dielectric Constant: $\underline{\epsilon'}$,

$$\frac{1}{\epsilon'} = \frac{\theta_f}{\epsilon_f'} + \frac{\theta_i}{\epsilon_i'}$$

Power Factor: $\underline{PF}$,

$$\left(\frac{1}{\epsilon'}\right) PF = \left(\frac{\theta_f}{\epsilon_f'}\right) PF_f + \left(\frac{\theta_i}{\epsilon_i'}\right) PF_i$$

FIG. 6. Endicott's equations relating the apparent dielectric constant and power factor of two materials in series.

to heat and vacuum dessication for a period of 16 hours, followed by tests on the paper under anhydrous conditions. A drying temperature of 170°C

and a pressure of 1 mm were employed in the tests. Temperatures below 25°C were obtained by surrounding the vacuum jar with dry ice. The results obtained are plotted in Fig. 5. While the dielectric constant changes only slightly with temperature, the power factor and dielectric loss factor are seen to increase markedly above 100°C. The apparent dielectric constant of the glass fiber paper is less than

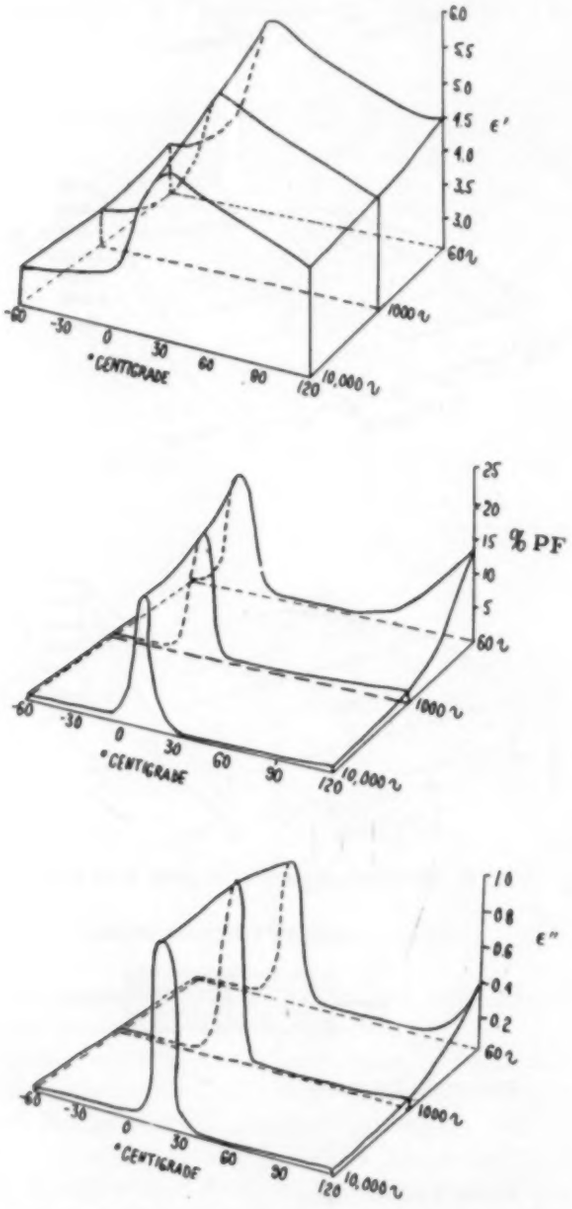

FIG. 7. Electrical properties of pentachlordiphenyl-impregnated glass fiber paper.

half that of the Kraft paper (3) while the power factor is as much as $\frac{1}{10}$th of the Kraft, and the dielectric loss factor of the glass fiber is as much as 20 times lower.

Following Endicott's thesis that the electrical qualities of a paper may be predicted if the characteristics of the substance comprising the fibers are known, the substitution of the acquired data in his equations (Fig. 6) leads to the table of information in the appendix. The calculated dielectric constant over the temperature range studied is the same as that obtained in tests.

Impregnated Glass Fiber Paper

In an effort to evaluate pentachlordiphenyl impregnated glass fiber paper, a dish was substituted for the flat base plate of the Endicott cell permitting the glass fiber paper to be desiccated and impregnated under vacuum, and the capacitive and loss characteristics determined at various temperatures and frequencies.

The results obtained are presented graphically in Fig. 7.

Conclusion

Examination of the data indicate that the Endicott equations may be employed successfully to predict the dielectric constant and dielectric loss factor of paper when the electrical properties of the pure substance are known and when the impregnant is air. Conversely, the electrical constants of the substance may be determined when those of the paper are known. When relatively low density papers and lossy impregnants with relatively high electrical losses are employed, the equations yield erroneous values due to the unknown part played by the fibers in absorbing or acting as a barrier to the ions. In the presence of pentachlordiphenyl, the glass fibers possess a positive charge and consequently exert an attractive force toward the free chlorides present in the impregnant. The glass fibers are also capable of exerting an attraction on the highly polarized pentachlordiphenyl molecule. When the large surfaces encountered by using submicron diameter fibers and the exceptional uniformity of the sheet are considered, it is thought that these reasons explain the lower electrical losses at moderate temperatures. The equations are of practical interest in predicting the quantitative limits which may be expected from the use of certain paper-making fibers in combination with a specified impregnant.

Acknowledgments

The author wishes to acknowledge the assistance given him in this study by Messrs. D. Labino and W. M. Temple of Glass Fibers, Incorporated, for producing the fibers; to Dean Walters, Naval Research Laboratory, for the analysis of the glass; to L. S. Birks, Naval Research Laboratory, for the electron micrographs; to R. T. Lucas for constructing the Endicott cell and impregnating the samples; and to R. C. Bowers, Naval Research Laboratory, for the statistical treatment of the fiber diameters. The glass paper samples were prepared by M. J. O'Leary, B. W. Scribner, J. Messimer, and J. Erving, of the National Bureau of Standards.

Any discussion of this paper will appear in a Discussion Section, to be published in the December 1953 issue of the JOURNAL.

REFERENCES

1. T. D. CALLINAN, R. T. LUCAS, AND R. C. BOWERS, *Elec. Mfg.*, **48**, No. 2, 94 (1951).
2. H. H. RACE, R. J. HEMPHILL, AND H. S. ENDICOTT, *Gen. Elec. Rev.*, **43**, No. 12, 492 (1940).
3. H. S. ENDICOTT, *Gen. Elec. Rev.*, **52**, No. 9, 28 (1949).
4. R. H. BARNARD, *Electrified Industry*, 24, Feb. (1950).
5. E. G. MEYER AND M. A. ELLIOTT, *Am. Soc. Testing Materials Bull.*, **147**, 63 (1947).
6. M. A. ELLIOTT, A. R. JONES, AND L. B. LOCKHART, *Ind. Eng. Chem. Anal. Ed.*, **18**, 10 (1947).
7. L. S. MCDOWELL AND H. L. BEGEMAN, *Phys. Rev.*, **33**, 55 (1929).
8. J. HOPKINSON, *Proc. Roy. Soc. London*, **31**, 148 (1881).
9. C. A. KRAUS AND E. H. DARBY, *J. Am. Chem. Soc.*, **44**, 2783 (1922).
10. W. A. YAGER AND S. O. MORGAN, *J. Phys. Chem.*, **35**, 2026 (1931)
11. A. H. WHITE AND S. O. MORGAN, *J. Franklin Inst.*, **216**, 635 (1933).

APPENDIX

I. The Electrical Properties of Unimpregnated Glass Fiber Paper Calculated

Frequency	Function	Temperature, °C								
		−40	−20	0	20	40	60	80	100	120
60 Cycles	Dielectric constant	1.071	1.072	1.072	1.072	1.073	1.073	1.074	1.074	1.075
	% Power factor	0.0041	0.0069	0.0096	0.0178	0.0216	0.0216	0.0267	0.0403	0.0452
	Loss factor	0.00004	0.00007	0.0001	0.0002	0.0002	0.0002	0.0003	0.0005	0.0005
1 Kc	Dielectric constant	1.071	1.071	1.071	0.071	1.072	1.072	1.073	1.073	1.074
	% Power factor	0.0178	0.0181	0.0184	0.0184	0.0192	0.0202	0.0190	0.0210	0.0227
	Loss factor	0.0002	0.0002	0.0002	0.0002	0.0002	0.0002	0.0002	0.0002	0.0002
10 Kc	Dielectric constant	1.069	1.070	1.070	0.071	0.071	0.072	0.072	0.072	0.073
	% Power factor	0.021	0.025	0.029	0.031	0.031	0.032	0.033	0.034	0.039
	Loss factor	0.0002	−.0002	0.0002	0.0002	0.0002	0.0003	0.0003	0.0003	0.0003
	Experimental									
60 Cycles	Dielectric constant	1.071	1.071	1.072	1.072	1.073	1.073	1.074	1.074	1.075
	% Power factor	0.012	0.012	0.016	0.020	0.021	0.022	0.023	0.024	0.045
	Loss factor	0.0001	0.0001	0.0002	0.0002	0.0002	0.0002	0.0002	0.0003	0.0005
1 Kc	Dielectric constant	1.070	1.071	1.071	1.072	1.072	1.072	1.073	1.073	1.074
	% Power factor	0.018	0.018	0.018	0.018	0.018	0.018	0.018	0.018	0.019
	Loss factor	0.0002	0.0002	0.0002	0.0002	0.0002	0.0002	0.0002	0.0002	0.0002
10 Kc	Dielectric constant	1.069	1.070	1.070	1.071	1.071	1.072	1.072	1.072	1.073
	% Power factor	0.020	0.020	0.020	0.020	0.020	0.020	0.022	0.023	0.023
	Loss factor	0.0002	0.0002	0.0002	0.0002	0.0002	0.0002	0.0002	0.0002	0.0002

II. The Electrical Properties of Impregnated Glass Fiber Paper Calculated*

Frequency	Function	Temperature, °C								
		−40	−20	0	20	40	60	80	100	120
60 Cycles	Dielectric constant	3.41	3.48	5.51	5.32	5.13	5.10	5.04	6.52	—
	% Power factor	0.08	1.06	1.25	0.15	0.95	7.13	20.61	46.02	—
	Loss factor	0.0027	0.0371	0.069	0.008	0.05	0.35	1.03	3.01	—
1 Kc	Dielectric constant	3.04	3.14	5.12	5.18	5.10	4.99	4.73	4.49	4.38
	% Power factor	0.12	0.20	12.91	0.29	0.31	0.42	0.99	2.39	5.31
	Loss factor	0.003	0.006	0.52	0.015	0.015	0.019	0.04	0.08	0.24
10 Kc	Dielectric constant	3.05	3.17	3.23	5.33	5.13	4.93	4.81	4.65	4.42
	% Power factor	0.13	0.80	7.0	2.0	0.08	0.06	0.5	0.9	0.21
	Loss factor	0.004	0.02	0.22	0.15	0.004	0.002	0.003	0.04	0.08
	Experimental									
60 Cycles	Dielectric constant	3.42	3.47	5.58	5.45	5.13	5.01	4.79	4.64	4.50
	% Power factor	0.18	10.06	11.54	0.18	0.23	0.36	1.21	2.88	7.82
	Loss factor	0.062	0.352	0.643	0.010	0.012	0.018	0.058	0.133	0.352
1 Kc	Dielectric constant	3.05	3.21	3.28	5.44	5.13	5.01	4.78	4.63	4.44
	% Power factor	3.15	2.51	17.47	0.23	0.04	0.05	0.11	0.22	0.65
	Loss factor	0.04	0.080	0.660	0.012	0.002	0.002	0.005	0.010	0.03
10 Kc	Dielectric constant	3.02	3.15	3.23	5.34	5.12	4.98	4.79	4.64	4.42
	% Power factor	0.04	0.74	5.0	1.90	0.065	0.041	0.048	0.071	0.11
	Loss factor	0.01	0.023	0.15	0.12	0.003	0.002	0.002	0.003	0.004

* Aroclor

Cathodic Lead Disintegration and Hydride Formation[1]

HUGH W. SALZBERG

Naval Research Laboratory, Washington, D. C.

ABSTRACT

Lead cathodes disintegrate into colloidal lead at high current densities in alkaline and weakly acid solutions. The rates of disintegration were studied in solutions of varying *p*H and salt concentration at different temperatures and current densities. It is concluded that the cause of this phenomenon is the formation and subsequent decomposition of a volatile unstable hydride of lead. The formula of this hydride is PbH_2. It is quantitatively formed at current densities above 10–50 ma/cm², depending on the other parameters. The equation for formation of PbH_2 is considered to be: $e + Pb(H) + H_2O \rightarrow PbH_2 + OH^-$. The implications of this on hydrogen overvoltage are discussed.

INTRODUCTION

During studies of the reducing properties of electrolytic hydrogen, it was observed that in both alkaline solutions and weakly acidic solutions containing no alkali ions lead cathodes disintegrate at high current densities, forming colloidal lead particles and, ultimately, sponge lead. The phenomenon was provisionally ascribed to the formation of a volatile unstable hydride of lead.

A literature search revealed only one report of the electrolytic formation of lead hydride. Paneth (1) obtained microquantities of a volatile material containing lead by alternately arcing and electrolyzing through acid solutions and cooling the evolved gases with liquid air. Jofa and Kabanov (2) reported a smoothing of the surface of a lead cathode in acid solutions at moderate current densities, which they interpreted as having been caused by lead hydride formation. The only reference to disintegration of a lead cathode was in the work of Bredig and Haber (3). They reported disintegration, at high current densities, of cathodes of lead, bismuth, antimony, mercury, arsenic, and rose metal and ascribed it to formation of a soluble alkali-metal alloy. They had no explanation of disintegration in acidic solutions.

EXPERIMENTAL METHOD

Procedure

The weight loss of a lead cathode of known dimensions under controlled conditions was determined by difference. The parameters studied were time, temperature, *p*H, salt concentration, and current density.

Since the true surface area was not known and the current distribution on the different portions of the cathode were certainly not uniform, the values reported here are not absolute current densities. Assuming however that neither the current distribution nor the area changed from run to run, the current densities are correct, relative to an unknown constant, and to each other.

The cell was a U-tube, 13.8 cm high with each limb 2.4 cm inner diameter. The bottom of the cathode limb contained a gas inlet equipped with a fritted disk so that the gas bubbles would be smaller and thus sweep out dissolved oxygen more effectively.

The electrodes were mounted in rubber stoppers since strong alkali would have destroyed ground glass joints. The anode was a bright platinum square, 2 cm on an edge. The cathode was a lead disk, 1.20 cm in diameter and 0.05 cm thick, with a lead wire spotwelded to the back. It was mounted on a glass tube, 0.72 cm outer diameter, which was held flush against the back face of the disk, so that electrolysis would not occur along the wire, which passed through the tube and out through the stopper. The area thus available for current passage was 1.95 cm. However, since leakage into the tube with consequent increase in surface area did occur and since the current densities reported were at best relative, the area was rounded off and considered as 2 cm².

The above electrode assembly was chosen so that after each run the cathode could be removed from cell and holder and weighed with fair precision. The cathodes weighed about a gram each and were weighed to a tenth of a milligram.

Materials

The lead used was Baker's Analyzed grade, giving an analysis of 99.99 per cent lead and 0.00000 per cent arsenic. The lead was cast into ingot form in an iron mold. The ingots were etched to remove any iron oxide or iron and then rolled into strips between steel rollers, cut into disks, and finally etched again with nitric acid and with a 90 per cent glacial acetic-10 per cent hydrogen peroxide solution. The results obtained with these lead disks were in agreement with

[1] Manuscript received August 11, 1952. This paper prepared for delivery before the Montreal Meeting, October 26 to 30, 1952.

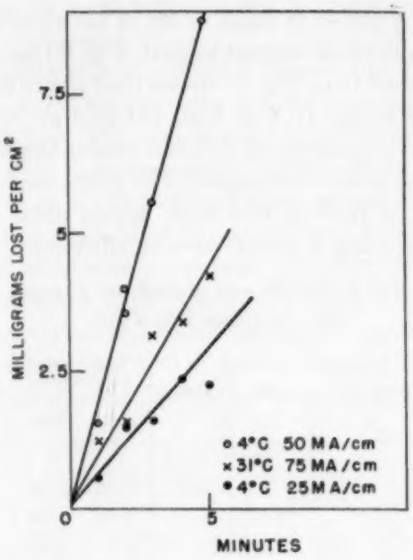

FIG. 1. Weight loss vs. time, in 4*N* NaOH at various temperatures and current densities.

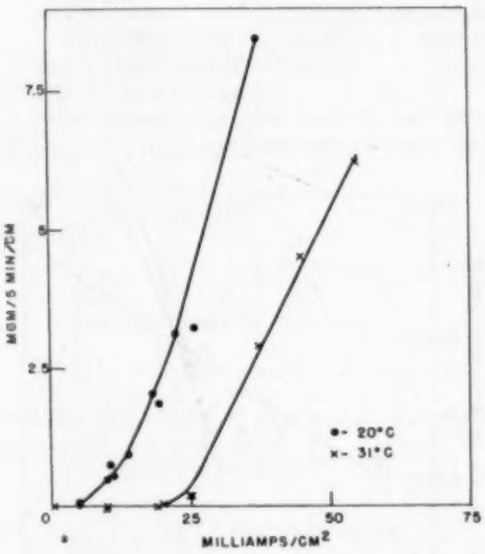

FIG. 2 Effect of temperature. Weight loss vs. current density for 0.04*N* NaOH at 20° and 31°C.

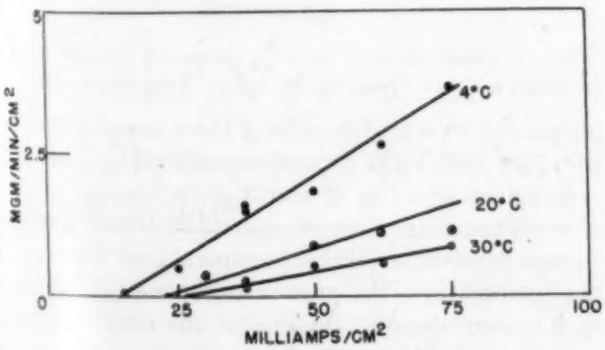

FIG. 3. Effect of temperature. Weight loss vs. current density for 4*N* NaOH at 4°, 20°, and 30°C.

those obtained from lead cast in Pyrex glass and used without rolling. Added impurities such as iron, silver, and antimony lowered the observed rates of disintegration.

Stock solutions were made from C.P. analyzed reagents titrated against standards and diluted as required. The *p*H of each dilution was determined with a Beckman *p*H meter. In the interests of time and economy, the solutions were used several times. However, unless the results of the final run in a solution agreed with these in a fresh solution, the runs in question were repeated, using fresh solution.

The gas used for scouring was tank hydrogen passed through the solution at a rate of 18–20 cc/min.

EXPERIMENTAL RESULTS

The final product of the reaction was a black precipitate of sponge lead. Although under the microscope this showed no apparent crystal structure, samples of it gave the x-ray pattern for lead.

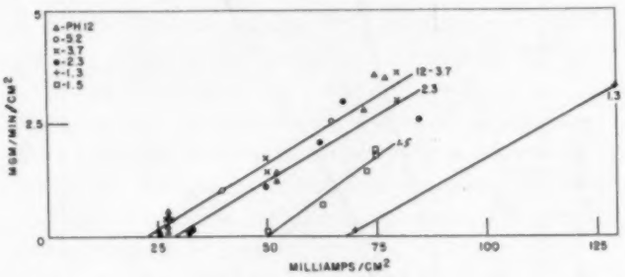

FIG. 4. Effect of *p*H. Weight loss vs. current density in 1*M* KCl at 20°C at various *p*H's.

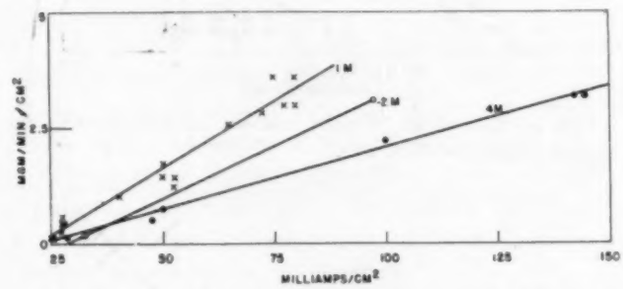

FIG. 5*a*. Salt effect. Weight loss vs. current density in alkaline solutions at 20°C in 1*M*, 2*M*, and 4*M* KCl solutions.

The results of the rate studies were as follows:

Time.—The weight loss vs. time curves were straight lines, indicating a constant rate. It was therefore permissible to make runs of varying duration. Results are shown in Fig. 1.

These straight lines did not pass through the origin, since each cathode had a film of lead oxide, on being immersed. The oxide film weighed between 0.1–0.3 mg, depending on the room temperature and time of exposure to air. Fig. 2 to 5 have been corrected for this oxide film.

Current density.—The shape of the rate of weight loss vs. current density curves is shown in Fig. 2 to 5. The curves are straight lines with sharp break points,

indicating that above a critical current density there is a direct proportionality between weight loss and current density.

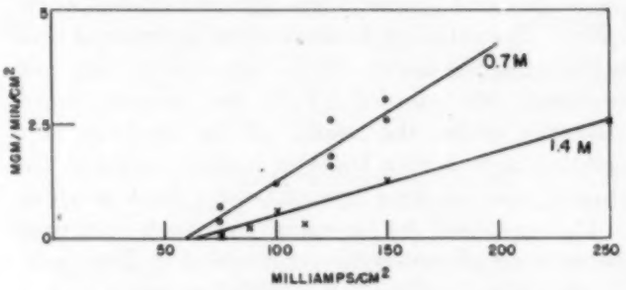

FIG. 5*b*. Salt effect. Weight loss vs. current density in alkaline solutions at 20°C in 0.7*M* and 1.4*M* (approximate concentrations) Na_2SO_4 solutions.

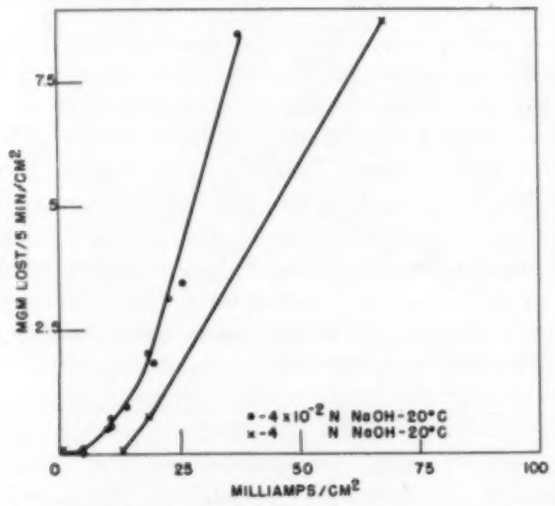

FIG. 5*c*. Salt effect. Weight loss vs. current density in 4*N* and 0.04*N* NaOH at 20°C.

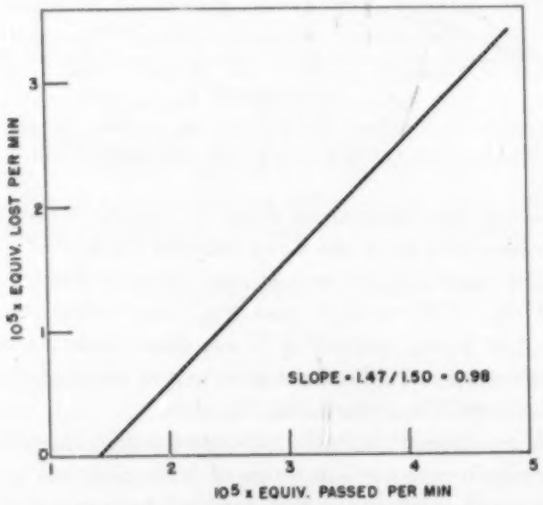

FIG. 6. Equivalents of lead lost per Faraday of current passed. Results obtained from straight line portions of graphs.

If the weight loss is plotted as equivalents of divalent lead per minute and the current is plotted as equivalents of current passed per minute, the slope gives the number of equivalents of divalent lead lost per equivalent of current passed. Fig. 6 (the straight line obtained from Fig. 5) shows that above the break point, for molar KCl at high *p*H and at 20°C, just about one equivalent of divalent lead is lost for every equivalent of current passed. The more concentrated solutions, if plotted this way, would show a lower slope indicating a lower current efficiency. The experimental error in determining these slopes is about 10–15 per cent. These data are summarized in Table I.

TABLE I. *Equivalents of lead per Faraday of current* (from Fig. 3–5b)

Electrolyte	*p*H	Temp	Equivalents per Faraday		i_o (Current at intercept)
			PbH_2	PbH_4	
					ma/cm²
1*M* KCl	12–3.7	20°C	0.98	1.96	23
	2.3		0.98	1.96	29
	1.5		1.1	2.2	50
	1.3		0.80	1.6	68
2*M* KCl	alk		1.05	2.1	29
4*M* KCl	alk		0.52	1.0	22
0.7*M* Na_2SO_4*	alk		0.46	0.92	59
1.4*M* Na_2SO_4*	alk		0.36	0.72	63
4*M* NaOH	alk	4°C	0.91	1.8	14
		20°C	0.46	0.92	22
		30°C	0.26	0.56	25

* Approximate concentration.

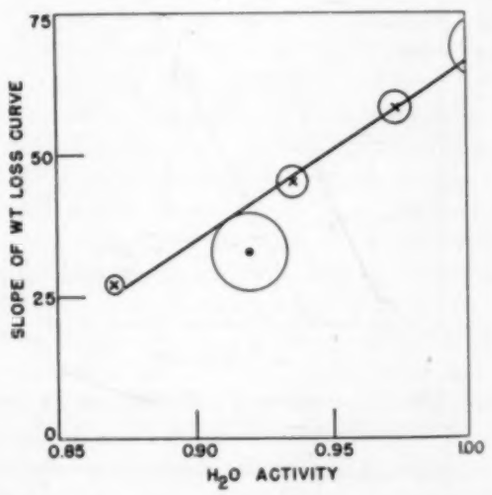

FIG. 7. Effect of water activity. Slope of straight lines vs. water activity, from Fig. 5*a* and 5*c*. Temperature 20° C.

Temperature.—Fig. 2 and 3 show the family of curves when weight loss per minute is plotted against current densities at different temperatures. The lower the temperature, the greater is the weight loss at each current density, the greater the slope and the more negative the intercept.

Acidity.—Fig. 4 shows the family of weight loss-current density curves at constant temperature and various *p*H. Apparently there is no change until the solution is fairly acid. At higher acidities, the break

in the curve is at higher current densities but the slope is unchanged.

Salt concentration.—Fig. 5 shows the family of weight loss-current density curves at constant temperature, high *p*H, and various salt concentrations. It is noted that the more dilute solutions show greater rates. If the slopes of these curves are plotted against the water activity, as in Fig. 7 and Table II, it is seen that there is a straight line relationship, the slope increasing with increased water activity.

To summarize the above results, the rate of weight loss is a direct function of current density and water activity. The rate of weight loss is an inverse function

TABLE II

Salt	Conc.	A_{H_2O}	Slope of rate-current curve
NaOH	4*N*	0.920	33 ± 7
	0.04	1.00	69 ± 7
KCl	4*N*	0.870	27 ± 1
	2	0.936	45 ± 5
	1	0.973	58 ± 3

of the temperature and the acidity. An empirical equation for this would be

$$\frac{\text{wt loss}}{\text{m}^2\text{-minute}} = k_1 i (A_{H_2O}) e^{+E_1/RT} - k_2 (1 + k_3 H_2O^+) A_{H_2O} e^{+E_2/RT} \quad (I)$$

where i = current density.

Discussion

The following diagram illustrates the suggested mechanism for this phenomenon.

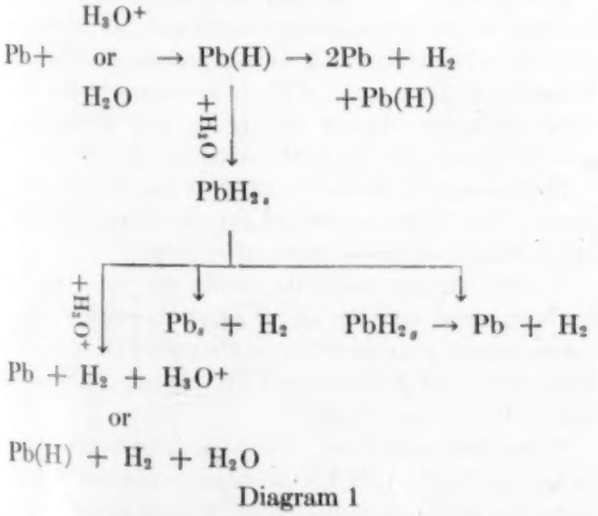

Diagram 1

where Pb(H) is chemisorbed hydrogen, the subscript s refers to the adsorbed or surface material and subscript g refers to the gaseous state.

If this summary is correct, at first, the chemisorbed atoms Pb(H) formed by discharge of either water or acid, leave the surface by combining as in equation (II)

$$2Pb(H) \rightarrow 2Pb + H_2. \quad (II)$$

When a critical current is reached, due to the attainment of a large enough potential, a volatile, unstable lead hydride, PbH_2, is formed, as in equation (III)

$$Pb(H) + H_2O + e \rightarrow PbH_2 + OH^-. \quad (III)$$

The amount of this hydride formed depends upon the current and the water activity. A fraction of the PbH_2 (depending upon the temperature) volatizes off the surface and then decomposes in the solution to Pb and gaseous H_2 as in equation (IV).

$$PbH_2 \xrightarrow[\text{gaseous}]{} Pb + H_2. \quad (IV)$$

A smaller fraction of the PbH_2 decomposes into Pb and H_2 before it has a chance to leave the surface.

In the presence of acid, the surface hydride is decomposed by the acid before it gets off the surface so that until the acid is depleted below a critical level, no PbH_2 is evolved. After this depletion, however, the rate of hydride evolution continues, independent of the initial acid concentration.

The formula PbH_2 is obtained from the slope of Fig. 6 and Table I. If the hydride were expressed as PbH_4, the observed yield would be greater than theoretical.

Fig. 5 and 7 indicate that the PbH_2 is formed directly from water, as shown in equation (III). This is also in accord with the inhibiting effect of H_3O^+ and the absence of any effect of OH^-.

The inverse temperature effect is considered as being due to the increased temperature speeding up the slow surface decomposition of the hydride more than it speeds up the volatization.

The instability of the gaseous PbH_2 is in accord both with the observations of Paneth and with the immediate formation of colloidal lead in the alkaline solutions discussed here.

The decomposition of the hydride by H_3O^+ before it leaves the surface is indicated by the results of Fig. 4. Here it is apparent that increased acidity has no effect on the slopes but only on the intercepts. In other words, the acid does not take part in the formation of the hydride but merely prevents weight loss until the current is sufficiently high.

This inhibition of the weight loss could be due to either acid catalyzed decomposition of the hydride before it leaves the surface, as in Equations (Va) and (Vb)

$$PbH_{2_{surf}} + H_3O^+ \rightarrow Pb_{surf} + H_2 + H_3O^+ \quad (Va)$$

or

$$PbH_2 + H_3O^+ e \rightarrow Pb(H) + H_2 + H_2O \quad (Vb)$$

or, it could be due to preferential discharge of the H_3O^+, as in equation (VI)

$$Pb(H) + H_3O^+ + e \rightarrow Pb + H_2 + H_2O. \quad (VI)$$

However, it is difficult to see why the PbH molecule should react differently toward a proton coming from H_3O^+ as in Equation (VI) than it reacts toward a proton coming from H_2O, as in equation (III). Also, the catalytic decomposition of the hydride by H_3O^+ before it has a chance to leave the surface would be in agreement with the observations of Jofa and Kabanov, as duplicated in this laboratory.

Several possible alternative explanations for this cathodic disintegration are as follows.

(*A*) The OH^- formed during the electrolysis attacks the lead and forms the $HPbO_2^-$ complex. Some of these complexes plate back on the cathode and being held loosely are blown off the surface by the evolved hydrogen. Arguments against this are:

1. Rate studies performed in these laboratories showed that the attack on lead in alkaline solutions is by H_2O and not OH^-.

2. This mechanism should lead to a positive temperature coefficient.

3. There should not be the direct proportionality between equivalents of current passed and equivalents of lead lost.

4. The attack by OH^- ions should result in a lower break point and higher slope in more alkaline solutions. The rates and intercepts, however, are about the same between *p*H 3–12.

5. The observed disintegration rates are several orders of magnitude greater than the corrosion rates in the absence of current.

(*B*) Formation of a Bredig arc, with production of colloidal lead. Arguments against this include:

1. No arc or spark is observed and the emf between electrode and solution is no more than 1–2 volts.

2. The magnitude of disintegration is far too great to be explained on the basis of an arc.

3. The temperature coefficient to be expected on this mechanism would be positive.

4. The arc process would not result in the linear relationship observed between equivalents of current and equivalents of lead lost.

5. A final, less direct argument here is the fact that Bredig himself, along with Haber, was the first to observe this phenomenon and he distinguished between this and the results of an arc or spark discharge.

(*C*) Formation of a water-soluble alloy between alkali and lead. Arguments against this are as follows.

1. No such water-soluble alloy is known.

2. This would not explain results in pure acid solutions, where no alkali-metal ions were present.

3. The volatility of such an alloy would not decrease with increasing temperature, although it might be in equilibrium with its constituents and the shift in equilibrium with temperature could explain a negative temperature coefficient.

4. If this mechanism were valid, increased alkali ion concentration would increase the disintegration, but it does not.

It is worth noting here, however, in connection with this last suggested mechanism that the explanation postulated in this paper is also the formation of an 'alloy.' The 'alloy' here, however, is a lead-hydrogen compound.

If the above results are valid there are certain implications in the field of cathodic hydrogen evolution and hydrogen overvoltage that must be considered.

1. If above the break points on the curve lead hydride is formed, obviously, below the break points no significant amount of lead hydride is formed.

Therefore, whatever the mechanism of hydrogen productions on lead at current densities below about 10 ma/cm², lead hydride is not rate-determining and, hydride formation cannot be considered as having anything to do with the observed alpha value of ½ in Tafel's equation.

In all probability, therefore, the slow, rate-determining step is either the slow discharge of an ion or a water molecule, or else the lateral diffusion of hydrogen atoms across the surface, which Pitman (4) has suggested for iron.

2. Hydride formation should involve chemisorbed hydrogen. Its occurrence is, therefore, an indication that at least above the break point, atomic hydrogen is present in significant amounts.

3. Hydrogen overvoltage measurements in the vicinity of the break point should give information as to the rate-determining step in hydrogen evolution. Referring to Diagram 1, if the overvoltage is due to a slow discharge, then a change in the mechanism should cause a change in the overvoltage equation.

Measurements in the vicinity of the break point should thus indicate whether the slow step involved production of atoms or removal of atoms.

4. The straight line relationship shown in Fig. 7 between water activity and slope of the weight loss/current density curve indicates that water is reduced, as shown above in equation (III), during the formation of PbH_2 from Pb(H).

Since PbH_2 is evolved, even in acid concentrations as high as 0.05*N*, (*p*H 1.5), it must be presumed that the water molecule is discharged in acid solutions, at least above the break point, which for *p*H 1.5 is at about 75 ma/cm².

This is in complete agreement with the work of Schuldiner (5) who found that on electrolyzing with

platinum cathodes in 0.1*N* acid, above 50–100 ma/cm², the source of the hydrogen was the water molecule.

From the surface changes noted by Jofa and Kabanov and duplicated by workers in these laboratories, it follows, since they reported hydride formations, that water is reduced even at current densities of about 1 ma in strong acids. Further consideration must, therefore, be given to the explanation of hydrogen overvoltage suggested by Glasstone, Laidler, and Eyring (6).

Summary

Lead cathodes disintegrate into colloidal lead at current densities above 10–50 ma/cm². The rate of dissolution is a direct function of current density and of water activity. The reaction was studied in solutions of sodium and potassium hydroxide, carbonates, chlorides and sulfates, and in sulfuric, phosphoric, and hydrochloric acids, in the presence and absence of neutral salts. The rates of disintegration are inversely proportional to temperature. Increased acidity displaces the rate curve toward lower values but does not change the slope.

The observed rates indicate the formation and subsequent decomposition of gaseous PbH_2.

Any discussion of this paper will appear in a Discussion Section, to be published in the December 1953 issue of the JOURNAL.

REFERENCES

1. F. PANETH, *Z. Elektrochem.*, **24**, 298 (1918); **26**, 452 (1920).
2. Z. A. JOFA AND B. KABANOV, *Doklady Akad. Nauk U. R. S. S.*, **10**, 616 (1939).
3. G. BREDIG AND F. HABER, *Ber.*, **31**, 2741 (1898).
4. A. L. PITMAN, unpublished.
5. S. SCHULDINER, *J. Electrochem. Soc.*, **99**, 488 (1952).
6. S. T. GLASSTONE, K. J. LAIDLER, AND H. EYRING, *J. Chem. Phys.*, **7**, 1055 (1939).

A Preliminary Study of the Ductility of Chromium[1]

H. B. Goodwin, R. A. Gilbert, C. M. Schwartz, and C. T. Greenidge

Battelle Memorial Institute, Columbus, Ohio

ABSTRACT

Chromium was found to be cold ductile if it is sufficiently pure and if low strain rates are used. Ductility is dependent on strain rate and purity. The slip mechanism was confirmed by x-ray and microscopic techniques.

Introduction

Chromium has so far found usefulness chiefly for plating and as a constituent of alloys containing generally less than 50 per cent chromium. This is true in spite of the fact that chromium-base alloys have excellent high temperature oxidation resistance and have shown high temperature strength superior to that of cobalt- and nickel-base alloys used at present for high temperature applications. The reason for the limited usefulness of chromium and chromium-base alloys is that these materials have always been so brittle at room temperature that they cannot be fabricated into useful structures. Most of the alloys have not been forgeable.

Experience with other metals strongly suggests that the brittleness of unalloyed chromium is not inherent, but is caused by impurities.

Other body-centered cubic metals are ductile. The ductility of molybdenum is destroyed by less oxygen than is present in the purest chromium so far obtained. Titanium, zirconium, and vanadium, once thought to be brittle, proved to be ductile when their purity was improved.

About two years ago, W. J. Kroll described (1) a process for making hot ductile chromium. This is additional evidence that the brittleness of chromium is caused by impurities, since the process is primarily a method of making chromium of higher purity than has heretofore been available. Another encouraging sign that the brittleness of chromium is not inherent is the demonstration by Greiner (2) of the slip mechanism in chromium. This has been confirmed independently here as described later.

Recently Gilbert, Johansen, and Nelson described production of chromium sheet which had some ductility when warm but could not be bent at room temperature (3). The sheet contained 0.001 per cent oxygen and slightly more nitrogen and was rolled by a special technique from arc-melted ingots which were melted from chromium previously deoxidized with hydrogen.

Earlier work by Marden and Rich (4) suggests that for chromium, like molybdenum and tungsten, special working schedules may be necessary to develop maximum ductility.

Preparation of High-Purity Chromium

The method used was: (*a*) to determine whether there were any signs of ductility in the purest chromium available, and (*b*) to compare the results with those obtained when small quantities of impurities were present in the chromium. In undertaking this work, it was not contemplated that pure chromium would find many uses. However, it was hoped that increasing the ductility of pure chromium would ultimately lead to chromium-base alloys of sufficient ductility for practical use.

In the past several years a number of approaches to making very pure chromium have been explored here. These included: (*a*) addition of deoxidizers to electrolytic chromium while arc melting in water-cooled copper crucibles under purified argon; (*b*) treatment of solid electrolytic chromium with molecular hydrogen; (*c*) treatment of molten electrolytic chromium with atomic hydrogen; (*d*) formation of chromic chloride from electrolytic chromium followed by fractional distillation of chloride in vacuum and reduction to chromium metal with hydrogen; (*e*) deoxidation of chromium with molten calcium; (*f*) deoxidation with anhydrous ammonia followed by vacuum annealing to remove nitrogen; (*g*) special methods of electrodeposition; (*h*) melting by induction in beryllia crucibles in vacuum, using carbon as a deoxidizer; (*i*) vacuum-arc melting using carbon as a deoxidizer; (*j*) combinations of the preceding techniques; and (*k*) purification by the "iodide" process. Although some of the first ten methods produced hot workable chromium and offer promise of further improvement, the highest purity chromium so far produced was made by the iodide process. The ductility studies described later were, therefore, carried out almost entirely with iodide chromium.

The iodide process for purification of chromium is a modification and improvement of the Van Arkel-De Boer process.

The chromium obtained by the iodide process was

[1] Manuscript received June 3, 1952.

in the form of many tiny individual crystals each adhering at one edge or corner to the filament on which they were deposited. Fig. 1 is a photograph of a typical chromium deposit made by the iodide process; it contains several hundred small crystals.

Several "buttons" were prepared by arc melting some of the chromium crystals in a cup-shaped depression about ½ in. in diameter in a water-cooled hearth plate. A water-cooled tungsten electrode was used. The melting was done in a highly purified argon atmosphere. These buttons were about ¼ in. in diameter and almost perfect spheres.

One button was hot rolled into a strip of 0.050-in. sheet about ½ in. wide and 6 in. long. The rolling was carried out in air and at a temperature of 980°C for the first pass. The temperature was gradually reduced at each pass. After a pass at 850°C, the sheet was annealed at 850°C for 15 minutes in air. It was rolled at 700°C for the final pass.

Vacuum-fusion and spectrographic analyses were run on the "as-deposited" crystals and on the rolled sheet. A carbon determination was made on the crystals by the standard combustion method. Table I gives the results of these analyses. For comparison, analyses for other types of chromium are also given. While chromium has been prepared with substantially lower oxygen content by vacuum fusion using carbon as a deoxidizer, such samples have had high residual carbon contents. When the amount of carbon was reduced, the oxygen content was higher. It appears that in this sample of iodide chromium, metallic impurities and hydrogen are substantially eliminated and oxygen has been reduced to a value well below that for most other types of chromium (except vacuum-fused chromium), while carbon and nitrogen are not significantly lower than in other chromium. The percentage value of oxygen is still well above the minimum which is permissible in ductile molybdenum or tungsten.[2] There is, then, still room for improvement in purity.

Ductility Tests

Because of the small quantity of iodide chromium available and because any agglomeration process might have changed the properties, most of the ductility studies were made on the small crystals as deposited. Most of these were not over ⅛ in. in the maximum dimension.

The crystals as deposited were quite soft, having Knoop hardness values averaging 136 which corresponds to less than zero on the Rockwell "C" scale. The Vickers hardness number ranged from 125 to 148 (10-kg load) on the crystals and was 210 on the rolled sheet.

The crystals as deposited could be shattered in a brittle manner by light hammer blows. However, it was discovered that the crystals were sensitive to strain rate and, if a low strain rate was used, they were surprisingly ductile. The tests were made by compressing individual chromium crystals between two flat polished steel plates in a hydraulic testing machine.

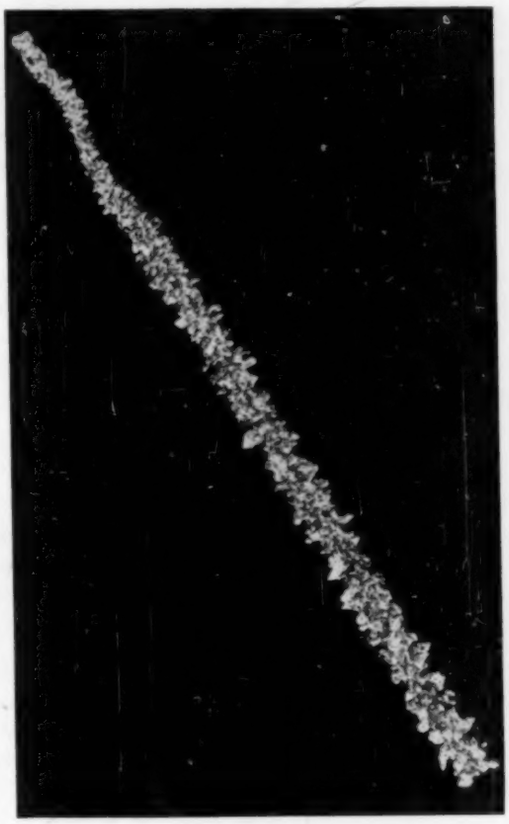

Fig. 1. Typical deposit of chromium obtained by thermal decomposition of chromous iodide on a tungsten wire filament.

It was found that at deformation rates of less than 0.050 in./min, the crystals could be flattened into tiny plates at room temperature and could withstand a total reduction in thickness of between 35 and 40 per cent before edge cracking developed. Even on examination at high magnification after etching, no signs of cracking were evident prior to the development of the edge cracks. When deformation rates somewhat higher than 0.050 in./min were used, the crystals cracked with less than 10 per cent reduction in thickness. As deformation rates increased, the amount of deformation before cracking decreased. Microscopic and x-ray diffraction examination showed the undeformed crystals to be single crystals. After compression, Laue photograms showed that

[2] Elements that are similar to chromium in being body-centered cubic and in being transition elements in the Periodic Table.

TABLE I. *Chemical composition of various types of chromium*

Material	Analysis, %																		
	O	H	N	C	Si	Fe	Cu	Mn	Mg	Co	Ni	B	Ti	Pb	Ca	Al	W	Mo	S
Iodide chromium, as deposited	0.014	0.0009	0.013	0.009	<0.001	<0.001	0.001	N.D.	0.001	0.001	N.D.	N.D.	N.D.	N.D.	0.001	N.D.	N.D.	N.D.	(Phosphorus and sulfur not determined)
Iodide chromium, sheet	0.053	0.0007	0.003*																
Special high-purity electrolytic chromium,†, as deposited	0.034	0.032	0.022		<0.001 to 0.01	<0.001 to 0.01	<0.001 to 0.01	<0.001 to 0.01	0.001 to 0.01	N.D. to 0.01	N.D.	N.D.	N.D.	0.001 to 0.01	0.001 to 0.01	0.001 to 0.01	N.D.	N.D.	
Commercial electrolytic chromium,‡, as deposited	0.1 to 0.3	0.07	0.01 to 0.02	0.01	<0.001 to 0.01	<0.001 to 0.05	<0.001 to 0.01	<0.001 to 0.01	0.001 to 0.01	N.D. to 0.01	N.D.	N.D.	N.D.	<0.001 to 0.01	0.001 to 0.01	<0.001 to 0.01	N.D.	N.D.	0.03
Regular electrolytic chromium, after arc melting					0.001 to 0.01	0.001 to 0.05	0.005 to 0.05	<0.001 to 0.01	<0.001 to 0.01	0.001 to 0.01	N.D.	0.001 to 0.01	N.D.	N.D.	0.001 to 0.01	0.001 to 0.01	0.5 to 1.5	N.D.	
Regular electrolytic chromium, after treatment with molten calcium					<0.001	0.001 to 0.01	0.001 to 0.01	0.001 to 0.01	<0.001 to 0.01	0.001 to 0.01	N.D.	N.D.	N.D.	N.D.	0.05 to 0.5	<0.001	N.D.	N.D.	

N.D. = Not detected.

* Nitrogen values in this range are not too reliable by the vacuum fusion method.

† The "special high purity" electrolytic chromium was prepared for Battelle by the Lancaster Electroplating Co. using the hot-bath method developed by the National Bureau of Standards (5).

‡ The "regular" electrolytic chromium is a standard commercial grade obtained from the Electro-Metallurgical Sales Corporation.

Note: Oxygen, hydrogen, and nitrogen were determined by vacuum fusion, the other elements spectrographically.

small areas, at least, were essentially monocrystalline, the lattice having suffered curvature because of plastic flow.

Having established that single crystals of iodide chromium were quite cold ductile at low deformation rates, it seemed desirable:

1. To determine whether polycrystalline iodide chromium exhibited as much ductility as had the single crystals.
2. To test similarly less pure chromium and determine how inpurities affected both the maximum permissible deformation rate and the maximum plastic deformation.
3. To determine whether the rolled iodide chromium was as ductile at low deformation rates in tension as the crystals had been in compression.
4. To determine whether any heat treatment could be found which would improve the ductility of iodide chromium crystals.
5. To establish by crystallographic studies the mechanism of plastic deformation of iodide chromium crystals.

The same results were obtained with polycrystalline iodide chromium as were obtained with single crystals. An arc-melted spherical button was compressed from an original diameter (of the almost perfect sphere) of 0.2028 in. to a "pancake" 0.1165 in. in thickness before edge cracks developed. This is a reduction in height of 42.6 per cent. The deformation rate was 0.002 in./min. Microscopic examination of the melted button after compression showed that it was polycrystalline, and it is assumed that it was also polycrystalline before compression.

The supply of iodide chromium was too small to permit additional testing of arc-melted buttons. In order to secure additional polycrystalline iodide chromium, a number of the single crystals, as deposited, were recrystallized by straining them about 30 per cent (at low deformation rates) and then annealing for 15 minutes at 2200°F in vacuum, followed by slow cooling. These were found, by microscopical examination, to be polycrystalline after the treatment. Low deformation-rate compression tests on these recrystallized crystals confirmed the previous observation that polycrystalline iodide chromium is cold ductile at low deformation rates, just as are single crystals.

For comparing the behavior of other less pure chromium with that of iodide chromium in compression at low deformation rates, two buttons were arc melted from electrolytic chromium. These buttons were about the same size and were arc melted by the same technique as the button of iodide chromium previously tested. One of the buttons was from the special high-purity electrolytic chromium and one from regular electrolytic chromium. In the compression tests, both buttons cracked into several pieces after a reduction in thickness of about 10 per cent, even though a deformation rate of only 0.001 in./min was used.

When tested in tension, the piece of sheet rolled from iodide chromium failed in a brittle manner at 46,000 psi with no measurable plastic elongation. A deformation rate of 0.001 in./min was used. Like all fractures observed in unalloyed chromium, the fracture was predominantly transcrystalline. The oxygen content of the sheet (Table I) was about four times that of the crystals as deposited, but it is not known if this is the whole explanation for the difference in ductility. The sheet was quite stiff but readily bent elastically to a 6-in. radius. It could not be bent permanently (plastically).

Several crystals of the as-deposited iodide chromium were heated in purified argon for one hour at 2950°F and then quenched in cold mercury[3] in an attempt to put any impurities present into solution or at least into a finely divided, evenly dispersed form which would be less harmful to the mechanical properties. The "quenched" crystals could be shattered under light hammer blows, but with somewhat more difficulty than as-deposited crystals. Microscopic examination showed that these were still single crystals after the heat treatment.

Testing of the heat-treated crystals by compression at low deformation rates showed that the heat treatment had greatly improved their ductility. A crystal 0.085 in. in thickness was compressed at room temperature in nine successive pressings to a final thickness of 0.017 in. The total reduction was 80 per cent of the original thickness. The specimen was removed and examined between pressings. Slight edge cracking of the crystal was evident after the fifth compression, at which time the thickness had been reduced to 0.036 in. These cracks did not propagate in the subsequent compressions, and the center of the piece was still free of cracks as examined under 25× magnification after the last compression. The first five pressings were at a deformation rate of 0.002 in./min. This was increased to 0.010 in./min for the last four pressings.

Another crystal was compressed from 0.047 to 0.039 in. in thickness (36 per cent) at a deformation rate of 0.1 in./min without cracking. This deformation rate is double that which was found to be the maximum permissible without cracking for as-deposited iodide chromium. A third crystal was compressed from 0.083 to 0.019 in. at a rate of 0.020 in./min without cracking, while a fourth crystal was compressed from 0.066 to 0.016 in. at a rate of

[3] Mercury was used because its low vapor pressure enabled the furnace to be evacuated prior to introducing the argon atmosphere.

0.150 in./min. At the end of this test, only small edge cracks were visible on the crystal.

From these tests it appears that the heat-treated crystals can be strained considerably more and at considerably higher rates without cracking than can untreated crystals.

FIG. 2. Light micrograph of an octahedral (111) face of a chromium crystal. Growth lines are on the right and lower sections of the crystal. Several scratches appear on the left. 25×.

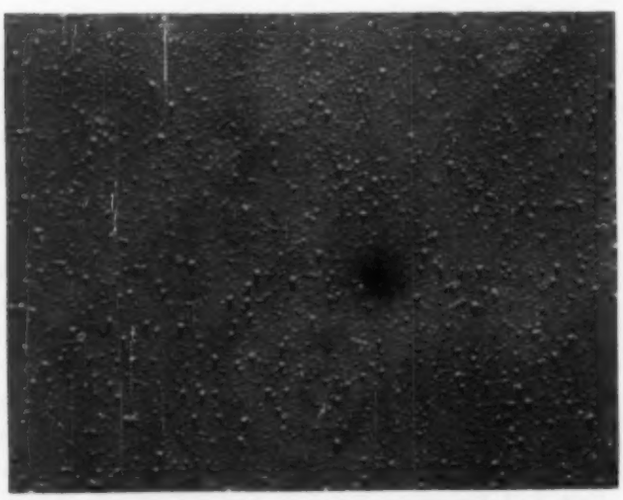

FIG. 3. Electron micrograph of the surface of a (111) face of a chromium crystal. Growth lines are shown faintly, as are the tiny bumps. Positive Formvar replica shadowed with platinum at arc tan 5. 15000×.

CRYSTALLOGRAPHIC STUDY OF HIGH-PURITY CHROMIUM

A detailed crystallographic study was made of the iodide chromium. The crystallographic study was convenient since the chromium was available in the form of single crystals. A density determination showed that the crystals were deposited at the theoretical density for chromium within the limits of accuracy of the determination.

The crystal habit, growth lines, and slip phenomena of the iodide chromium crystals were studied by microscopical and x-ray methods. The crystals were deposited as distorted octahedra. Cube faces are present on about one-half of the crystals. The octahedral faces (111) are rough and partly covered with

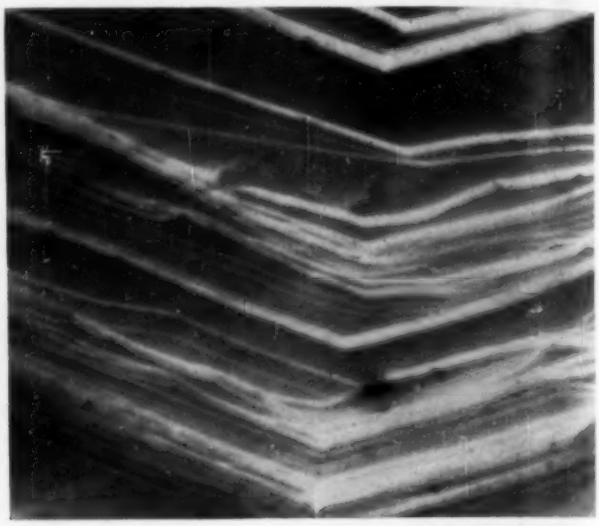

FIG. 4. Light micrograph showing the surface of a (111) face of a chromium crystal after compression. The shallow V's are growth lines. Slip lines are present, running diagonally upward from left to right. 800×.

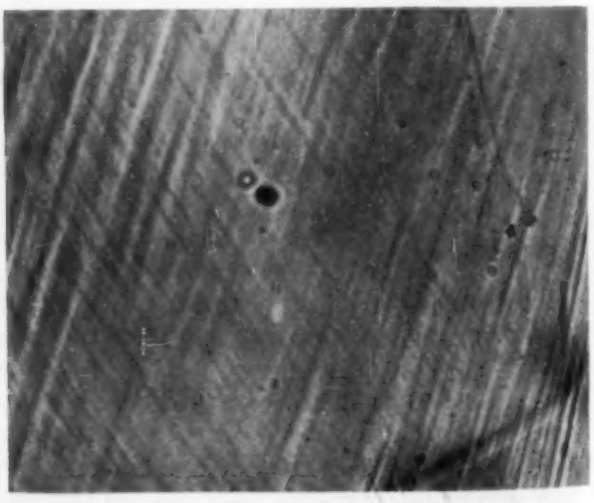

FIG. 5. Light micrograph showing two sets of slip lines on the (111) face of a chromium crystal. 800×.

growth lines or contours, the edges of which are nearly concentric about a point. These lines are shown in Fig. 2, 3, and 4. In the low-power light micrograph, Fig. 2, they appear to be edges of growth layers which nucleated at the point and have not completely spread across the face of the crystal. Fig. 3 shows an electron micrograph of a (111) face at a magnification of 15,000 times. Four faint growth lines appear. The surface is covered with small

nodules which may be oxide. The cube faces (100) are smooth and featureless under the light microscope, but in the electron microscope the small nodules are again visible.

A number of crystals having well developed faces were strained (at low deformation rates) to varying degrees, and the progress of slip was followed by observation of traces of slip planes in the crystal facets. Slip lines were observed on the octahedral faces of the deformed crystals. Fig. 4 shows slip lines

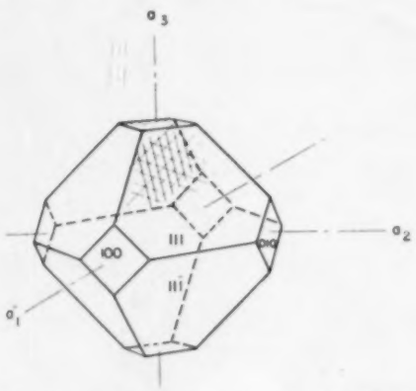

FIG. 6a. Clinographic projection of idealized chromium crystal. The fine lines on the (111) and (001) faces represent slip lines. Crystallographic axes are labeled a_1, a_2, and a_3.

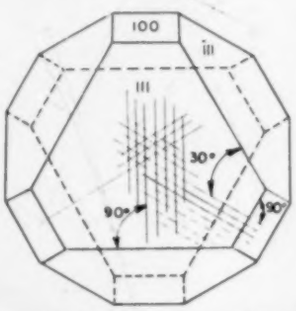

FIG. 6b. Orthographic projection of idealized chromium crystal showing octahedral face (111) in the plane of the drawing. The fine lines show the traces of the slip plane (110) on both the (111) and the (100) faces. The angle between sets of slip lines on the (111) face is 60°.

crossing growth contours while Fig. 5 shows two sets of intersecting slip lines. The crystallographic orientation of these lines was studied in the light microscope and the results are summarized in Fig. 6. The slip plane was identified as (110) from the trace orientations. The traces of two or more sets of these slip planes in the (111) face should form angles of 60°. In Fig. 5, however, the lines appear to form angles of about 50°. This is because secondary slip which occurred in a different direction has deformed the first set of slip lines. This deformation is on such a small scale that it is not visible in the light microscope. Electron micrographs of these intersecting slip lines show that the angle between them is truly 60° (see Fig. 8).

Fig. 7 and 8 show slip lines on the (111) face of a deformed chromium crystal. In Fig. 7, the slip lines cross growth contours. The distance between slip bands varies but in Fig. 7 it is about 1 to 2 microns. The growth lines show a gradual curvature which ends abruptly in a narrow line. Across this line the

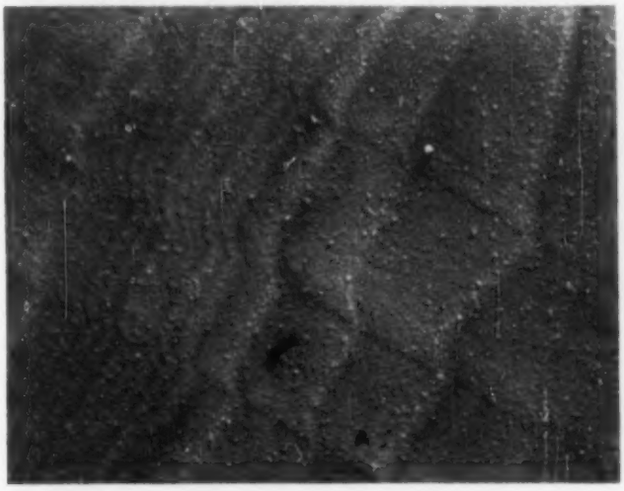

FIG. 7. Electron micrograph of a (111) face of a chromium crystal showing slip lines crossing growth lines. The slip lines run diagonally downward from left to right. Positive Formvar replica shadowed with platinum at arc tan 5. 15000×.

FIG. 8. Electron micrograph of a (111) face showing 2 sets of slip lines intersecting at 60 degrees. Growth lines are visible in the lower right. Positive Formvar replica shadowed with platinum at arc tan 5. 15000×.

growth lines resume their original direction. It is probable that the slip band where curvature is present consists of a large number of slip lines so fine as to be unresolved under these conditions. It seems likely that the slip started at the beginning of the curvature. Each succeeding plane slipped a little farther until finally the stress was relieved and the process stopped abruptly, thus ending the curve in a sharp

line. The width of the resulting slip band is about 0.6 micron.

Fig. 8 shows what is interpreted to be two sets of slip lines crossing each other. The angle between lines is 60°, but one set of lines is markedly stepped. It is evident that the average direction of the stepped trace differs from the true direction, confirming the conclusions drawn with respect to the angle of intersection shown in Fig. 5. Some growth lines appear in the lower right area of Fig. 8, but in the region of double slip they have practically lost their identity.

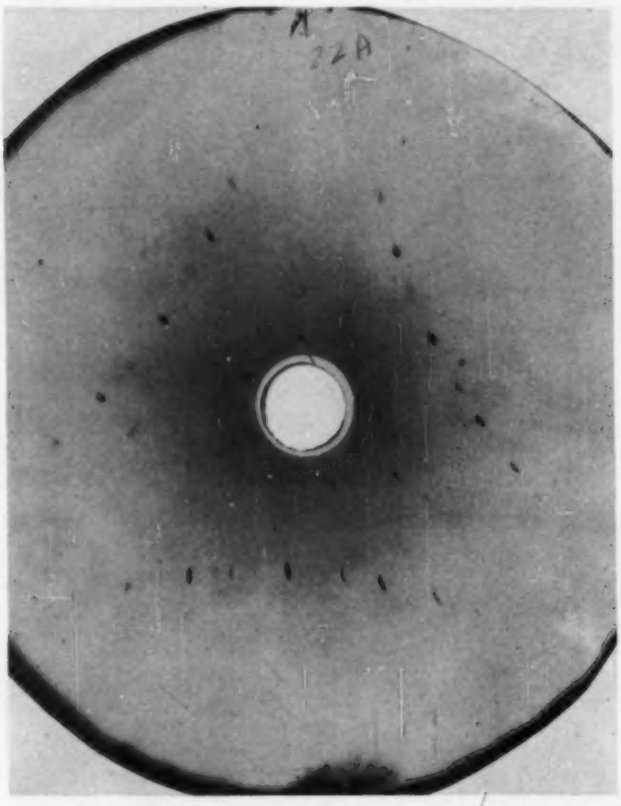

FIG. 9. Back-reflection Laue pattern of (111) face of chromium crystal compressed 7 per cent. Laue spots are elongated in a single direction.

X-ray diffraction methods provided additional information concerning the slip process. Deformed crystals of iodide chromium examined by back-reflection Laue techniques showed streaked Laue spots which indicated that lattice rotation had occurred during squeezing. An example of one such Laue photograph is Fig. 9, taken with the x-ray beam normal to an octahedral face of a crystal compressed 7 per cent. The elongation of the spots in a single direction may be explained by local curvature of the lattice (6, 7) at the slip plane. When crystals were compressed so as to develop several sets of slip planes, the spots appeared to be smoothly distorted in more complex manners such as shown in Fig. 10. Except for the systematic distortions of the spots, the Laue patterns were essentially those of single crystals. The slip direction has not been determined. However, it should be possible to do so by extending the investigation.

When electrolytic or iodide chromium is hammered, it does not pulverize but flattens into flakes with {100} planes parallel to the surface. The malleability in itself is an indication of ductility, and the preferred orientation indicates movement along crystallographic planes.

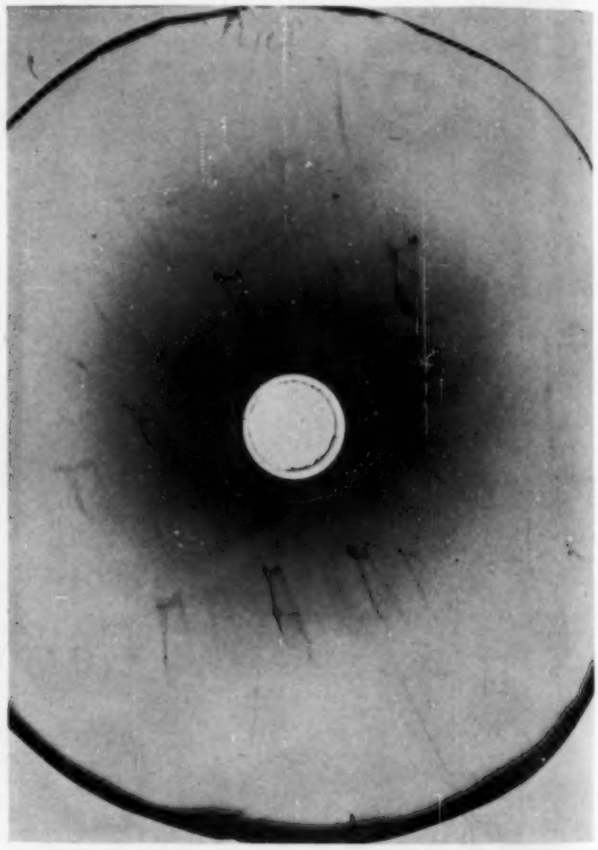

FIG. 10. Back-reflection Laue pattern of (100) face of chromium crystal compressed 30 per cent. Each Laue spot is distorted into a complex pattern presumably caused by slip along more than one set of slip planes.

An attempt was made to determine the effect of deliberate additions of oxygen and nitrogen on the ductility and slip in chromium. One crystal was heated in an atmosphere of each of these gases. Each crystal was strained and then examined microscopically and by x-rays for evidence of slip. After straining, slip was observed in the crystal treated with oxygen, but not in that treated with nitrogen. (This does not necessarily mean that slip did not occur, since the crystals are odd shaped and compression does not always take place in such a manner as to cause the particular face under ob-

servation to slip.) The oxygen-treated crystal appeared to have less ductility than an untreated crystal, but slip was observed on the same plane, indicating a change in degree, rather than a change in slip system. The nitrogen-treated crystal was shown by the Laue photograms to have split into two or more grains after compression.

It was determined that the cleavage plane of the crystals is predominantly the (100) plane.

Significance of Results

The work described in this paper gives strong evidence that chromium is inherently ductile. This has important implications for chromium-base alloys. Although the presence of a sigma phase may sometimes be responsible for brittleness in chromium-base alloys (8), it has been suggested (9) that this is not always the case. There is evidence that the brittleness of chromium-base alloys, in which the amount of sigma phase is small, is due to the brittleness of the chromium-rich solid-solution matrix and that, when the elements which embrittle unalloyed chromium are identified, the elimination of these same elements from chromium-base alloys will make the alloys ductile also.

The importance of this lies in the fact that certain chromium-base alloys have exhibited high temperature strengths superior to those of the best heat-resistant alloys commercially available. Test bars of an alloy[4] containing 58 per cent chromium, 25 per cent molybdenum, 15 per cent iron, and 2 per cent titanium had rupture times of up to 1764 hours at 1600°F and 40,000 psi and in excess of 100 hours at 1800°F and 25,000 psi. High temperature oxidation resistance was also adequate.

If oxygen and nitrogen are shown to be among the impurities which embrittle chromium, and this is quite likely, it may well be that originally ductile chromium-base alloy parts, working at elevated temperatures in atmospheres containing these gases, will gradually become embrittled after being placed in service. This is not necessarily too serious, since for many uses high ductility may not be required in service, with the only need for high ductility being during fabrication.

The desirability of producing ductile chromium-base alloys is emphasized by the scarcity of cobalt, the major constituent of the best present heat-resistant alloys and by the fact that the low melting point of cobalt (2723°F[5]) makes significant improvement in cobalt-base alloys unlikely.

Although it is desirable that the work reported here should be confirmed by further research, it is believed that this work provided some important clues in the problem of the ductility of chromium. The evidence suggests that chromium may be inherently ductile and strongly favors the "impurity" theory for the brittleness of chromium.

Summary

Efforts were made to produce chromium of the highest possible purity. The method chosen was that of the thermal decomposition of distilled chromous iodide on a hot wire filament. The chromium resulting from the iodide process was in the form of tiny individual crystals averaging about ⅛ in. in their largest dimension.

Qualitative estimates of the ductility of the crystals were made by testing them, as deposited, in compression at low deformation rates. By testing the crystals themselves, the danger of contamination during melting was eliminated. The test was also prompted by the small supply of material available. Several small spherical buttons, about ¼ in. in diameter, were arc melted from some of the crystals, in a water-cooled copper crucible using a tungsten electrode and an argon atmosphere. One of these was rolled into sheet at an initial rolling temperature of 980°C and a final temperature of 700°C.

It was found that the amount of deformation which the crystals could undergo in the simple compression test, before cracking, increased with increasing purity. Some of the higher purity crystals could be reduced in thickness by as much as 40 per cent at room temperature without cracking, if sufficiently low deformation rates were used. The crystals were quite sensitive to deformation rate. All could be cracked by light hammer blows. The deformation rate above which cracking was likely to occur was higher on the average for the higher purity chromium. Arc-melted buttons were also tested in compression and showed that the same general behavior was obtained with polycrystalline material as with single crystals. Quenching from 2950°F improved the ductility of single crystals.

When a tensile test was made on the single piece of sheet, it failed in a brittle manner even though the deformation rate was only 0.001 in./min. However, analysis showed it had become contaminated during rolling.

Since high ductility is possible only when slip occurs, the compressed crystals of iodide chromium were examined for various manifestations of slip. Slip bands were easily detected in the light microscope and their general shapes were observed at

[4] This alloy was made and tested at Battelle Memorial Institute under sponsorship of the Office of Naval Research. This general type of alloy was developed at Climax Molybdenum Company.

[5] The melting point of chromium is still in dispute because sufficiently pure chromium has not been available for accurate determination, but it is known to be above 3400°F.

higher power, using electron microscopy. The observation of slip traces in crystals with well-developed octahedral and cube facets made it simple to determine the slip plane. The traces were parallel to the edges on the cube faces and bisected the angles between the edges of the octahedral face. These facts shows the slip plane to be (110), as is the case in some other body-centered cubic metals, including molybdenum.

Evidence of ductility was also observed from x-ray diffraction patterns of compressed crystals taken by the Laue method. The Laue spots from a crystal compressed 7 per cent were elongated in a single direction, as a result of the local curvature of the lattice which occurs during slip. The spots from crystals deformed about 30 per cent were distorted in a more complex manner, but the patterns were essentially those of single crystals. A preliminary micrographic and x-ray study of crystals exposed to oxygen and nitrogen was also made to detect effects of these impurities on ductility.

Iodide crystal chromium, when hammered, tears at the lateral edges. Continued beating produces a thin foil having a (100) orientation.

Acknowledgment

Studies of the ductility of chromium have been made at Battelle under sponsorship of the U. S. Air Force's Project RAND. The work which is described in this paper was conducted at Battelle Memorial Institute under subcontract of Prime Contract AF 33(038)-6413, Project RAND.

Any discussion of this paper will appear in a Discussion Section, to be published in the December 1953 issue of the JOURNAL.

REFERENCES

1. W. J. KROLL, W. F. HERGERT, AND L. A. YERKES, *J. Electrochem. Soc.*, **97**, 258 (1950).
2. EARL S. GREINER, *Trans. Am. Inst. Mining Met Engrs.*, **188**, 891 (1950).
3. H. L. GILBERT, H. A. JOHANSON, AND R. G. NELSON, *J. Metals*, p. 63, January 1953.
4. J. W. MARDEN AND M. N. RICH, U. S. Pat. 1760367, 1930.
5. A. BRENNER, P. BURKHEAD, AND C. JENNINGS, *J. Research Nat. Bur. Standards*, **40**, 31 (1948).
6. C. S. BARRETT, "Structure of Metals," p. 359, McGraw-Hill Book Co., New York (1943).
7. R. W. TURNER, T. L. WU, AND K. SMOLUCHOWSKI, *Rev. Sci. Instr.*, **21**, 440 (1950).
8. J. W. PUTNAM, N. J. GRANT, AND D. S. BLOOM, "Sigma Phase in Chromium Molybdenum Alloys With Iron or Nickel," American Society for Testing Materials Special Technical Publication No. 110, entitled "Symposium on the Nature, Occurrence, and Effects of Sigma Phase" (1950).
9. W. L. HAVEKOTTE, C. T. GREENIDGE, AND H. C. CROSS, *Am. Soc. Testing Materials Proc.*, **50**, 1101 (1950).

Effect of Germanium on the Transformation of White to Gray Tin, at Comparatively Low Temperature[1,2]

R. R. Rogers and J. F. Fydell

Mines Branch, Department of Mines and Technical Surveys, Ottawa, Canada

ABSTRACT

At a comparatively low temperature, gray tin may appear on white tin when the latter (*a*) is in contact with elementary germanium, (*b*) contains a certain proportion of germanium in the form of an alloy, or (*c*) is in contact with solutions in which certain germanium compounds have been dissolved. Data also are presented regarding the rate of spread of gray tin on white tin castings and coatings containing various proportions of germanium.

Introduction

Ordinary tin, which is ductile and useful for many important purposes, is stable above 13.2°C (55.8°F). On the other hand, gray tin, which is quite brittle and useless for most purposes, is stable below that temperature. Fortunately the transformation to gray tin frequently occurs very slowly, although at times it does take place with considerable rapidity. Even after the gray tin has been reconverted into the white variety by increase in temperature the material usually is of little value until it has been remelted.

The term "tin disease" has been used in the literature when referring to this phenomenon, probably due to the wart-like appearance of the gray tin, and to the fact that a sample of gray tin may "inoculate" samples of white tin which are in contact with it. Sometimes the first indication of the transformation appears spontaneously, i.e., without inoculation.

A summary of the previously published information on gray tin has been compiled (1). From this it would appear that much remains to be learned regarding the subject. For this reason a research program was initiated at the Mines Branch of the Department of Mines and Technical Surveys to investigate the various factors which have an influence on the transformation to gray tin. During this research it became evident that germanium, when present, may have a considerable effect on the transformation. The results of the experiments which were performed in this connection are given in the present paper.

Although the authors have not investigated this phase of the problem extensively, it is of interest to note that germanium has been found in certain tin minerals. Papish (2) reported the presence of this element in five of the twelve tin minerals which he investigated, the proportion varying between 0.001 and more than 0.005 per cent. The sources of these germanium-containing minerals were: Yukon, Nevada, Mexico, Bolivia, and New South Wales.

The tin used in all of the present experiments was obtained in the form of cast bars, and the following analysis was supplied by the manufacturer: antimony, 0.0005%; lead, 0.0005%; copper, 0.0002%; bismuth, 0.0002%; iron, 0.0002%; arsenic, trace; silver, trace.

The sulfur content was found to be 0.006 per cent in these laboratories. This tin will be referred to as "pure tin" in this paper.

The germanium used was a pure grade obtained from the Eagle-Picher Company of Cincinnati, Ohio.

Experimental

Cast Tin and Tin Alloys

It is known that different types of tin have different degrees of susceptibility to gray tin formation. Early in the investigation it was found that the pure tin used in these experiments had quite a high susceptibility. A cast bar 37 cm (15 in.) long x 0.8 cm (0.3 in.) in diameter (Fig. 1) was converted completely into gray tin (Fig. 2) in 13 days when inoculated with gray tin and exposed to a temperature of −30°C. The gray tin appeared approximately one day after inoculation.

Later experiments showed that similar results could be obtained if elementary germanium was used as the inoculating agent instead of gray tin. While in contact, the tin and germanium were immersed in an aqueous solution containing calcium chloride (450 g/l) acidified with hydrochloric acid to *p*H 1.5. The gray tin appeared approximately two days after inoculation.

Gray tin was produced on similar bars of pure tin

[1] Manuscript received January 29, 1952. This paper was prepared for delivery before the Philadelphia Meeting, May 4 to 8, 1952.

[2] Published by permission of the Director-General of Scientific Services, Department of Mines and Technical Surveys, Ottawa, Canada.

when they were immersed for four months in calcium chloride solution (450 g/l) in which germanium dioxide (0.15 g/l) had been dissolved. The temperature was maintained at −30°C throughout the experiment. No such result was obtained in the absence of germanium dioxide.

In some of these experiments the germanium dioxide was replaced by a soluble salt of one of the following metals: bismuth, antimony, silver, copper (ic), lead, iron (ous), lithium, zinc. Although some of the more noble of these metals were deposited on the

FIG. 1. A 5-in. cast bar of commercially pure tin prior to inoculation with gray tin.

FIG. 2. The cast bar of commercially pure tin shown in Fig. 1 after inoculation with gray tin and 13 days at −30°C.

tin bars by electrolytic replacement, no evidence of gray tin formation was observed.

A number of small pure tin castings of the same size and shape, containing various proportions of germanium and zinc, were produced and then exposed to temperatures of +4°, −29°, −40°, and −51°C (40°, −20°, −40°, and −60°F) without inoculation. The length of time which elapsed before gray tin appeared spontaneously on each casting is given in Table I.

The rate of spread (m) of the gray tin on these castings is given in Table II. (Note: In this research it has been found that the relation $A^{1/2} = mt + b$ exists where A is the area in square millimeters which has been infected with gray tin in t days, and b is a constant for any particular area. Although the dilatometer method of measuring rate of spread has been used considerably in the past, it is not applicable in the case of comparatively thin coatings. In the present work the same method of measuring rate of spread was used for both coatings and castings, in order to permit comparisons to be made.)

TABLE I. *Spontaneous formation of gray tin on castings*

Composition (wt, %)			Time to spontaneous appearance of gray tin (days)			
Sn	Ge	Zn	+4°C	−29°C	−40°C	−51°C
100	—	—	>220*	31	>56*	1.9
98	2	—	>220*	4	0.9	0.9
86	14	—	>220*	0.9	0.9	0.9
98	—	2	>220*	41	7	5.9
96	2	2	>220*	14	14	4.0

* No gray tin had formed on samples within period stated and experiment was discontinued.

TABLE II. *m values for gray tin on castings*

Composition (wt, %)			m		
Sn	Ge	Zn	−29°C	−40°C	−51°C
100	—	—	1.41	—	4.9
98	2	—	0.9	3.7	0.85
86	14	—	0.38	4.6	3.3
98	—	2	0.07	0.43	0.07
96	2	2	0.03	0.03	0.12

TABLE III. *Spontaneous formation of gray tin on coatings*

Germanium content (wt, %)	Time to spontaneous appearance (days)		
	−29°C	−40°C	−51°C
0.00	>370*	>37*	0.8
0.01	>370*	12	>4.9*
0.03	88	18	>4.9*
0.12	32	2.7	1.7
0.17	17	1.7	0.8
0.45	17	0.9	1.7
1.10	17	0.7	1.7

* No gray tin had formed on sample within period stated and experiment was discontinued.

Hot Dip Tin Coatings

Sheet steel coupons were electroplated on both sides with about 0.005 cm (0.002 in.) of iron, following a procedure previously used (3). After rinsing in water and then in a slightly acidified aqueous solution of the flux, they were dipped into a molten bath of pure tin which was covered with molten flux ($ZnCl_2$ 75%, NaCl 11%, KCl 14%) and was oper-

ated at a temperature of 306 ± 2°C (583°F). Various small amounts of germanium were added to the molten bath and a number of the plated steel coupons were dipped in the bath after each addition. The germanium content of the resulting coatings was determined spectrographically.

Coupons with tin coatings having different germanium contents were exposed to temperatures of −29°, −40°, and −51°C. Those in which spontaneous transformation to gray tin occurred, and the length of time required in each case, are given in Table III. In every case except one, this transformation took place in the comparatively thick coating at the bottom of the coupon.

A similar set of coupons was inoculated with gray tin and exposed to the same temperatures. The rate of spread of the gray tin on each coupon was determined. The values of m are given in Table IV.

TABLE IV. *m values for gray tin on coatings*

Germanium content (wt, %)	m		
	−29°C	−40°C	−51°C
0.00	0.06	0.32	0.70
0.01	0.07	0.11	0.87
0.03	0.07	0.11	0.34
0.12	0.08	0.05	0.86
0.17	0.04	0.11	3.00
0.45	0.04	0.34	2.30
1.10	0.03	0.11	0.05
Average	0.06	0.16	1.16

Discussion

It was shown that white tin of the type used in these experiments could be transformed into gray tin when the former was brought into contact with a particle of gray tin at a suitable temperature. This phenomenon has been known for a considerable number of years.

It was also shown that the white tin could be transformed into gray tin when the former was brought into contact with a particle of elementary germanium in the presence of acidified calcium chloride solution at a suitable temperature. No transformation took place when the white tin was in contact with the acidified chloride solution only. A concentrated solution of calcium chloride was used because such a solution does not freeze at −30°C. No doubt a solution of any other electrolyte which would remain liquid at this temperature would give similar results. Apparently the function of the acid in the solution was to keep the surfaces of the germanium and tin free from oxides or other compounds. Films of such compounds would have prevented a direct contact between germanium and tin.

The transformation took place in the presence of an aqueous solution in which germanium dioxide had been dissolved. It is assumed that elementary germanium was slowly deposited on the white tin by electrolytic replacement and this caused the transformation to gray tin by inoculation. No doubt solutions containing a number of other germanium compounds would have given the same result.

It also was shown that the transformation to gray tin did not take place when solutions of a wide variety of metal salts were in contact with the white tin. This was true even when a metal, such as silver or copper, was deposited on the tin by electrolytic replacement.

At a suitable temperature, gray tin appeared spontaneously on tin castings containing certain proportions of germanium. It would appear from the constitutional diagram (4) that elementary germanium separates out when alloys of tin and germanium are cooled below 232°C. It is assumed that this particular germanium acted similarly to that used in producing gray tin by inoculation. The time which elapsed before the spontaneous appearance took place was decreased as the germanium content was increased. When zinc was present in the alloy the time which elapsed was increased. This may be caused by the fact that the gray tin was produced in a tin-zinc combination rather than in tin alone. Zinc was used in some of these experiments because it tends to increase the rate of spread of gray tin, when it is present in certain proportions.

It was shown that the rate of spread (m) of gray tin was greatest on the casting of pure tin and decreased as the germanium content was increased. There was a great decrease in rate in the case of the castings containing zinc. This probably was attributable to the fact that the gray tin was being produced in a tin-zinc combination rather than in pure tin. It is interesting to note that, in the case of the tin-germanium combinations, those which had the greatest tendency to produce gray tin spontaneously were the ones which had the lowest rate of spread.

The steel sheet coupons were electroplated with iron so that the tin coating could not come into contact with the nonferrous constituents present in the steel. These might possibly have had some effect on the results of the experiments.

It will be observed that in general the time to spontaneous appearance tended to decrease as the germanium content was increased and as the transformation temperature was lowered.

It is important to note that the values of m and of time elapsed before spontaneous appearance probably would have been somewhat different if tin of a

different composition had been used in producing the various castings and coatings.

It has been known for a considerable length of time that gray tin, when placed in contact with white tin under suitable conditions, causes the formation of gray tin on the latter. However, it is rather unexpected that a different element, such as germanium, behaves as an inoculant in a similar manner. In this connection it is interesting to note that germanium and tin are quite close together in the same group (IV) of the Periodic Table, and that the properties of germanium are somewhat similar to those of gray tin. For instance, they both crystallize in the cubic system, whereas white tin crystallizes in the tetragonal system.

In passing it may be noted that Goryunova recently reported that she had been unable to produce gray tin by inoculation with germanium (5).

Conclusions

Perhaps the most important conclusion to be drawn is the fact that white tin may be transformed into gray tin, at a suitable temperature, when the former (*a*) is in contact with elementary germanium; (*b*) is in contact with aqueous solutions in which certain germanium compounds have been dissolved; and (*c*) contains a certain proportion of germanium in the form of an alloy. Further, the rate of spread of gray tin in tin castings and coatings depends to a considerable extent upon the amount of germanium present and the transformation temperature.

Any discussion of this paper will appear in a Discussion Section, to be published in the December 1953 issue of the Journal.

References

1. R. R. Rogers and W. R. G. Stewart, Investigation No. MD2609, Mines Branch, Dept. of Mines and Technical Surveys, Ottawa, Canada, Nov. 23, 1949.
2. J. Papish, F. M. Brewer, and D. A. Holt, *J. Am. Chem. Soc.*, **49**, 3028 (1927).
3. R. R. Rogers, *Ind. Eng. Chem.*, **27**, 785 (1935).
4. "Equilibrium Data for Tin Alloys," p. 30, Tin Research Institute, Greenford, England (1949).
5. N. A. Goryunova, *Proc. Acad. Sci., U. S. S. R.*, **75**, 51 (1950).

The Caustic Electrolytic-Zinc Process[1]

CHARLES T. BAROCH, R. V. HILLIARD, AND R. S. LANG

Bureau of Mines, U. S. Department of the Interior, Boulder City, Nevada

ABSTRACT

Zinc is extracted from oxidized ores with NaOH solution, and the zincate electrolyte is purified with zinc powder and lime. The zinc is recovered electrolytically as "flake" powder consisting of pinnate crystals. At 12.9 amp/dm² (120 amp/ft²) about 1.5 kw hr/lb of zinc is required. Many types of oxidized ores have been tested in the laboratory and some pilot-plant work has been done; the process appears to be feasible.

INTRODUCTION

The caustic-leach electrolytic-zinc process offers a possible method of treating many oxidized zinc-lead ores that cannot be beneficiated by ore dressing or flotation. Many such deposits, especially in the west, are too far from cheap fuel for consideration of any of the fuming methods, and generally they consume too much acid or chlorine for any acidic or cloridizing process. Furthermore, leaching siliceous ores with acid forms gelatinous silica which prevents separation of solutions from the residue.

The solubility of zinc and lead oxides in sodium hydroxide was an early chemical discovery, and a caustic process for recovering zinc and lead was suggested at the turn of the century (1). A decade later Johnson (2) again mentioned the possibilities of a caustic zinc process and stressed the facts that ferric oxide was insoluble in caustic solutions and that the silica problem is less troublesome. Little can be found in the literature since then to indicate that caustic processes have been considered seriously. Today, the use of caustic soda is much more practical than formerly, because a plentiful supply is available at the many modern caustic-chlorine plants located in all sections of the country.

OUTLINE OF THE PROCESS

A generalized flowsheet of the caustic electrolytic-zinc process is shown in Fig. 1. The process follows the usual pattern used in electrowinning by hydrometallurgy, namely, leaching, purification, and electrolysis. Oxidized ore or roasted concentrate is leached in depleted solution returned from electrolysis and, after separating from leach residue, the solution is purified by treatment with zinc dust to remove the metals electropositive to zinc, chiefly lead and copper. The zincate electrolyte is electrolyzed in a simple type of nondiaphragm cell, and the zinc is recovered in a powder which is called "flake" zinc to distinguish it from the usual blown powdered metal.

[1] Manuscript received August 18, 1952. This paper prepared for delivery before the Montreal Meeting, October 26 to 30, 1952.

Leaching

Solubility of zinc in caustic solutions.—Most oxidized minerals and compounds of zinc will dissolve in caustic solutions, presumably forming therein a compound called zincate. The zincate can be crystallized only from relatively strong caustic solutions—in the case of caustic soda, those containing about 440 g/l NaOH or more. Zincates can be retained in solution only when a great excess of alkali is present, otherwise they will hydrolyze to form zinc oxide or hydroxide which precipitates in the solution. Therefore, the reaction between caustic and zinc compounds is not as positive as that between acids and the same zinc compounds. For instance, a certain amount of acid will react stoichiometrically with a definite amount of zinc oxide, but this is not true with caustic soda solution, as several times the stoichiometric amount of caustic soda is necessary to dissolve a certain amount of zinc oxide and retain it in solution.

Goudriaan (3, 4) determined the solubilities of specially prepared ZnO and $Zn(OH)_2$ in caustic soda solutions, and summaries of his data have been reproduced in the International Critical Tables (5), Seidell (6), and Mellor (7). His data are expressed in percentages Na_2O, ZnO, and H_2O, and they cannot be converted into the volumetric units because densities of the solutions were not given. Similar solubility determinations have been reported by Muller (8) and by Scholder and Hendrich (9), which are stated in normalities or moles per liter.

Zinc hydroxide and oxide are artificial compounds not found in ores, although solubilities of the oxide would be of considerable value if the leaching of roasted sulfide or carbonate ores is to be attempted. The most common oxidized zinc ores are composed of carbonates and silicate minerals. The principal carbonate minerals are smithsonite, having the chemical formula $ZnCO_3$, and the basic carbonate known as zinc bloom or hydrozincite with the formula

$ZnCO_3 \cdot 2Zn(OH)_2$. The silicates vary from an anhydrous silicate called willemite, $2ZnO \cdot SiO_2$, to the hydrated zinc silicate known in this country as calamine or hemimorphite, $2ZnO \cdot SiO_2 \cdot H_2O$.

In the dissolution of zinc carbonate minerals by caustic solutions, sodium zincate is formed, and a corresponding amount of caustic soda is converted to sodium carbonate:

$$ZnCO_3 + 4NaOH = Na_2ZnO_2 + Na_2CO_3 + 2H_2O. \quad (I)$$

Saturation, therefore, is approached by a simultaneous reduction in caustic concentration. When

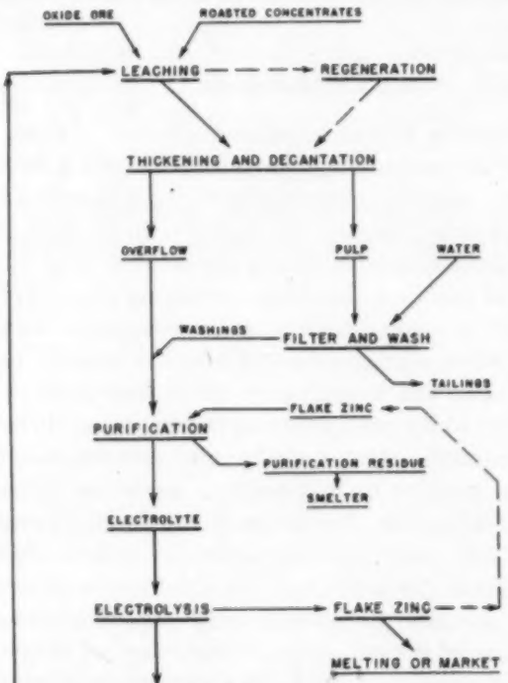

FIG. 1. Flowsheet of the caustic electrolytic-zinc process.

saturation is reached, any excess of zinc carbonate present continues to react with the caustic soda:

$$ZnCO_3 + 2NaOH = Na_2CO_3 + Zn(OH)_2. \quad (II)$$

Under these conditions, the lowering of the caustic concentration causes hydrolysis of dissolved sodium zincate, resulting in the lowering of the zinc content of the solution. To all outward aspects the following reaction appears to take place:

$$ZnCO_3 + Na_2ZnO_2 + 2H_2O = Na_2CO_3 + 2Zn(OH)_2. \quad (III)$$

If sufficient zinc carbonate is present, reactions (II) and (III) will continue until all the NaOH is converted to Na_2CO_3 and all the zinc is precipitated from the solution.

Zinc silicate dissolved in caustic soda solutions forms sodium zincate and sodium silicate, both of which are retained in solution. An excess of ore causes no change in the solubilities, and when a solution is saturated with zinc, it will no longer attack zinc silicate mineral.

Fig. 2 summarizes data on the solubilities of different zinc compounds in solutions of varying caustic concentrations. The upper curve represents the solubilities of specially prepared $Zn(OH)_2$ as reported by Muller (8) and Scholder and Hendrich (9), and the lowest curve represents the solubilities of ZnO as determined by Muller, supplemented by data of one of the authors. The two intermediate curves are the maximum solubilities obtained by adding nearly pure hydrozincite and hemimorphite in increments to caustic solutions and plotting the residual caustic concentrations.

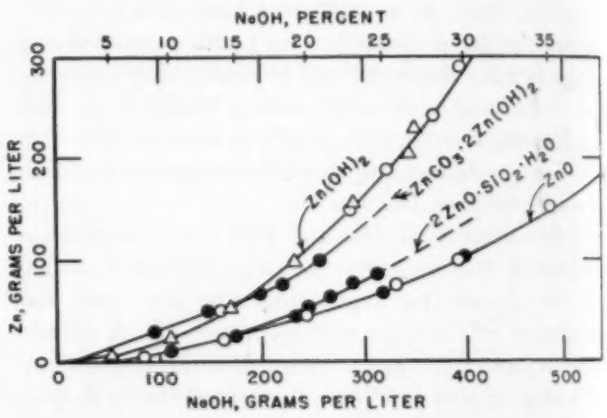

FIG. 2. Solubilities of zinc compounds in caustic soda solutions. (△ Scholder and Hendrich; ○ Muller; ● Author's data).

Hydrozincite formed solutions of stronger zinc content than $Zn(OH)_2$ up to about 190 g/l NaOH, but in stronger caustic it was slightly less soluble. The solubility of hemimorphite closely followed that of ZnO up to about 170 g/l NaOH, but above that the zinc silicate ore produced slightly stronger zinc solutions. The amount of dissolved SiO_2 followed the quantity of zinc stoichiometrically, a condition that was not changed by an excess of ore.

The data show that different minerals yield widely varying zinc concentrations for a given NaOH concentration, and that a much stronger zinc electrolyte can be made from ores containing carbonate zinc minerals than from hemimorphite ores. Furthermore, it was found that leach solutions saturated with respect to either zinc oxide or hemimorphite would still dissolve zinc from hydrozincite. This means that ores containing both hydrozincite and hemimorphite, which are quite common, can be saturated close to the hydrozincite line by using at least 2 stages of countercurrent leaching.

Other factors affecting leaching.—To show the range of leaching conditions necessary for different ores, comparative tests were made on 22 samples gathered from mines in many districts which varied widely in tenor and mineralogical composition. NaOH concentration and leach temperature had the greatest influence of all factors on the dissolution of zinc from these ores. The fineness of grind, up to as coarse as 8-mesh, had relatively insignificant effect, and the duration of leach beyond the first 4 hours increased the extractions only slightly. The degree of agitation was important, and good extractions were obtained only when a positive, active agitation of the leach pulp was used.

As might be expected from experiences with the solubilities of different zinc compounds, a wide variation in the leachabilities could be attributed to mineralogical composition. Some variation was found in ores composed of the same minerals but, broadly speaking, leachability of different ores varied with the 4 most common mineralogical types.

1. Hydrozincite was the easiest to leach, and it dissolved rapidly in any strength of caustic, even at room temperature.

2. Smithsonite dissolved completely in cold 15 per cent NaOH, but at temperatures above 60°C it would dissolve in caustic as weak as 5 per cent NaOH.

3. Hemimorphite, hydrated zinc silicate, responded only to the stronger solutions, and the necessity for heating was marked. Leached for 4 hours at 90°C, 9 different ores yielded 78.8 to 93.2 per cent of their zinc in 15 per cent NaOH, and the extraction rose to above 90 per cent for all the ores when leached similarly in 20 per cent NaOH. Room temperature and 60°C leaches of these ores in 20 per cent NaOH resulted in only 36.9 to 62.8 per cent extraction.

4. Willemite required at least 30 per cent NaOH solution, boiling temperature, and very violent agitation for good extractions. Abrasion seems to be very helpful in leaching all zinc silicate ores.

Removal of zinc minerals by leaching results in an appreciable decrease in the amount of solids remaining as leach residue. The weight loss is a direct function of the zinc content and will be nearly twice the zinc analysis in per cent. For instance, ore containing 17.1, 30.6, and 44.6 per cent Zn lost 32.9, 57.5, and 82.7 per cent, respectively, of their original weight during leaching. Leaching also disintegrates the ore; consequently, it is desirable to start with ore ground as coarsely as possible to prevent the formation of excessive amounts of slime residue. Leach residues are often porous, friable, and soft, so that rough treatment, such as excessively rapid agitation and pumping through high-velocity centrifugal pumps, tends to disintegrate the residue into slimes. In none of the ores tested, however, were these slimes of the dispersed colloidal type that refused to settle. Standard settling tests (10) on leach residues from the 22 test ores gave ultimate pulp densities, after 16 to 19 hours of settling, that ranged from 17.3 to 44.8 per cent leach residue in pregnant solutions consisting of 20 per cent NaOH. In all cases the supernatant solutions were clear. The lower pulp densities were always associated with the higher grade ores and the corresponding amounts of pulp were small.

Recausticization

Two of the most common caustic-soluble impurities found in ores are carbonate and silica, and both can be removed with lime.

Carbonates of zinc, lead, copper, iron, and most metals are completely decomposed by caustic solutions of any strength. Dolomite and dolomitic limestones from different localities show differing degrees of reactivity, probably because a protective coating of impervious magnesium hydroxide forms over the surfaces of particles. The solubility of carbonate from calcium carbonate, either as limestone, aragonite, or calcite, is dependent on an equilibrium condition which varies with the concentration of NaOH and Na_2CO_3 in the solvent. This equilibrium can be expressed by the following reversible reaction:

$$Na_2CO_3 + Ca(OH)_2 \rightleftharpoons 2NaOH + CaCO_3. \quad (IV)$$

Causticization of soda ash with lime has long been used for manufacturing caustic soda (11). Goodwin (12) and Olsen and Direnga (13) have discussed the equilibrium in the causticizing process, which is affected very slightly by temperature because the heat change of the reaction is low. However, heat influences the speed of the reaction, and equilibrium is established completely in 2 hours at 94° to 98°C.

Caustic makers seldom use a solution containing more than about 12½ per cent Na_2CO_3 (equivalent to 9.4 per cent NaOH), and the cited data do not consider the equilibrium for the higher strengths needed for caustic leaching of zinc. Consequently, additional work had to be done on stronger solutions. The technique adopted was very similar to that of Olsen and Direnga (13). The tests were made in resistance glass, calcium carbonate in excess was added to a caustic solution, and the mixture was boiled under reflux for 3 hours. After settling, a portion of the clear liquid was decanted into a test tube and allowed to cool to 20°C so that accurate volumetric samples could be taken, which were analyzed for NaOH and Na_2CO_3. As checks, a number of tests were made by the reverse reaction, using solutions of Na_2CO_3 treated with hydrated lime.

The experimental results are plotted in Fig. 3 for

solutions containing from 90 to 240 g/l NaOH. A caustic solution containing 90 g/l NaOH and in equilibrium with $CaCO_3$ and $Ca(OH)_2$ will contain only about 5 g/l Na_2CO_3, and the proportion of Na_2CO_3 rises as the NaOH content is increased. The rise is especially rapid for NaOH concentrations above 180 g/l. At about 195 g/l NaOH the equilibrium curve reaches the limit of saturation of Na_2CO_3, designated by the point X. Theoretically, all solution of greater NaOH concentration than that shown by point X should, given sufficient $CaCO_3$ and time for reaching equilibrium, end up at point X with the excess Na_2CO_3 crystallized out.

Actually, point X is very difficult to locate exactly, as one is confronted with the phenomena of solutions

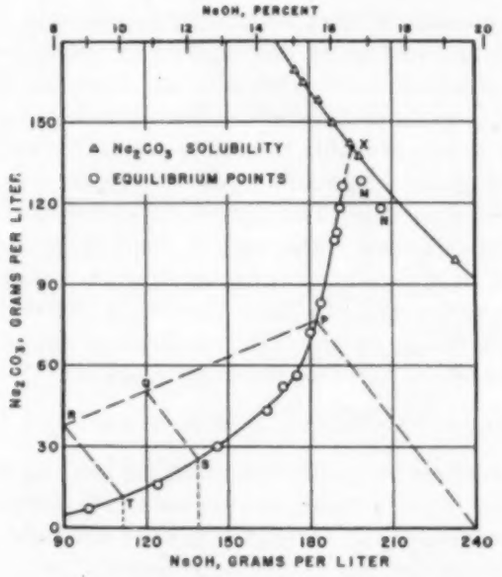

FIG. 3. Equilibrium curve of the reversible reaction: $Na_2CO_3 + Ca(OH)_2 \rightleftharpoons 2NaOH + CaCO_3$.

supersaturated with Na_2CO_3, further complicated by the formation of the double salts of sodium and calcium carbonate known as pirsonnite, $Na_2CO_3 \cdot CaCO_3 \cdot H_2O$, and gaylussite, $Na_2CO_3 \cdot CaCO_3 \cdot 5H_2O$ (14, 15). These double salts form slowly in strong soda solutions and are most in evidence in solutions containing over about 180 g/l NaOH. Formation of these salts is presumed to have caused the dislocation of points M and N below the solubility curve of Na_2CO_3 in NaOH. As further evidence of this, sample N was retained and shaken intermittently; the Na_2CO_3 content dropped slowly and the solution at the end of 30 days contained 201 g/l NaOH but only 45 g/l Na_2CO_3. Over half the Na_2CO_3 had precipitated as a double salt with $CaCO_3$. These double salts of Na_2CO_3 and $CaCO_3$ tend to form whenever calcareous ores are leached with strong caustic solutions, and the resulting compound precipitates with the leach residue. This does not represent a loss of soda salt, because the double salt dissociates readily on dilution and washing.

To visualize how this equilibrium curve can be used for calculating recausticization, assume that a solution contains 240 g/l NaOH, initially. In leaching ore, the solution picks up carbonate from leached minerals and limestone, and its composition with respect to soda salts follows the line to point P (Fig. 3), providing the volume remains constant. The slope of this line will be 1.325 to 1, because a unit weight of NaOH is converted into 1.325 unit weights of Na_2CO_3. At point P, the solution contains about 182 g/l NaOH and 77 g/l Na_2CO_3, and up to this point reaction (IV) has proceeded from right to left. At point P, the solution will no longer react with $CaCO_3$, but it can still react with metal carbonates. However, so long as any $Ca(OH)_2$ is present, the solution will remain at the concentrations represented by point P.

Recausticization of any part of the Na_2CO_3 content represented by point P can be obtained only by dilution. Dilution will follow a line drawn from P to the zero point of the graph, represented by the line through Q and R. Point Q represents about 50 per cent dilution where the concentration should be about 122 g/l NaOH and 52 g/l Na_2CO_3. But, at this point equation (IV) will reverse, and the solution composition will follow line QS to the equilibrium curve. At S, the solution will contain about 140 g/l NaOH and 27 g/l Na_2CO_3, and approximately one-half of the sodium carbonate originally contained at point P would be recausticized.

Similarly, if the original solution is diluted 100 per cent, the new concentration would be that of point R, and lime treatment to equilibrium would result in a composition represented by point T, where the concentrations are about 111 and 11 g/l, respectively, for NaOH and Na_2CO_3. In this case, about 72 per cent of the original Na_2CO_3 would be recausticized.

The presence of zinc or lead in the solution permits recausticization to occur at higher caustic concentrations. These metal-caustic compounds seem to "neutralize" a portion of caustic and, in effect, displace the equilibrium curve as plotted in Fig. 3 downward and toward the right. For example, a caustic solution initially containing 272 g/l NaOH only, will come to equilibrium with $CaCO_3$ at 190 and 109 g/l, respectively, of NaOH and Na_2CO_3; with 40 g/l Zn present in the same strength solution, the equilibrium point becomes 213 and 78 g/l NaOH and Na_2CO_3, respectively. This means that it is possible to leach and recausticize at the same time, by adding the necessary lime directly to the leach.

Some ores contain such large amounts of caustic-

soluble carbonate that roasting to remove most of the carbonate seems to be most practical. Such a scheme has been suggested for concentrates produced from ore of the Horn Silver mine at Milford, Utah. Zinc and iron carbonates are closely associated in this ore, and the owners state that coarse-mesh concentration of their low grade ore is possible by simple heavy media separation. Typical concentrate submitted contained 25.3 per cent Zn, 18.3 per cent Fe, 4.6 per cent CaO plus MgO, and 21.2 per cent CO_2. Roasted for 2 hours from 400° to 500°C, the concentrates lost about 20 per cent of their weight, and the resulting calcine contained 31.5 per cent Zn and only 3.7 per cent CO_2. Recovery of over 90 per cent of the zinc was obtained with solutions containing 200 g/l NaOH and 58 g/l Na_2CO_3 in 3-stage, 2-hour leaches at temperatures as low as 40°C; carbonate pickup was practically nil.

TABLE I. *Range in analyses of typical purified electrolytes*

Constituent	Range
	g/l
Zn	38 to 52
Pb	0.002 to 0.0003
Cu	0.0002
Fe	0.0006
SiO_2	0.38 to 1.96
Na_2CO_3	42 to 60
NaOH	179 to 209

Silica is also removed by treatment with lime, forming calcium silicate, probably in some hydrated form. Like the reaction with carbonate, lime will not remove silica completely, but an equilibrium is established which depends on the strength of caustic. With an excess of lime present, silica will be removed to about 1 g/l in 200 g/l NaOH solution and to about 3 g/l in 300 g/l NaOH solution. Residual silica in these amounts is not harmful. The silica is precipitated stoichiometrically by the lime, and the reaction proceeds best at temperatures above 60°C. Precipitates made below this temperature are gelatinous and give settling and filtering troubles.

Purification

The pregnant solution, after separation from the leach residue, is purified by treatment with zinc dust to precipitate lead, copper, and any other metallic impurities electropositive to zinc. The electrodeposited flake zinc made by this process is better for purification than the regular blown dust, because the flake product consists of fern-leaf clusters of very small single crystals which present a large specific surface area compared to the spherules of blown dust. Only a slight excess over the stoichiometric quantity is required, and adding the dust in increments seems to be most effective. Virtually complete removal of lead and copper can be determined by a simple test. Adding a few drops of a soluble sulfide in solution to a test sample of purification liquor gives a dark precipitate even when traces of lead or copper are present, and a pure white precipitate when only zinc remains.

Purification residue is a sponge metal that settles readily, and it shows a tendency to coagulate slimes that might be present in the solution. Rapid agitation is an aid to quick purification, but aeration is not desirable, as any air coming in contact with sponge residue quickly oxidizes and causes re-solution of lead and copper. Filtering continuously through a filter press without allowing the cake to run dry until the end of a run offers an excellent method of separating purification residue and giving the solution a final clarification at the same time.

TABLE II. *Analysis of a typical purification residue*

Constituent	Analysis
	per cent
Pb	52.1
Zn	13.8
Cu	4.0
Fe	0.8
SiO_2	3.5
Na_2O	0.54

Batch purification, as in the acid process, seems to offer the best possibilities of perfect control of electrolyte purity. Batches as large as 1200 gal were purified at 35° to 50°C in as little as 1½ hours, using mechanical agitation. The range in analyses of typical purified electrolytes made in leaching tests on Goodsprings (Nevada) hydrozincite ore is shown in Table I.

The sponge metal produced was well oxidized by the time residues were washed, dried, and sampled. An analysis of a typical residue is given in Table II.

Electrolysis

The electrolysis of sodium zincate solution for the production of zinc dust was suggested early in the first World War (16). A similar process was used in Germany around 1939 when I. G. Farbenindustrie was equipped to produce at least 110 pounds daily of zinc dust which was used for reduction of organic compounds. This plant and a good description of zincate electrolysis was described in a report by Eckardt (17) which became available after the war through operations of the Office of Military Government for Germany (U. S.). Many of the facts and conclusions discovered by Eckardt were worked out

independently at Boulder City before his report became available.

Electrolysis is conducted in open type (nondiaphragm) cells, and the zinc is deposited as a moss-like sponge which is recovered as a powder or dust. Attempts to deposit solid plates consistently have not been successful to date. Physically, the electrodeposited powder is different from the spherical particles of condensed or atomized zinc dust. Flake zinc consists of pinnate-shaped flakes with serrated edges giving a fern-leaf appearance, each flake consisting of a cluster of very small loosely connected crystals. Flake zinc made in the test work varied from 2.0 to 23.4 per cent plus-65-mesh and from 22.3 to 46.4 per cent minus-35-mesh material.

The best cathode material tried was standard rolled magnesium sheet metal, but steel, stainless steel, and nickel were also satisfactory. Iron-containing metals are not desirable, however, as particles of rust add one of the least desired impurities to the zinc. All metals electropositive to zinc were quickly covered by a flash coating of zinc metal when used as cathodes, then the loose flake zinc would start depositing. Zinc does not plate over and cover magnesium; therefore, the flake zinc adheres very lightly to magnesium cathodes, and it can be easily removed by a slight jarring of the electrode, a light touch of the deposit, or even by a movement of the electrolyte. Aluminum, used universally for cathodes in the acid electrolytic-zinc process, is soluble in caustic solutions.

Nickel appears to be virtually indestructible in caustic zincate solutions, even under the highly corrosive influence of anodic oxidation, and it is by far the most satisfactory anode material. A large variety of iron and steel samples were tested, and all showed measurable corrosion rates when used as anodes. Plain low carbon steel, such as that used for high quality sheet metal, was the best. High carbon steels and cast iron disintegrated quite rapidly, as did the alloy steels, especially those containing chromium. Sheet steel, carefully cleaned and plated with from 0.04 to 0.05 mm (0.0015 to 0.002 in.) thickness of nickel, was as corrosion-resistant as the pure nickel. Nickel-plated copper was not successful, as the copper would dissolve rapidly under the influence of anodic oxidation if even the slightest pinhole marred the nickel coating.

Current densities up to 27 amp/dm^2 (250 amp/ft^2) have been used successfully. Below about 5.3 amp/dm^2 (50 amp/ft^2) the current efficiency becomes lower with decreasing current density; typically, the current efficiencies were 92.0 and 82.8 per cent, respectively, at 4.3 and 0.5 amp/dm^2 (40 and 5 amp/ft^2). Above 5.3 amp/dm^2, the current efficiency showed little variation from 95 per cent. These data held true so long as the zinc concentration was held above 18 g/l, as the current efficiency dropped as the zinc concentration was depleted below this point, being only 80.4 per cent at 10 g/l Zn.

At the usual operating temperatures, 18° to 50°C, caustic soda solutions have the highest specific conductance in the concentration range between about 160 and 280 g/l NaOH (18). This range conforms ideally with the concentrations of NaOH desired for effective leaching of most ores. The specific conductance of caustic solutions is lowered by the presence of other substances, including zinc and silica. The effects of these factors are relatively insignificant compared to the effects of current density and temperature.

The decomposition voltage of zinc in zincate solutions is around 1.95 v, as compared to about 2.35 v in zinc sulfate solutions. At 45°C and 7.62 cm (3 in.) cathode-to-cathode spacing, the voltage from anode to cathode rose almost linearly with the current density from 2.12 v at 2.2 amp/dm^2 (20 amp/ft^2) to 3.60 v at 27.0 amp/dm^2 (250 amp/ft^2). For over-all general purposes, a current density of 12.9 amp/dm^2 (120 amp/ft^2) seems to be satisfactory. At this current density, the cell voltage varied from 3.2 v at 30°C to 2.72 v at 45°C, using electrolyte containing 29 g/l Zn. While the cell voltage lessens with increasing electrolyte temperature, it is impractical to operate a cell above about 50°C, because re-solution of the zinc powder accelerates very rapidly at temperatures above this.

Using a current density of 12.9 amp/dm^2 (120 amp/ft^2), a large number of tests gave an average of 3.0 v drop directly across the cells. Allowing for line and connector losses, it is believed that a well-designed circuit of commercial cells in series would require between 3.3 to 3.5 v per cell at the d-c output board. Well-purified electrolyte containing from 35 to 40 g/l Zn was electrolyzed to produce a depleted solution averaging 10 g/l Zn at an average current efficiency of around 85 per cent. The calculated d-c power consumption, therefore, was between 1.44 and 1.53 kwhr per lb of zinc.

All of several cells used for large-scale laboratory or pilot plant testing were constructed of welded sheet steel. The interiors were coated with a non-metallic liner, because metallic zinc wet with an electrolyte forms a voltaic couple with iron, causing the zinc to dissolve quite rapidly with the evolution of hydrogen. Small cells painted with several coats of alkali-resistant synthetic plastic coating, after careful sandblasting and cleaning, withstood over a year of use. Two larger cells similarly coated with the same compound cracked and peeled badly after a month's use. The next group of 5 welded steel cells were rubber-lined, and these proved to be very satisfactory.

The flake zinc can be removed by a wholly

mechanical operation, thereby eliminating the laborious hand stripping of sheet metal of the acid process. The economic success of this method of zinc recovery from solutions will depend largely on developing a continuous and rapid system for removing the flake zinc from the cells and separating it from the electrolyte. Considerable progress was made in 1948 and 1949, when the Bureau had the privilege of cooperating with Basic Reduction Company, Boulder City, Nevada, in pilot plant development of the process. Unfortunately, the company was unable to finance the complete development and commercial adaptation of the process; nevertheless, large steps in process developments were made, particularly in electrolysis and zinc recovery.

The first system tested comprised 2 cells each containing 5 cathodes 46 by 51 cm (18 by 20 in.) totalling 232 dm^2 (25 ft^2) and operated at 3000 amp. The second system consisted of 5 rubber-lined cells each containing 5 cathodes aggregating 325 dm^2 (35 ft^2) of effective area and operating normally at 4200 amp. The cathode and anode assemblies were fixed permanently in the cells, and the cells were hopper-bottomed for collecting the flake zinc as it fell off the cathodes. The confluence of the hoppers terminated in standard rubber-lined 2-in. pipe flanges which were opened and closed by diaphragm valves operated by compressed air. These valves were actuated by an automatic timer, which would open to drain a pulp of flake zinc and electrolyte at intervals of 4 to 10 minutes and remain open for 5 to 10 seconds. The withdrawn pulp was pumped to a cone settler where the flake zinc pulp was thickened, and the decanted electrolyte returned to the electrolytic cells.

Opening of the valve would lower the liquid level of the cell from 2 to 4 in., depending on the duration of the open period of the cycle. Ordinarily, this movement of the solution was sufficient to dislodge the deposited zinc but, occasionally, small patches of the moss-like deposit would become firm enough to continue growing outward until short-circuiting against the anode would occur. Lightly rapping or vibrating each cathode remedied this, but the pilot plant tests did not continue long enough to install mechanical devices for this. Another suggestion was to install motor-actuated wands to move periodically across the cathodes, similar to the action of a windshield wiper; it would seem that this method would be more positive in removing the zinc and would have the advantages of smooth, vibrationless operation.

The thickened flake-zinc pulp was filtered on a wire screen and spray-washed with sufficient water to displace most of the electrolyte. The flake zinc easily formed a cake several inches thick which filtered and washed very rapidly. This cake was repulped with a small amount of water and pumped to a basket centrifuge where the last traces of caustic were readily displaced with a water spray, and the final moisture reduced to about 20 per cent.

The centrifuged product was next passed through an aluminum-tube dryer through which warm dry air circulated and dried the zinc without raising the temperature at any time above 110°C. Dried in this manner, the zinc did not oxidize perceptibly. Dry flake zinc was produced which analyzed 99.30 per cent Zn, which contained less than 0.05 per cent combined Pb, Fe, and Cu, and 0.06 per cent SiO_2. The difference of 0.59 per cent, presumed to be oxygen, would account for 3.00 per cent ZnO; therefore, the flake zinc was calculated to be 96.8 per cent metallic zinc. Several tons of such zinc was produced from Goodsprings (Nevada) oxidized zinc ore containing from 22 to 38 per cent Zn and up to 5.2 per cent Pb. Later, in some large-scale laboratory tests, several batches of leach solution were purified with flake zinc more carefully than usual and clarified carefully to remove the finest of colloidal iron compounds. Samples of this zinc, analyzed spectrographically in the laboratory of American Zinc Company, showed 0.004 per cent Pb, as low as 0.0011 per cent Fe, no Cd, and 0.001 per cent Cu, meeting the specifications for Special High Grade or "Four-Nines" (99.99) zinc.

About 25,000 tons of zinc dust is produced each year, but it remains to be seen whether flake zinc could capture any part of this market. On the other hand, it might create a demand of its own, especially as a chemical agent where the crystalline flakes present a more reactive surface than the spherical particles of zinc dust. The flake zinc may be melted and cast to form the slab zinc of commerce. Several tons produced in the pilot plant were sold to a zinc works on the Pacific Coast, and they had no difficulty in melting the unconsolidated flake zinc material, according to reports.

The effects of various minor impurities or trace elements on the electrolysis of zincate solutions have been studied for some time, and a report on these findings will form the basis of a future paper. Suffice to say here, trace impurities appear to be much less harmful in zincate solutions than in acid zinc solutions.

Discussion

The results of the work on this process to date indicate that the caustic electrolytic-zinc process is technologically feasible for many types of oxidized zinc ores, drosses, and calcines. Details applying to a specific source of zinc will need additional work, while attempts to evaluate the economic feasibility of the process and the development of certain mechanical expediencies should be preceded by testing in a pilot

plant operation. The success of the Bayer process, which produces the world's supply of alumina for aluminum at a very low cost, should dispel any notions that leaching with caustic solutions is impractical. In fact, many of the techniques used in the Bayer process should be of considerable help in planning the development of the leaching part of the caustic zinc process.

Caustic is not consumed by any common ore elements except sulfates and chlorides, which are comparatively rare. None of the ores tested have shown any tendency to form insoluble complexes such as the sodium aluminosilicate formed by leaching bauxite in the Bayer process. The alumina encountered has always been almost totally insoluble in caustic. Consequently, the only caustic loss in the process is by mechanical entrainment. The purification sponge can be squeezed in a press and lightly washed so it will retain very little caustic. Similarly, the flake zinc can be washed very effectively by a displacement spray on a centrifuge. Countercurrent washing of repulped filter cake, consisting of both leach and recausticization residues, and using about 2 tons of wash water per ton of ore, showed a loss of 51 lb of NaOH per ton of ore in a 3-stage system, and a 19-lb loss in a 4-stage system. It is believed that a properly worked out displacement wash on a suitable filter could equal this performance with a single unit operation and use less wash water.

In many respects, the construction of a caustic leach plant would be cheaper and simpler than an equivalent acid process plant. Corrosion problems are relatively simple, and one has the choice of many equipment items that would be difficult to fabricate for the acid process. Standard steel construction would replace heavy and expensive lead-lined equipment, although the cost savings would be offset somewhat by the necessity for rubber or plastic linings in cells.

Acknowledgments

This project has been conducted at the Boulder City (Nevada) Experiment Station of the Bureau of Mines, now designated as the Electrometallurgical Branch of the Metallurgical Division, Region III. The work was under the general supervision of the late C. W. Davis and R. R. Lloyd, former and present chiefs of the Branch, both of whom have been enthusiastic in their support and encouragement. Many of the results were possible only through the combined efforts of the station personnel, and it is difficult to mention all who have contributed. P. R. Perry, in charge of the chemical and physical laboratories, deserves particular mention, as do T. A. Sullivan and J. H. Linck, chemists, for their patient analytical work; and R. W. Lewis and H. A. Heller, also chemists, for assisting with the physical chemistry and special spectrographic work. Miss Alice Buse, W. R. Vreeland, and R. D. Van Gilder, recently added to the staff, assisted materially in compiling data on recausticization, settling rates, and the effects of trace impurities, respectively.

Any discussion of this paper will appear in a Discussion Section, to be published in the December 1953 issue of the JOURNAL.

REFERENCES

1. E. C. KETCHUM, U. S. Pat. 592,055, October 19, 1897.
2. W. M. JOHNSON, *Trans. Am. Electrochem. Soc.*, **11**, 272 (1907).
3. F. GOUDRIAAN, *Proc. Acad. Sci. Amsterdam*, **22**, 179 (1919).
4. F. GOUDRIAAN, *Rec. trav. chim.*, **39**, 505 (1920).
5. National Research Council, E. F. Washburn, Editor, "International Critical Tables," Vol. IV, 1st ed., pp. 377 and 393, McGraw-Hill Book Co., Inc., New York (1928).
6. A. SEIDELL, "Solubilities of Inorganic and Metal Organic Compounds," 3rd ed., p. 1327, D. Van Nostrand Co., New York (1940).
7. J. W. MELLOR, "A Comprehensive Treatise on Inorganic and Theoretical Chemistry," Vol. 4, p. 529, Longmans, Green and Co., New York (1923).
8. E. MULLER, *Z. Elektrochem.*, **33**, No. 4, 134 (1927).
9. R. SCHOLDER AND G. HENDRICH, *Z. anorg. u. allgem. Chem.*, **241**, 76 (1939).
10. A. F. TAGGART, "Handbook of Mineral Dressing," Section 15, p. 7, John Wiley and Son, Inc., New York (1945).
11. T. P. HOU, "Manufacture of Soda," Ch. XIX, 2nd ed., American Chemical Society Monograph Series No. 65, Reinhold Publishing Corp., New York (1942).
12. L. F. GOODWIN, *J. Soc. Chem. Ind. London*, **45**, 360-T (1926).
13. J. C. OLSEN AND O. G. DIRENGA, *Ind. Eng. Chem.*, **33**, 204 (1941).
14. J. H. PRATT, *Z. Krist. Mineral. Petro.*, **27**, 416 (1897).
15. O. BUTSCHLI, *J. prakt. Chem.*, (2) **75**, 556 (1907).
16. H. J. MORGAN AND O. C. RALSTON, *Trans. Am. Electrochem. Soc.*, **30**, 229 (1916).
17. W. ECKARDT, FIAT Microfilm Reel MM 106, frames 82–101 on file as Publication Board Document 41411 in Office of Technical Services of the U. S. Department of Commerce. This document was translated by O. C. Ralston and issued as Bureau of Mines *Information Circular* 7466, May 1948.
18. National Research Council, E. P. Washburn, Editor, "International Critical Tables," Vol. VI, 1st ed., p. 254, McGraw-Hill Book Co., Inc., New York (1929).

Effect of Local Action Currents on the EMF of the Weston Standard Cell[1]

HERBERT H. UHLIG

Corrosion Laboratory, Department of Metallurgy, Massachusetts Institute of Technology, Cambridge, Massachusetts

ABSTRACT

Local action currents on the surface of cadmium-amalgam are shown to decrease slightly the measured emf of a Weston standard cell. The reversible emf, E(therm.), is related to the observed steady state emf, E(obs.), and a function of local action currents $f(i)$ as follows:

$$E(\text{therm.}) = E(\text{obs.}) + f(i).$$

Local action currents, calculated for a 10–13 per cent Cd amalgam from hydrogen overvoltage data on mercury, are at least equal to 2.1×10^{-9} amp/cm² corresponding to liberation of 0.008 ml H_2/cm²/year. Measurements of anodic polarization of the amalgam show that this current affects the reversible emf not less than the order of 3×10^{-8} volt, with the actual value being possibly larger by a factor of 100 times or more because of local action currents additional to those used in the calculation. The emf of the Weston cell is decreased whenever local action currents increase; by deposition, for example, of low overvoltage impurities from the electrolyte on the amalgam, and by presence of mercurous ions and dissolved oxygen plus other depolarizers. Factors increasing the observed emf include diffusion of low overvoltage impurities from the surface into the amalgam, reduction of oxygen and other depolarizers on aging, and neutralization of electrolyte by the glass. The latter factors offer an explanation for the reported positive drift in emf of some Bureau of Standards cells.

Apart from considerations of standard cells, the observed potential of any metal, thermodynamically capable of reaction with water to form hydrogen, is the corrosion potential and not the reversible potential, even though the two values may nearly coincide. The deviation from reversibility depends on the corrosion rate and the extent to which the metal polarizes as anode.

INTRODUCTION

The saturated Weston standard cell is the following:

Cd amalgam, sat'd $CdSO_4 \cdot \frac{8}{3}H_2O$, sat'd Hg_2SO_4, Hg.

The emf at 25°C is 1.0181 international volts, and the over-all simplified reaction[2] is:

$$Cd(s) + Hg_2SO_4(s) = CdSO_4(s) + 2Hg(l).$$

[1] Manuscript received June 9, 1952. This paper prepared for delivery before the Philadelphia Meeting, May 4 to 8, 1952.

[2] The more accurate equation is the following:

$$x\text{Cd}(y\text{Hg})(1+s) + \text{Hg}_2\text{SO}_4(s) + \frac{8/3}{m - 8/3}\text{CdSO}_4 \cdot m\text{H}_2\text{O}(l) = \frac{m}{m - 8/3}(\text{CdSO}_4 \cdot 8/3\text{H}_2\text{O})(s) + 2\text{Hg}(l) + (x-1)\text{Cd}(y\text{Hg})(1+s)$$

where x moles of Cd are associated with y moles of Hg in the amalgam electrode and m is the number of moles of water associated with 1 mole of $CdSO_4$ in the saturated solution. This equation differs from that given by Vinal (1) in that Cd amalgam instead of Cd(s) appears on the left-hand side and a diluted amalgam on the right-hand side, in accord with the actual reaction of the cell.

Cells properly prepared maintain a constant potential over many years. However, careful comparisons at the National Bureau of Standards show that even under optimum conditions, a slight drift occurs such that the potential for some cells may increase with time in the order of 2 microvolts (μv) per year (2). The drift has been ascribed to various causes, such as change in crystal size of mercurous sulfate or cadmium sulfate, or neutralization of the electrolyte by the glass container. However, changes in polarizing local action currents on the surface of the cadmium amalgam electrode can also account for the drift, and this very likely is one of the major causes as is shown herewith.

The surface of an amalgam can be considered to be a network of short-circuited anodes and cathodes making up local action cells, in accord with the electrochemical theory of corrosion. The magnitude of electric current produced by these cells is determined by the rate of the cathodic reaction (usually discharge of hydrogen ions). The anodes are polarized by this local action current to some potential more cathodic than the reversible potential, the exent of the polarization depending on the magnitude of current. The over-all potential of cadmium amalgam in

contact with saturated cadmium sulfate, therefore, is the corrosion potential and *not the equilibrium potential*, even though these two values in practice differ only slightly one from the other. The deviation of measured potentials from reversible values caused by local cell action has been discussed qualitatively by Mears and Brown (3).

In the absence of depolarizers, the value of the corrosion potential can be calculated from a knowledge of the overvoltage of hydrogen on mercury and the anodic polarization characteristics of cadmium amalgam in saturated cadmium sulfate. This calculation makes use of observations by Wagner and Traud (4) to the effect that the corrosion rate of a zinc amalgam in hydrochloric acid solution can be expressed quantitatively, in accord with Faraday's

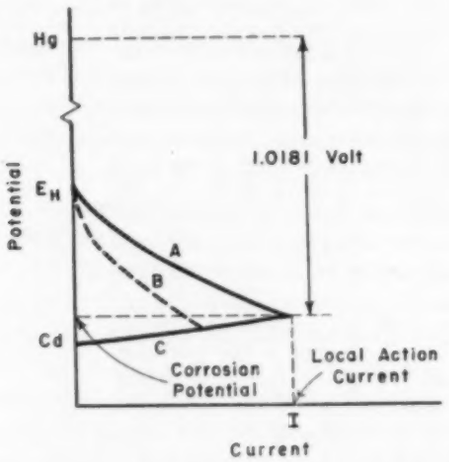

FIG. 1. Diagram of cathodic and anodic polarization of Cd amalgam in contact with saturated $CdSO_4$.

law, as an equivalent current which polarizes mercury cathodically to the potential of the amalgam in the same acid environment. Their experiments constitute proof that amalgams, like most metals, corrode by reason of local action cells, even though mercury cathodes and zinc anodes of a zinc amalgam are presumably on an atomic scale.

Fig. 1 describes polarization curves for the anodic and cathodic elements of a 10–13 per cent cadmium amalgam, the activity of which is independent of precise composition, in contact with deaerated saturated cadmium sulfate. When the amalgam is first exposed to the electrolyte, the cathodic elements, illustrated by Hg, are rapidly polarized to the hydrogen electrode potential E_H by depletion of Hg_2^{++} in the electrolyte at the immediate amalgam surface. This occurs with only momentary electric current. When the potential reaches E_H, hydrogen ions begin to discharge, accompanied this time by continuous current and, hence, continuous corrosion of Cd to Cd^{++}. The rate of hydrogen formation depends on the magnitude of the local action currents, in turn controlled by the hydrogen overvoltage value of the cathodic areas.

The final corrosion potential of the amalgam is determined by the intersection of the cathodic polarization curve A and the anodic polarization curve C. Corresponding current I is the local action current equivalent to the corrosion rate of the amalgam and rate of liberation of hydrogen.

Should polarization or overvoltage of the cathodic areas, for some reason, increase in accord with curve B, the local action current determined by intersection with C is less than for curve A, and the corrosion potential then moves in the anodic direction toward the reversible potential marked Cd. This corresponds to a drift of potential for the Weston cell in the positive direction. A drift in the same direction results from a change of E_H in the anodic direction caused, for example, by increase in *p*H of the electrolyte. In all cases, the observed emf of the Weston cell is *always* slightly less than the reversible potential.

Calculation of Local Action Currents

To calculate the order of local action currents, the first step involves calculation of the ratio of activity of Cd^{++} to activity of cadmium in the cadmium amalgam. This ratio is obtained from the emf of the Weston cell (1.0181 int. volts at 25°C), the E^0 values for $Cd \rightarrow Cd^{++} + 2e^-$ (0.402 volt) and $2Hg \rightarrow Hg_2^{++} + 2e^-$ (−0.799 volt), and the activity of Hg_2^{++} in saturated $CdSO_4$. The expression for the emf of the cell at 25°C is the following:

$$1.0181 = 0.402 + 0.799 - \frac{0.0591}{2} \log \frac{(Cd^{++})}{(Cd)} - \frac{0.0591}{2} \log \frac{(Hg)^2}{(Hg_2^{++})} \qquad (I)$$

where $(Hg)^2 = 1$.

The activity of Hg_2^{++} can be calculated from the activity of SO_4^{++} in saturated $CdSO_4$ and the solubility product of Hg_2SO_4 equal to 6.2×10^{-7} (5). The activity of SO_4^{--} is obtained from the solubility of $CdSO_4 \cdot \frac{8}{3}H_2O$, namely, 0.06627 mole $CdSO_4$/mole H_2O (6) or 3.68 molal, and the activity coefficient for 3.5 molal $CdSO_4$ equal to 0.035 (7).

Therefore,

$$(Hg_2^{++}) = \frac{6.2 \times 10^{-7}}{3.68 \times 0.035} = 4.8 \times 10^{-6}.$$

Substituting this value into equation (I), the log ratio of the activity of Cd^{++} to activity of Cd in Hg is:

$$\log \frac{(Cd^{++})}{(Cd)} = 0.88. \qquad (II)$$

From this value, it is possible to calculate the equilibrium potential difference E_H of the hydrogen electrode and the Cd amalgam electrode in saturated $CdSO_4$. The electrolyte in a practical cell may be about 0.03*N* in H_2SO_4 (8), the *p*H of which is assumed for present purposes to be 1.5, and the partial pressure of hydrogen is equal to one atmosphere.

Then

$$E_H - E_{Cd} = 0.402 - \frac{0.0591}{2} \log \frac{(Cd^{++})}{(Cd)} - 0.059\ pH = 0.29 \text{ volt.} \quad \text{(III)}$$

If the pressure of H_2 is less than one atmosphere, as is expected, this value would be somewhat larger, but, as explained later, the final calculations are not affected.

It is the above emf that is available to polarize Hg beyond the equilibrium potential for evolution of hydrogen. The accompanying current, equal to the local action current, can be calculated from the hydrogen overvoltage value (O.V.) for mercury. Kortüm and Bockris (9) give the following value for Hg in 0.2*N* H_2SO_4.

$$\text{O.V.} = \frac{2.303RT}{0.52\mathbf{F}} \log \frac{I}{6 \times 10^{-12}}$$

where I is in amp/cm². The overvoltage is not changed appreciably by change in *p*H(10); addition of cadmium sulfate may alter the value slightly, but the magnitude and direction of change are uncertain. Measurements by deBéthune at low current densities in 0.1*N* hydrochloric acid indicate that hydrogen overvoltage on mercury is depressed by $CaCl_2$ addition, but is increased by KCl addition (11). Setting the value of overvoltage above equal to 0.29 volt and solving for I, one obtains 2.1×10^{-9} amp/cm². This is equivalent to the liberation of 0.008 ml H_2/cm²/year.

It might be assumed that the low partial pressure of hydrogen in the anode compartment, when the cell is set up initially, accounts for an increase in local action currents through increase in the available potential for hydrogen evolution. However, low partial pressures of hydrogen are accompanied by increase in hydrogen overvoltage (12), with a resultant cathode potential that is largely independent of pressure.

On the basis of this discussion, the reversible emf for the Weston cell, E(therm.), can be expressed in terms of the steady state or observed emf, E(obs.), as follows:

$$E(\text{therm.}) = E(\text{obs.}) + f(i)$$

where $f(i)$ is the additive term to the potential resulting from polarization of the Cd electrode corresponding to the local action current I.

Anodic Polarization of Cd Amalgam

The actual value for $f(i)$ in volts can be obtained from anodic polarization data for cadmium amalgam. These data were obtained by opening a saturated Weston cell, breaking up the cadmium sulfate crystals, inserting a saturated $CdSO_4$ salt bridge to just above the amalgam surface; the bridge, in turn, making contact with an Ag-AgCl electrode in 0.1*N* KCl. Current up to 1 ma was passed through the cell and potentials between the amalgam and the silver chloride electrode measured to ±1 mv with an electronic potentiometer. The measurements are recorded in Fig. 2. The amalgam polarizes to the

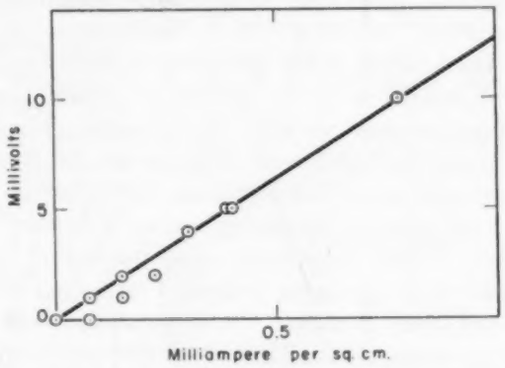

Fig. 2. Anodic polarization of 10–13 per cent Cd amalgam in saturated $CdSO_4 \cdot \frac{8}{3}H_2O$.

extent of about 13 mv/ma/cm². This turns out to be the same value as that obtained for anodic polarization of zinc amalgam by Wagner and Traud (4).

Corresponding Potential Drift

The polarization, therefore, corresponding to 2.1×10^{-9} amp/cm² is 3×10^{-8} volt. Consequently, under ideal conditions the Weston cell is expected to deviate from its reversible emf by at least −0.03 μv.

But the calculated local action current was obtained using overvoltage data for mercury in contact with solutions of greater purity than corresponds to mercury and solutions usually composing a standard cell. Therefore, −0.03 μv is the minimum value of the expected deviation from reversibility caused by corrosion of the amalgam with accompanying hydrogen evolution. Under practical conditions, the deviation is expected to be greater perhaps by a factor of at least 100 (3 μv) or more.

Evidence for this comes from the fact, as Bowden and Rideal showed (13), that overvoltage data for so-called pure mercury may deviate from the logarithmic or Tafel equation when polarizing currents

are below 5×10^{-7} amp/cm². Corresponding current is then greater than that predicted by the Tafel equation. Where improved experimental precautions are used, deviations occur at currents below 10^{-9} or 10^{-10} amp/cm² (14), but such precautions are probably seldom considered necessary in the production of Weston cells. A local action current of 5×10^{-7} amp/cm², for example, would cause a deviation of the Weston cell emf of 6.5 μv below the theoretical reversible value.

Further evidence that a deviation of 0.03 μv may be a limiting lower value comes from the larger accumulation of hydrogen in some aged practical cells than the value 0.008 ml hydrogen/cm²/year. A polarizing current of 5×10^{-7} amp corresponds to 2 ml of hydrogen per year, a value, which, although probably high, corresponds more closely to the measurable quantities of hydrogen sometimes observed.

A third factor is the presence of mercurous ions and depolarizers in the electrolyte which increase local action currents and cause corresponding deviations in emf of the cell. Whether or not dissolved oxygen and organic depolarizers (for example, from cork) are present, mercurous ion is a certain component of the electrolyte, some portion of which diffuses to the amalgam surface. That which reaches the cadmium amalgam reacts in accord with the same approximate reaction as for the cell itself. The corresponding increased local action current polarizes the anodic elements of the amalgam to a more cathodic value similar to local action currents accompanying hydrogen evolution.

How large such currents may be in a practical cell depends on the diffusion rate of mercurous sulfate. The rate of diffusion from the saturated solution at the mercury electrode to essentially zero concentration at the amalgam electrode (equilibrium concentration of Hg_2^{++} at the amalgam surface is calculated to be 6×10^{-39} molal) can be calculated by Fick's law.

$$\frac{dm}{dt} = -AD\frac{dc}{dx}$$

where $\frac{dm}{dt}$ is the diffusion rate for m moles of Hg_2SO_4 passing cross section A (1 cm²); D is the diffusion constant (1×10^{-5} cm² sec^{-1}) (15) and $\frac{dc}{dx}$ is the concentration gradient in moles/ml/cm. The latter value is equal to the solubility of mercurous sulfate in saturated cadmium sulfate (5.5×10^{-6} moles/ml) (16) divided by 5 cm, the estimated length of the diffusion path. The current i is then equal to $2\mathbf{F}\frac{dm}{dt}$ where **F** is the Faraday, and where 2 enters because of divalent mercurous ion. The diffusion current density for this situation turns out to be 2×10^{-6} amp/cm². This value is undoubtedly high because diffusion is retarded by a mass of cadmium sulfate crystals on the amalgam surface. Local action currents derived from this source, therefore, cannot be calculated accurately, but whatever their finite value, they certainly supplement the local action currents accompanying hydrogen evolution. It is obvious that under abnormal conditions where convection currents are allowed to take place, or the cell is disturbed mechanically, the emf of the Standard cell can be appreciably reduced by increased local action at the amalgam electrode caused by reaction with mercurous ions.

Conclusion

In summary, factors causing drift which decrease the observed emf are those that increase local action currents.[2] These include:

1. Precipitation of low overvoltage impurities on the amalgam surface. In this respect, difference in overvoltage of the solid cadmium amalgam compared with the liquid amalgam phase in equilibrium can also alter rate of hydrogen discharge as the relative amounts of each phase change on aging of the cell. The direction of this effect depends on the comparative values of overvoltage for the two phases.
2. Leaching out of organic and inorganic depolarizers from cork, if cork is present.
3. Presence of dissolved oxygen.
4. Diffusion of Hg_2^{++} to the amalgam electrode.

Factors decreasing local action currents and thereby increasing the emf of the Weston cell are:

1. Diffusion of low overvoltage impurities from the surface into the amalgam. The effect of liquid and solid phases may also enter, as described above.
2. Gradual reduction of depolarizers and of dissolved oxygen through corrosion of the cadmium amalgam.
3. Neutralization of acid by glass. This decreases the potential of E_H vs. Cd and, hence, decreases local action currents. For a change of 0.1 unit in pH, the corresponding change in cell potential, using overvoltage values for pure mercury, is calculated to be about 3.3×10^{-9} volt, but for less pure Hg and a local action current of 5×10^{-7} amp/cm², the value is 7.8×10^{-7} volt.

[2] The major factor causing drift in the unsaturated type Weston cells using unsaturated $CdSO_4$ electrolyte differs from those discussed above. Unsaturated cells tend to decrease in emf on aging by perhaps 50–100 μv/year. This is accounted for by increase in activity of Cd^{++} brought about by slow reaction of the amalgam with Hg_2^{++} to form Hg, and with the electrolyte to form hydrogen. This effect overshadows the irreversible or nonthermodynamic influences on the saturated cell emf listed in this paper.

This effect is in the same direction, but smaller than the thermodynamic effect of sulfuric acid on the over-all free energy change or emf for the cell reaction. The observed effect is expressed (17) by the equation

$$\Delta E = -855x$$

where ΔE is the difference of emf in microvolts from the "neutral" cell when the electrolyte is made x normal in sulfuric acid. An increase of pH by 0.1 unit at pH 1 is accompanied, therefore, by an observed increase in emf of about 20 μv, this being about 25 times the irreversible effect calculated above for the larger polarizing current.

These effects suggest that cells of maximum stability in emf can be constructed by:

1. Using highest purity mercury and solutions in accord with rigid experimental precautions employed in hydrogen overvoltage measurements.

2. Constructing the cell of an inert material which on aging will not alter pH of the electrolyte, or supply anions or cations to the electrolyte capable of altering hydrogen overvoltage on mercury. This suggests use of quartz, tetrafluorethylene, and similar substances.

3. Instead of sulfuric acid, addition of a weak acid having maximum buffer capacity. This will make possible a higher pH for saturated cadmium sulfate with less tendency for reaction with cadmium amalgam to form hydrogen. Any such acid must be compatible with saturated cadmium sulfate and must not precipitate mercurous ions from saturated mercurous sulfate. It must not reduce at a mercury cathode.

4. Designing the cell so that diffusion is retarded from the mercury to the amalgam electrodes.

It is also evident from the discussion above, that the observed potential of any metal in an aqueous electrolyte, whether an amalgam or not, capable of reaction with water to form hydrogen, is actually the corrosion potential and not the reversible potential. Deviations from reversibility are in the cathodic direction and depend on magnitude of local action currents and the extent to which the metal is polarized anodically per unit of current. Since the corrosion rates for metals more active than hydrogen are usually greater than for amalgams, it is a reasonable conclusion that deviations from reversibility are, in general, greater than the deviations calculated above.

Any discussion of this paper will appear in a Discussion Section, to be published in the December 1953 issue of the JOURNAL.

REFERENCES

1. G. VINAL, "Primary Batteries," p. 171, John Wiley & Sons, Inc., New York (1950).
2. L. H. BRICKWEDDE AND G. VINAL, *J. Research Natl. Bur. Standards*, **27**, 487 (1941).
3. R. B. MEARS AND R. H. BROWN, *J. Electrochem. Soc.*, **97**, 75 (1950).
4. C. WAGNER AND W. TRAUD, *Z. Elektrochem.*, **44**, 391 (1938).
5. "Corrosion Handbook," p. 1138 (H. H. Uhlig, editor) John Wiley & Sons, Inc., New York (1948).
6. L. H. BRICKWEDDE, *J. Research Natl. Bur. Standards* **36**, 377 (1946).
7. H. HARNED AND B. OWEN, "The Physical Chemistry of Electrolytic Solutions," 2nd ed., p. 427, Reinhold Publishing Co., New York (1950).
8. L. H. BRICKWEDDE AND G. VINAL, *J. Research Natl. Bur. Standards*, **27**, 489 (1941).
9. G. KORTÜM AND J. O'M. BOCKRIS, "Electrochemistry," Vol. II, p. 759, Elsevier Press, Inc., Houston (1951).
10. G. KORTÜM AND J. O'M. BOCKRIS, "Electrochemistry," Vol. II, p. 423, Elsevier Press, Inc., Houston (1951).
11. A. DEBÉTHUNE, *J. Am. Chem. Soc.*, **71**, 1556 (1949).
12. J. O'M. BOCKRIS, *Chem. Revs.*, **3**, 538 (1948).
13. F. P. BOWDEN AND E. K. RIDEAL, *Proc. Royal Soc., London*, **120A**, 59 (1928).
14. F. P. BOWDEN AND K. E. GREW, *Disc. Faraday Soc.*, **1**, 86 (1947).
15. LANDOLT-BORNSTEIN, Vol. I, p. 68.
16. G. VINAL, "Primary Batteries," p. 183, John Wiley & Sons, Inc., New York (1950).
17. G. VINAL, "Primary Batteries," p. 202, John Wiley & Sons, Inc., New York (1950).

Some Electrochemical Properties of New Synthetic Ion Exchange Membranes[1]

ALVIN G. WINGER, GEORGE W. BODAMER, AND ROBERT KUNIN

Rohm and Haas Company, Philadelphia, Pennsylvania

ABSTRACT

The physical, chemical, and electrochemical properties of ion exchange membranes Amberplex C-1 and Amberplex A-1, recently developed for commercial application by the Rohm and Haas Company, were investigated and interpreted in the light of a discussion of the Donnan membrane equilibrium for polyelectrolyte membranes. A homogeneous, single-phase model was assumed valid for these membranes. The cation exchange membrane Amberplex C-1 was found to be preferentially permeable to cations and the degree of permselectivity was found to vary with concentration of surrounding electrolyte. Similarly, anion exchange membrane Amberplex A-1 was found to be preferentially permeable to anions. The conductivity of both membranes was found to be a function of the concentration and nature of the surrounding solution. The electrochemical properties of the membranes were correlated with their fixed-ion concentrations and degrees of hydration.

Several possible applications of these membranes having commercial interest are suggested and discussed briefly.

INTRODUCTION

The early history of the study of membranes showing selective ion permeability is closely associated with biochemistry. Starting about 1890, the realization grew among biochemists that many bioelectric phenomena could be explained on the assumption that certain membranes permitted the transfer of cations but not anions, and vice versa. Since that time the number of workers in this field has become legion, so that it is scarcely possible to mention all of them, much less describe their contributions in detail. Many have attacked the problem by synthesizing membranes, which might be simpler to study than the natural varieties. Notable work along this line has been done by Michaelis (1) and by Sollner (2–5), using collodion membranes, and by Juda and coworkers (6–8) and Kressman (9) using synthetic ion exchange membranes.

A different interest led Wyllie and Patnode (10) to the synthesis of model membranes. These men were concerned with the fact that oil shales show characteristic membrane potentials depending on the oil and brine concentrations. Their models consisted of compressed disks of finely ground ion exchange resins and a plastic binder.

More recently there have become available synthetic ion exchange membranes of sufficient size and with sufficient electrical conductance to render them commercially useful. These membranes are particularly suited to industrial applications because, along with high conductivity and selective ion permeability, they possess considerable flexibility and tensile strength, and excellent chemical durability. They are not appreciably affected by concentrated alkaline or acid solutions, by oxidizing agents, or by many solvents.

Properties of Ideal Permselective Membranes

For the purpose of this paper, an ideal permselective membrane will be defined to be a membrane which, when subjected to a potential gradient, permits passage of cations to the exclusion of anions, or the reverse. The transport number of the mobile ion is thus unity within the membrane, while that of the ion of opposite charge is necessarily zero. This will be the case for the ideal membrane regardless of the concentration of the outside solution. As will be apparent shortly, an ideally permselective membrane is in practice impossible to produce, but can be closely approximated by a careful choice of such membrane variables as composition and physicochemical properties. Choice of proper operating conditions of concentration and temperature is also important.

The basic theory of permselective membranes and their electrochemical properties was first extensively developed by Teorell (11, 12) and by Meyer and Sievers (13). Extensions of the theory and tests to determine its validity have been made by numerous investigators (1–5, 11–20) chiefly on membranes of limited capacity equilibrated in dilute solutions of electrolytes. According to this theory, the permselective properties of certain natural and artificial membranes can be explained by the existence within

[1] Manuscript received July 24, 1952. Paper prepared for delivery before the Philadelphia Meeting, May 4 to 8, 1952.

the membrane of easily dissociated ions loosely bound to fixed groups of opposite charge. If the fixed groups are anionic and the mobile ions, or counter-ions, are cationic, the membrane will be preferentially permeable to cations when placed under a potential gradient, while fixed cationic groups and mobile anions will give the membrane anion permeable properties. When a permselective membrane, e.g., a cation exchange membrane, is equilibrated with a solution of binary electrolyte such as potassium chloride, a Donnan equilibrium is established in due time, provided the membrane is at least slightly permeable to the solvent. Unequal numbers of the two oppositely charged mobile ions are then present in the membrane to satisfy the conditions of Donnan equilibrium, viz.,

$$[K^+][Cl^-]f_\pm^2 = a_\pm^2 \qquad (I)$$

$$[K^+] = [Cl^-] + [A^-] \qquad (II)$$

where $[K^+]$, $[Cl^-]$, and $[A^-]$ are the concentrations of potassium ion, chloride ion, and fixed ion in the membrane at equilibrium; $a_\pm$ is the mean ionic activity of the external KCl solution in equilibrium with the membrane. $f_\pm$ can be interpreted as a mean activity coefficient of the potassium and chloride ions in the membrane.

It is obvious from equations (I) and (II) that at equilibrium there will be widely different concentrations of potassium and chloride ions within the membrane if the fixed ion concentration of the membrane is large, as will be the case, for example, with membranes composed of synthetic ion exchange materials. Since the transport numbers of the ions in a system depend on both their relative concentrations and their mobilities, the transport number within the membrane of the more concentrated ion (potassium ion in the above case) will be greatly increased over its value in the electrolytic solution. If $[A^-]$ is large, $[Cl^-]$ will be relatively small and the transport number of the chloride ion nearly zero. Hence the membrane is highly permselective for cations, in this case potassium ions. If the activity of the external solution, $a_\pm$, is high, $[Cl^-]$ in the membrane will be large in spite of high $[A^-]$. This effect increases the transport number of chloride ions and decreases the cationic permselectivity. In decreasing electrolyte concentrations, the permselectivity approaches the theoretical maximum for an ideal membrane. However, in any electrolytic process ion concentrations are appreciable and perfect permselectivity is an idealized situation of little practical interest. It is approached at moderate concentrations of electrolyte by membranes of high exchange capacity or fixed ion concentration.

From the above considerations, Teorell (11) and Meyer-Sievers (13) derived an expression for the potential across a membrane separating two solutions of concentration C_2 and C_1 of a uni-univalent electrolyte. Modified to include activities (14) instead of concentrations within the membrane as well as in the external solutions, this expression becomes

$$E = \frac{RT}{\mathbf{F}}\left[U \ln \frac{\sqrt{K^2a_1^2 + 1} + U}{\sqrt{K^2a_2^2 + 1} + U} + \tfrac{1}{2} \ln \frac{(\sqrt{K^2a_2^2 + 1} + 1)(\sqrt{K^2a_1^2 + 1} - 1)}{(\sqrt{K^2a_2^2 + 1} - 1)(\sqrt{K^2a_1^2 + 1} + 1)}\right] \qquad (III)$$

where $K = \dfrac{2}{Af_\pm}$, $U = \dfrac{U_c - U_a}{U_c + U_a}$, R = the gas constant, T = the absolute temperature, and $\mathbf{F}$ = the Faraday. a_1 and a_2 are the mean ionic activities of the solutions, $f_\pm$ the mean activity coefficient of the ions within the membrane, U_c and U_a the mobilities of cation and anion in the membrane, and A the selectivity constant or fixed-ion concentration of the membrane. If the fixed-ion concentration A is large compared to the concentrations of the external solutions, equation (III) reduces to the Nernst potential expression for a reversible electrode,

$$E_0 = \frac{RT}{\mathbf{F}} \ln \frac{a_2}{a_1}. \qquad (IV)$$

This is the value of the membrane potential if the membrane is perfectly permselective, permitting passage of either cations or anions, but not both. If the fixed-ion concentration is small compared to the concentrations of the external solutions, or $a_\pm > Af_\pm$, equation (III) reduces to the diffusion potential between two solutions of an electrolyte of different concentration,

$$E = \frac{U_c - U_a}{U_c + U_a}\frac{RT}{\mathbf{F}} \ln \frac{a_2}{a_1} = (t^+ - t^-)\frac{RT}{\mathbf{F}} \ln \frac{a_2}{a_1} \qquad (V)$$

where t^+ and t^- are the average transport numbers of cation and anion, respectively, in the solutions. Equation (V) is a special case of both the Henderson equation and the Planck equation for liquid junction or diffusion potentials, for a uni-univalent electrolyte, obtained by special integrations of the general differential equation for liquid junction potentials (21).

This latter expression is derived for any liquid junction between two solutions and will hold for a membrane boundary, with the transport numbers involved being those within the membrane.[2] With

[2] The form of the expression for a junction potential obtained by integration of the general differential equation for the liquid junction potential will depend on the assumption made concerning the distribution of the ions in the boundary region. Teorell (12) assumed a distribution in the membrane boundary similar to that assumed by Planck for liquid boundaries and arrived at equations similar to Planck's.

this in mind, we can write, for a membrane electrode involving a uni-univalent electrolyte,

$$E = (t_+ - t_-)\frac{RT}{\mathbf{F}} \ln \frac{a_2}{a_1} \qquad \text{(VI)}$$

where t_+ and t_- are the transport numbers of cation and anion within the membrane. This equation will hold over all concentration ranges of external solution, reducing to equation (IV) and equation (V) for very low and very high values of that concentration, respectively. Since $t_- = 1 - t_+$, equation (VI) can be written in the form,

$$E = (2t_+ - 1)\frac{RT}{\mathbf{F}} \ln \frac{a_2}{a_1}. \qquad \text{(VII)}$$

The measured potential across a membrane separating two solutions of a uni-univalent electrolyte of activities a_2 and a_1 will be given by equation (VII) provided a_2 and a_1 are quite similar, an assumption required in the derivation of equation (V), and hence (VII), from general liquid junction potential theory. If the membrane, e.g., a cation exchange membrane, is ideal, $t_+ \rightarrow 1$ and equation (VII) becomes the Nernst potential expression (IV). The voltage is then the maximum possible voltage E_0 for any membrane in those particular solutions, and it can obviously be calculated from data on the activities of the ions in solution. Dividing the measured potential by the calculated E_0, or equation (VII) by (IV), we obtain

$$E/E_0 = 2t_+ - 1 \qquad \text{(VIII)}$$

or

$$t_+ = \frac{E + E_0}{2E_0}. \qquad \text{(IX)}$$

Thus, an average transport number of the cation in the membrane is defined.

TABLE I. *Physical and chemical properties of ion exchange membranes*

Property	Amberplex C-1	Amberplex A-1
Tensile strength	370 lb/in.^{2}	350 lb/in.^{2}
Bursting strength*	25.2 lb/in.^{2}	13.3 lb/in.^{2}
% Elongation	29%	16%
% Swelling from dry to hydrated state	56%	42%
% H_2O, hydrated state	34%	28%
Total exchange capacity, meq./dry gram	3.0	1.5
Fixed ion concentration equiv./l imbibed water	5.7	3.9

* Measured on Mullen Burst Strength Tester; apparatus similar to that described in A.S.T.M. Test Method D774.

The degree of permselectivity of a membrane can be expressed in terms of the change in the transport number of the mobile ion in a solution, when the membrane is introduced into the solution in series with it electrically. Thus the degree of permselectivity P can be defined by,

$$P = \frac{t_{\text{mobile ion}} - t^0_{\text{mobile ion}}}{1 - t^0_{\text{mobile ion}}} \qquad \text{(X)}$$

where $t_{\text{mobile ion}}$ refers to the value of the transport number in the membrane and $t^0_{\text{mobile ion}}$ the value in the free electrolyte solution. This represents the fraction of the maximum possible increase in the transport number of the mobile ion which is achieved by introduction of the membrane.

The conductance of permselective ion exchange membranes is chiefly electrolytic in nature, hence their conductivity will be a function of the concentration and mobility of the ions within the membrane. Since the concentrations of the ions within the membrane depend on their concentrations in the external solution(s) with which the membrane is equilibrated, the conductivity of the membranes will increase as the external solution concentration increases, or vice versa. As infinite dilution of the external solution is approached, the concentration of mobile ions within the membranes approaches a minimum value, $[A^{\pm}]$, the fixed ion concentration of the membrane. The conductivity of the membrane would thus be expected to approach a limiting minimum value which is characteristic of that particular membrane at low concentrations of external solutions.

Within the membrane, the mobile ions have a mobility which is sharply reduced from their mobility in free aqueous solution, probably due to complex electrostatic and interionic attractive forces in the membrane. The conductivity of the membrane would be expected to be less than that of the surrounding electrolyte solution of moderate and high concentration. As before noted, at low external concentrations the membrane conductivity approaches a minimum, while that of the external solution goes to zero at infinite dilution. At some value of external concentration, the two conductivities will be equal, giving an apparently homogeneous system.

Experimental Results

The physical, chemical, and electrochemical properties of ion exchange membranes Amberplex C-1 and Amberplex A-1, recently developed by the Rohm and Haas Company, will be presented in the light of the foregoing remarks on the membrane properties that might be considered ideal. Table I summarizes various physical and chemical properties of the two membranes.

It is evident that these membranes have excellent physical properties, listed above for the hydrated state. When dry, the films are less flexible, but they may be repeatedly desiccated and hydrated without damage to physical or chemical properties. The films should be hydrated by soaking several hours before they are rigidly clamped into position. However, in salt, acid, or alkali solutions of ordinary concentration, the membranes shrink only slightly and will not crack when changing solutions. These membranes are highly resistant to passage of water under a hydrostatic head, a square foot of the membrane, 25 mils thick, permitting leakage of 10–25 ml/hr under one atmosphere pressure.

The chemical stability of Amberplex C-1 and Amberplex A-1 is excellent. The films are resistant to strong acid and alkali solutions and solutions containing free halogens. They are unaffected by many common solvents and can be used at temperatures up to about 95°C.

TABLE II. *Permselectivity of ion exchange membranes in* KCl *solution*

KCl C_2	KCl C_1	$\bar{N}$	E(mv)	E_0 (mv)	$t_{\text{mobile ion}}$	$t^0_{\text{mobile ion}}$	$P \times 100$	$(E/E_0) \times 100$
Amberplex C-1								
0.04	0.02	0.03	16.1	16.6	0.985	0.490	97.1	97.0
0.10	0.05	0.075	15.8	16.3	0.984	0.490	96.9	97.0
0.20	0.10	0.15	15.0	16.1	0.966	0.490	93.4	93.2
0.40	0.20	0.30	14.3	16.0	0.947	0.489	89.8	89.5
1.0	0.50	0.75	13.1	16.0	0.910	0.489	82.5	81.9
2.0	1.0	1.5	11.1	16.5	0.837	0.489	68.1	67.3
Amberplex A-1								
0.04	0.02	0.03	−16.4	−16.6	0.995	0.510	99.0	98.9
0.10	0.05	0.075	−15.9	−16.3	0.988	0.510	97.6	97.6
0.20	0.10	0.15	−15.3	−16.1	0.976	0.510	95.2	95.0
0.40	0.20	0.30	−14.2	−16.0	0.944	0.511	88.6	88.8
1.0	0.50	0.75	−12.9	−16.0	0.903	0.511	81.2	80.8
2.0	1.0	1.5	−10.5	−16.5	0.818	0.511	62.8	63.7

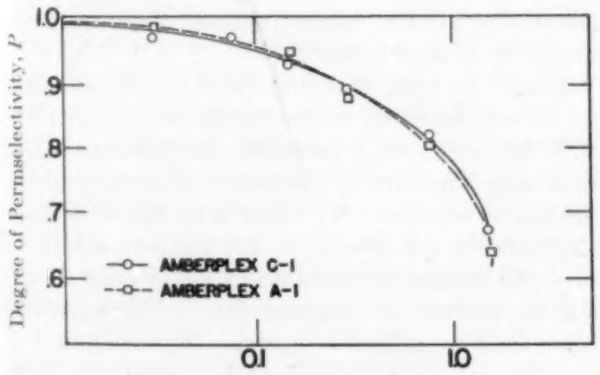

FIG. 1. Permselectivity of ion exchange membranes in KCl solutions.

TABLE III. *Specific conductivity of ion exchange membranes in electrolytic solutions*

External solution	Conc N of sol'n	Specific conductance of membrane (ohm^{-1}cm^{-1}) $\times 10^3$	Specific conductance of sol'n (ohm^{-1}cm^{-1}) $\times 10^3$	Resistance of 25 mils thickness in ohm/cm^2
Amberplex C-1 (23 mils)				
NaCl	2.00	4.10	—	14.1
	1.00	3.32	98*	19.2
	0.500	1.95	50*	32.5
	0.100	1.06	10.67	60.0
	0.010	0.54	1.18	116
	0.000	0.46*	0	138*
HCl	1.00	21.4	—	2.96
	0.10	7.90	39.13	8.0
	0.01	3.98	4.12	15.9
	0.00	3.6*	0.0	17.6*
KCl	2.00	6.20	—	9.50
	1.00	3.77	—	15.5
	0.10	2.05	12.90	28.6
	0.01	1.16	1.41	50.3
	0.00	1.0*	.00	58.5*
Amberplex A-1 (26 mils)				
NaCl	2.00	2.84	—	22.3
	1.00	1.90	98*	33.4
	0.100	0.844	10.67	75.4
	0.050	0.698	5.55	100
	0.010	0.511	1.18	124
	0.000	0.46*	00	138*
NaOH	1.00	12.1	—	5.25
	0.10	3.35	22.21	18.9
	0.01	1.50	2.38	42.3
	0.00	1.1*	0.0	57.6*
KCl	1.00	2.73	—	24.2
	0.10	1.47	12.90	45.0
	0.01	1.04	1.41	63.6
	0.00	0.97*	0.00	68.0*

* Extrapolated values

The concentration potentials of the following cell were measured in order to determine the membrane potentials of Amberplex C-1 and Amberplex A-1 over a range of solution concentrations:

Hg, Hg_2Cl_2	KCl (sat'd in agar)	KCl (C_2)	mem-brane	KCl (C_1)	KCl (sat'd in agar)	Hg_2Cl_2, Hg

Saturated calomel electrodes, whose equivalence was checked, were used as reference electrodes, and the measurements were made at 25°C ± 0.5° using a Type K-2 Leeds and Northrup potentiometer. The membranes were equilibrated in a solution of concentration $\bar{N} = (C_2 + C_1)/2$ before being clamped

between two Plexiglas half cells containing the solutions C_2 and C_1. $\bar{N}$ ranged from 0.03 to 1.5 equivalents per liter and C_2/C_1 was kept constant at a value of 2. The measured potentials were corrected for the asymmetric junction potential between the agar bridges and the two solutions, a correction amounting to about 0.3 mv for $C_2/C_1 = 2$ for KCl solutions. The values of E are considered reproducible to ±0.2 mv and were constant with respect to time if the solutions were renewed frequently to eliminate effect of diffusion through the membrane.

In Table II the results of the measurements, along with the transport numbers and the degrees of permselectivity calculated from the potentials, are tabulated.

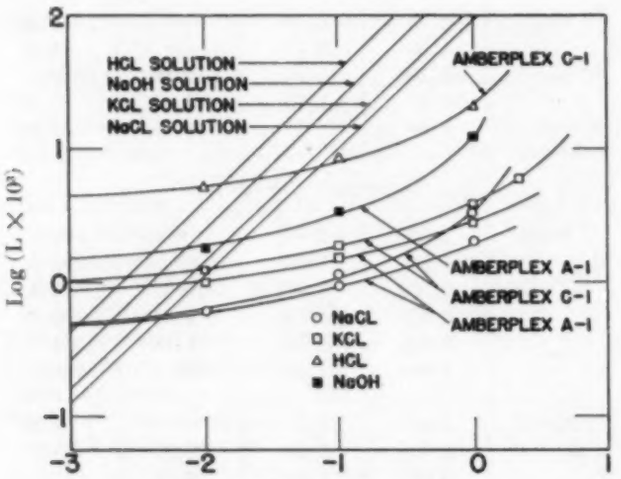

FIG. 2. Specific conductance, L, of ion exchange membranes and of electrolytic solutions in equilibrium with them.

Fig. 1 shows a plot of permselectivity as a function of concentration $\bar{N}$ for both membranes.

The conductivity of the membranes equilibrated with electrolytic solutions of varying strength is given in Table III and Fig. 2, expressed in terms of specific conductivity. The thickness of the membrane is also given, hence it is easy to calculate the resistance per unit area of the membrane from the specific conductance. The measurements were made using a 1000-cycle a-c bridge constructed of Leeds and Northrup equipment, including a Wagner ground to eliminate sound in the earphones due to current flow from the bridge circuit through the earphones to ground. The Plexiglas cells were used to measure the resistance of the solutions without the membrane, then the resistance of both solution and membrane equilibrated with the solutions. From the membrane dimensions and difference between the resistance measurements, the specific conductivity and the resistance per cm² of the membrane were calculated. The measurements, usually made at 25°–27°C were corrected to 25°C by assuming a temperature dependence of membrane resistance similar to that of aqueous electrolytic solutions.

Discussion

The electrochemical properties of Amberplex C-1 and A-1 are shown to be such as would be predicted from theoretical considerations. Table II and Fig. 1 show that permselectivity of either membrane approached 100 per cent at low concentrations, dropping steadily with mounting concentration of the surrounding solution. Even at a relatively concentrated solution of 1.5$\bar{N}$ both membranes have a permselectivity of about 65 per cent. It is interesting to note that for dilute solutions the anion exchange membrane Amberplex A-1 has about the same permselectivity in KCl solutions as the cation exchange membrane Amberplex C-1, despite a somewhat lower fixed-ion concentration in the former. The explanation for this may involve the effect of the electroendosmotic transport of water across the membrane, neglected in the derivation of equation (III). In solutions of low concentration, this effect would cause considerable transport of water per unit charge transferred across the membrane. Moreover, the electroendosmotic transport of water would be proportional to the fixed ion concentration (18) and would thus be more serious for Amberplex C-1 than for Amberplex A-1, reducing its calculated permselectivity at low concentrations more markedly than that of Amberplex A-1.

It can be seen that the ratio of the measured membrane potential to the maximum potential possible for a perfectly permselective membrane is a close approximation of the degree of permselectivity defined by equation (X). There is no formal relationship between the ratio E/E_0 and the permselectivity property defined by equation (X). The close numerical approximation between the values calculated using these equations is possible only for an electrolyte whose cation and anion have nearly the same mobility in aqueous solution, e.g., potassium chloride.

Table III and Fig. 2 demonstrate that the conductivity of the permselective ion exchange membranes approaches a minimum value at low concentrations of external solutions. As would be expected from analogy with aqueous solutions, the hydrogen form of the cation exchange membrane Amberplex C-1 is much more conducting than the salt form. Similarly, the hydroxyl form of anion exchange membrane Amberplex A-1 has a relatively high conductivity. For all forms of the membranes, the membrane conductivity and solution conductivity

are similar in the region of external concentration equal to about 0.01*N*. Below this concentration, the current limiting resistance of a membrane-solution system is the solution, while above it the membrane is the limiting resistance.

Applications

From the study of a number of applications, it has become evident that the ion exchange membranes Amberplex C-1 and Amberplex A-1 are particularly suited to many electrochemical processes in which the object is to produce pure chemicals. For example, instead of adjusting the *p*H of solutions by the addition of acids or bases, it is a simple matter to cause the proper ions (either cations or anions) to migrate through a membrane when a voltage is applied. The electrical power involved is frequently less than the cost of chemical agents which would otherwise be required. At the same time, the solution being treated does not suffer from the introduction of a salt, which often complicates subsequent operations such as crystallization and distillation. In addition, in most cases a useful by-product, such as an acid or base, is recovered in the other electrode compartment and it may even be worthwhile to collect the gases—hydrogen, oxygen, or chlorine—which are liberated at the electrodes.

A specific example of the use of the cation exchange membrane is the preparation of sebacic acid from its sodium salt. Current practice involves the addition of sulfuric acid to a water solution of sodium sebacate so as to form sodium sulfate and free sebacic acid, the latter of which precipitates. The organic acid is filtered, washed and dried. The electrochemical process is carried out in a two-chamber cell, in which the electrode chambers are separated by a cation exchange membrane. The anolyte is the solution of sodium sebacate, while the catholyte is a dilute sodium hydroxide solution. Under an impressed potential, sodium ions migrate readily through the cation permeable membrane out of the anode chamber into the cathode chamber, while at the anode hydrogen ions are produced and oxygen is liberated. As the acidity of the anolyte increases, sebacic acid settles out as a soft, white precipitate. The concentration of caustic in the cathode compartment meanwhile increases. Migration of hydroxyl ions toward the anode is substantially impeded by the permselective cation exchange membrane.

There are, thus, three advantages in the electrolytic process as compared with the conventional method; no additional chemical agent (sulfuric acid) is required; the desired product is not contaminated by added salts; sodium hydroxide is recovered for re-use in the treatment of castor oil to produce sodium sebacate.

An example of the use of the anion exchange membrane is the liberation of ethylenediamine from its hydrochloride. Normally, the step is carried out by neutralizing with caustic. Unfortunately, the sodium chloride so introduced creates a considerable operational problem in the subsequent recovery of the free amine by distillation. The electrolytic process can again be carried out in a two-chamber cell, the separating membrane in this case being an anion exchange membrane. The catholyte is the ethylenediamine hydrochloride solution, and the anolyte is dilute hydrochloric acid. Chloride ions migrate from the cathode chamber through the anion permeable membrane and into the anode chamber. Hydroxyl ions are formed and hydrogen is liberated at the cathode and the free amine is left in the cathode chamber. Migration of hydrogen ions from the anode chamber into the catholyte is prevented by the permselective nature of the anion exchange membrane. Chlorine is liberated at the anode if the hydrochloric acid solution is sufficiently concentrated, and can be collected.

Here again the saving in additional chemical reagents, the liberation of the amine in a solution uncontaminated by salt, and the recovery of a useful by-product are advantages of the electrolytic process.

Many similar applications involving the use of a single ion exchange membrane separating two electrode chambers have been examined. Space permits mentioning only a few, such as the recovery of sodium hydroxide and sulfuric acid from waste sodium sulfate, production of caustic by the electrolysis of brine, and precipitation of magnesium hydroxide from sea water.

Three-chamber cells, using two membranes, have been used to advantage in several cases. For example, sodium hydroxide and sulfuric acid have been produced from sodium sulfate in a cell made up according to the scheme:

cathode: dilute NaOH: cation exchange membrane: sodium sulfate solution: anion exchange membrane: dilute H_2SO_4: anode.

Finally, it should be mentioned that two-, three-, and higher-multiple chamber cells have been operated successfully in flowing systems with the obvious benefits which accrue to continuous operation.

Acknowledgment

The authors wish to acknowledge the assistance of Mr. Charles F. Ryan, Miss Irene Rodalewicz, and Miss Rita Palm during the course of the experimental work.

Any discussion of this paper will appear in a Discussion Section, to be published in the December 1953 issue of the JOURNAL.

REFERENCES

1. L. MICHAELIS AND A. A. WEECH, *J. Gen. Physiol.*, **11**, 147 (1927).
2. K. SOLLNER, *J. Electrochem. Soc.*, **97**, 139C (1950).
3. K. SOLLNER AND H. P. GREGOR, *J. Phys. Chem.*, **51**, 299 (1947).
4. K. SOLLNER AND H. P. GREGOR, *J. Coll. Sci.*, **6**, 557 (1951).
5. K. SOLLNER AND H. P. GREGOR, *J. Coll. Sci.*, **7**, 37 (1952).
6. J. T. CLARKE, J. A. MARINSKY, W. JUDA, N. W. ROSENBERG AND S. ALEXANDER, *J. Phys. Chem.*, **56**, 100 (1952).
7. W. JUDA, N. W. ROSENBERG, J. A. MARINSKY AND A. A. KASPER, *J. Am. Chem. Soc.*, **74**, 3736 (1952).
8. W. JUDA AND W. A. MCRAE, *J. Am. Chem. Soc.*, **72**, 1044 (1950).
9. T. R. E. KRESSMAN, *Nature*, **165**, 568 (1950).
10. M. R. J. WYLLIE AND H. W. PATNODE, *J. Phys. Chem.*, **54**, 204 (1950).
11. T. TEORELL, *Proc. Soc. Exp. Biol. Med.*, **33**, 282 (1935).
12. T. TEORELL, *Z. Elektrochem.*, **55**, 460 (1951).
13. K. H. MEYER AND J. F. SIEVERS, *Helv. Chim. Acta*, **19**, 649, 665 (1936).
14. K. F. BONHOEFFER, L. MILLER, AND U. SCHINDEWOLF, *Z. Phys. Chem.*, **198**, 270 (1951).
15. G. MANECKE, *Z. Elektrochem.*, **55**, 672 (1951).
16. G. MANECKE AND K. F. BONHOEFFER, *Z. Electrochem.*, **55**, 475 (1951).
17. C. E. MARSHALL AND W. E. BERGMAN, *J. Am. Chem. Soc.*, **63**, 1911 (1941).
18. G. SCHMID, *Z. Elektrochem.*, **54**, 424 (1950).
19. G. SCHMID, *Z. Elektrochem.*, **55**, 229 (1951).
20. C. E. MARSHALL, *J. Phys. and Colloid Chem.*, **52**, 1284 1948).
21. D. MACINNES, "Principles of Electrochemistry," Reinhold Publishing Corp., New York (1939).

Acid Strengths of the Phenylacetic Acids[1]

MARY L. KILPATRICK

Department of Chemistry, University of Pennsylvania, Philadelphia, Pennsylvania

AND

EDWARD FACKENTHAL[2]

Department of Chemistry, Illinois Institute of Technology, Chicago, Illinois

ABSTRACT

The ratio of dissociation constants $K_{\text{substituted acid}}/K_{\text{acetic acid}}$ was determined in methanol and ethanol for mono-, di-, and triphenylacetic acid by the electrometric and colorimetric methods. In water, the insolubility of triphenylacetic made another procedure necessary with that acid, and the solubility method of Löwenherz was employed. The ratio increases in all three solvents in going from mono- to diphenylacetic, but in going from di- to triphenylacetic it remains constant in water, within the error of the measurements, and decreases in methanol and ethanol. Various explanations of these results are discussed.

INTRODUCTION

From the time of Ostwald on, studies have been made of the effect of substitution upon the dissociation constants of the fatty acids. Derick (1) observed that the change in the logarithm of the dissociation constant, $\log K_s - \log K_u$, depends on the nature and position of the substituent; that the change is one-third that for a similar substitution, one atom nearer to the carboxyl group; and that the change decreases as the acid strength increases, being proportional to $-\log K_s$. For substitution on the alpha carbon his equation becomes

$$\log K_s = \frac{\log K_u}{1 + d} \qquad \text{(I)}$$

where d is the effect caused by one substitution. Applying this equation successively to the phenyl-substituted acetic acids, one obtains for di- and triphenylacetic acids the constants shown in the last column of Table I.

A more detailed examination of the effect of substitution was made by Branch and Calvin (5). For the phenylacetic acids, their equation reduces to

$$\log K_s = \log K_{\text{HAc}} + \frac{A\Sigma I}{1 + |B\Sigma I|} \qquad \text{(II)}$$

where I is the inductive constant for the phenyl group, A a parameter expressing the enhancement of the resonance effect caused by the presence of the substituent, and B is a parameter expressing the fact that saturation occurs with increasing substitution. Putting in the values given by Branch and Calvin for I, A, and B, viz., 1.5, 0.3, and 0.03, respectively, one calculates that

$$K_{\text{H}\phi\text{Ac}} = 4.7 \times 10^{-5};$$
$$K_{\text{H}\phi_2\text{Ac}} = 1.2 \times 10^{-4};$$
$$K_{\text{H}\phi_3\text{Ac}} = 2.7 \times 10^{-4}$$

in water at 25°C.

Jenkins (6) suggested that the number of resonance forms in the anion determines the effect of substitution on acid strength. He also suggested that a linear relationship exists between the dissociation constant of a phenyl-substituted acid and n, the number of resonance forms in the anion. Setting

$$K = 1.65 \times 10^{-5}(n - 1) \qquad \text{(III)}$$

where $n = 2$ for acetic acid, 4 for phenylacetic, and 8 for diphenylacetic, the calculated values

$$K_{\text{HAc}} = 1.65,\ K_{\text{H}\phi\text{Ac}} = 4.95,\ K_{\text{H}\phi_2\text{Ac}} = 11.6 \times 10^{-5}$$

are in fair agreement with the observed (cf. Table I) and the value predicted for triphenylacetic acid is

$$K_{\text{H}\phi_3\text{Ac}} = 15(1.65 \times 10^{-5}) = 24.8 \times 10^{-5}$$

which is close to the values computed from equations (I) and (II). Although the fit of the data to equation (III) is as good as to (I), it seems difficult to justify equation (III). In the phenyl-substituted acetic acids there is no benzenoidal-quinoidal resonance along the carbon chain, the aromatic nucleus being insulated from the acidic portion of the molecule by the alpha carbon atom, so that the aromatic nucleus can be regarded as a unit, with its own polar effect (5). There would accordingly be half as many resonance forms in the acid as in the anion in

[1] Manuscript received August 5, 1952. Paper prepared for delivery before the Philadelphia Meeting of The Electrochemical Society, May 4 to 8, 1952. Abstracted from the dissertation of Edward Fackenthal, to be presented to the Faculty of the Graduate School of the University of Pennsylvania in partial fulfillment of the requirement for the degree of Doctor of Philosophy, January 1953.

[2] Present address: The School of Pharmacy, Temple University, Philadelphia, Pennsylvania.

each case. It seems best to consider equation (III) to be empirical.

An equation of the form

$$\log K_s = \log K_{HAc} + qx - t(x - 1) \quad \text{(IV)}$$

was suggested by Baughan (7) for the chloro- and the phenyl-substituted acetic acids. Here x is the number of substituents, and q and t are adjustable parameters; if q and t for the latter series are obtained from K_{HAc}, $K_{H\phi Ac}$ and $K_{H\phi_2Ac}$, $K_{H\phi_3Ac}$ is calculated to be 27×10^{-5}.

It will be observed that the empirical equations (I) to (IV) all call for an increase in acid strength upon introduction of the third phenyl group into acetic acid, just as is found upon introduction of the third chlorine in the chloroacetic series.

Following Bjerrum (8) a number of authors have treated the problem of the effect of substitution on acid strength in terms of the electrostatic interaction between the dissociating proton and the dipole of

TABLE I. *Application of Derick's equation to the phenyl-substituted acetic acids*

Solvent, water; temp, 25°C

$d = [\log K_{HAc}/\log K_{H\phi Ac}] - 1 = 0.103$

Acid	$10^5 \times$		
	K	K_u	(K_s) calc.
Acetic	1.75[a]		
Phenylacetic	4.88[b, c]		
Diphenylacetic	11.5[b]	4.88	12.3
Triphenylacetic		11.5	26.9

[a] MacInnes and Shedlovsky (2).
[b] Dippy and Williams (3).
[c] Jeffery and Vogel (4).

the substituent. For two nonresonating, monobasic carboxylic acids HA_1 and HA_2

$$\Delta w = kT \ln K_1/K_2 \quad \text{(V)}$$
$$= [W(HA_1) + W(A_2^-) - W(HA_2) - W(A_1^-)]$$

where $W(HA_1)$, $W(A_2^-)$ are the electrostatic free energies of the respective species in the given solvent, it being assumed that the structural contribution to the total work of removing a proton from the acid HA_1 is balanced by that of adding a proton to base A_2^-. Eucken (9) proposed that in computing Δw an "effective" dielectric constant D_E intermediate between that of the solvent and that of the molecules be employed, in place of the dielectric constant of the solvent as in Bjerrum's treatment. Then, if HA_2 is the parent acid and HA_1 the acid formed by replacement of hydrogen by a polar substituent having the dipole moment M,

$$\ln K_1/K_2 = \frac{eM \cos \zeta}{2kTD_E R^2} \quad \text{(VI)}$$

where R is the distance between the proton and the point dipole, and ζ the angle of inclination of the dipole to the line joining it to the proton. A theoretical derivation of D_E has been given by Kirkwood and Westheimer (10) for the cases where the molecules may be considered to be (*a*) spherical cavities, and (*b*) prolate spheroidal cavities, of dielectric constant D_i, placed in a continuous medium of dielectric constant D equal to that of the solvent. For the spherical model

$$\frac{1}{D_E} = \frac{1}{D_i}\left[1 - \frac{4x^{3/2}}{(1+x)^2}\right] + \frac{1}{D}\left[\frac{8x^{3/2}}{(1+x)^2} + \frac{4x^{1/2}}{1+x} - \frac{4 \ln (1+x)}{x^{1/2}}\right] \quad \text{(VII)}$$

Here $x = (R/2)^2/b^2$, where b is the radius of the spherical cavity. The center of the cavity is considered to lie at the midpoint of R.

The application of equations (VI) and (VII) to the phenyl-substituted acetic acids will be discussed in the last section of this paper. It is seen from equations (VII) and (VI) that D_E should decrease, and the relative acid strength increase, on going from a solvent of high to one of low dielectric constant.

Experimental

Preparation of Materials

Phenyl-substituted acetic acids.—Samples of mono-, di-, and triphenylacetic acid from the Eastman Kodak Company were purified by recrystallization from freshly distilled petroleum ether or benzene, were dried in an Abderhalden drier, and stored in separate desiccators over phosphorus pentoxide. Four determinations of the melting point of phenylacetic acid were made, averaging 77.0°C as compared with The International Critical Tables value of 76.5°C. Two determinations of the melting point of diphenylacetic acid gave 148.1° and 148.0°C; the value listed is 148.0°C. Triphenylacetic acid decomposed before melting, but analyses by electrometric titration with standard sodium hydroxide solution, in an atmosphere of nitrogen, gave 99.88 and 99.94 per cent purity.

Lithium salts of the phenyl-substituted acetic acids.—The salts were prepared by neutralization of aqueous lithium carbonate solution with equivalent amounts of alcoholic solutions of the acids. They were crystallized from their solutions, and then recrystallized twice more from absolute ethanol. Lithium triphenylacetate failed to crystallize spontaneously from its alcoholic solution but the addition of petroleum ether precipitated it quite effectively. No analyses of the salts were made, agreement between the results obtained with buffer

solutions prepared from the solid salts, and buffer solutions prepared by partial neutralization of the corresponding acids being considered sufficient evidence of purity.

α-Dinitrophenol.—A sample of 2,4-dinitrophenol from the Eastman Kodak Company was vacuum-sublimed in an Abderhalden drier for five hours at 39°C, and then for twelve hours at 46°C. After recrystallization of the sublimed material from absolute ethanol the melting point was found to be 113.1°C as compared with The International Critical Tables value of 112.6°C.

γ-Dinitrophenol.—A sample of 2,5-dinitrophenol from LaMotte was recrystallized twice from water, and dried in a desiccator over phosphorus pentoxide; mp, 106.1–106.3°C.

Methanol and ethanol.—The alcohols were purified by the method of Lund and Bjerrum (11). Their purity was checked by density measurements.

Acetic acid.—The acid was prepared from a sample of Kahlbaum acetic acid which was found on titration to be 99.55 per cent pure. It was assumed that water was the only impurity present, and an amount of Kahlbaum acetic anhydride equivalent to 110 per cent of the water was added to the acid, the mixture was refluxed for 32 hours, and distilled at 118.3 ± 0.1°C, at 765.5 mm. The corrected boiling point of 118.1°C is in agreement with the value in The International Critical Tables. Analysis by titration with standard sodium hydroxide solution gave 100.05 per cent purity.

Lithium methylate and ethylate solutions.—Each solution (about 0.03*M*) was prepared by dissolving the computed amount of freshly cut metal in the alcohol contained in a bottle fitted with a suction filter, through which the solution was drawn to its permanent container with attached burette. Carbon dioxide was excluded.

Lithium chloride.—Lithium chloride from Kahlbaum was fused in an atmosphere of hydrogen chloride and dried in an Abderhalden drier; the product was neutral.

Quinhydrone.—Quinhydrone from Leeds and Northrup was used without purification.

Electrometric Measurements

The acid strengths of the three phenyl-substituted acetic acids relative to acetic acid were determined by use of the concentration cell

Au	HAc	0.005*M*	.	HX	0.005*M*	Au
	LiAc	0.005*M*	LiCl	LiX	0.005*M*	
	LiCl	0.045*M*	1.00*M*	LiCl	0.045*M*	
	Quinhydrone			Quinhydrone		

where X represents the anion of the substituted acid. For a discussion of the theory underlying the use of the cell, the apparatus, the method of carrying out an experiment, and the computation of the ratio of the dissociation constants of the two acids from E, the measured emf,

$$E = \frac{RT}{\mathbf{F}} \ln \{[H^+]_{HX}/[H^+]_{HAc}\} \qquad \text{(VIII)}$$

the reader is referred to a paper by Elliott and Kilpatrick (12). The symbol $[H^+]$ used in equation (VIII) represents the concentration of the solvated proton.

A test was carried out with water as solvent and phenylacetic acid as HX in order to compare $K_{H\phi Ac}/K_{HAc}$ determined electrometrically with the ratio computed from the individual constants $K_{H\phi Ac}$ (3) and K_{HAc} (2) obtained conductimetrically. Letting

$$K_{HX}/K_{HAc} = K_{A_xB_0} \qquad \text{(IX)}$$

the value found for $\log K_{A_xB_0}$ was 0.448, as compared with 0.445 computed from the conductimetric values for $K_{H\phi Ac}$ and K_{HAc}. As in the cases given by Elliott and Kilpatrick, the agreement between the electrometric value at $\mu = 0.05$ and the conductimetric at $\mu = 0$ shows that the ratio of dissociation constants does not change with ionic strength up to $\mu = 0.05$.

The precision measure of the electrometric determinations was estimated to be 0.01 in $\log K_{A_xB_0}$. All measurements were made at 25 ± 0.1°C. The results obtained are given in Table III.

Colorimetric Measurements

The strength of the substituted acid, relative to that of acetic acid, was also obtained by determining colorimetrically the equilibrium constants K_{AiB_0} and K_{AiB_x} for the reactions

$$Ac^- + HP \rightleftharpoons P^- + HAc$$
$$X^- + HP \rightleftharpoons P^- + HX$$

where HP represents the acid form of the indicator (α- or γ-dinitrophenol) and P^- the basic form. It follows that

$$K_{HX}/K_{HAc} = K_{A_xB_0} = K_{AiB_0}/K_{AiB_x} \qquad \text{(X)}$$

where $K_{A_xB_0}$ is the equilibrium constant for the reaction

$$HX + Ac^- \rightleftharpoons X^- + HAc.$$

The measurements were made with an Evelyn photoelectric colorimeter manufactured by the Rubicon Company, Philadelphia. The filters and the galvanometer were also supplied by Rubicon. With water as solvent, the absorption was measured in calibrated test tubes, about 10 ml of solution being used. With ethanol or methanol, it was measured in a cylindrical cup whose effective depth was main-

tained constant by means of a plunger; here about 1 ml of solution was used. The cup and plunger were always cleaned in the same manner before refilling with a new solution. Both were washed with distilled water, then with alcohol, and dried, first with absorbent tissue and finally with a linen handkerchief free from lint.

The colorimeter was adjusted at the start to give a galvanometer reading of 100.0 with pure solvent in the absorption cell ($G_0 = 100.0$), and the constancy of illumination was checked at frequent intervals during the experiment, readjustment to $G_0 = 100.0$ being made whenever necessary.

The procedure in carrying out an experiment was to determine E_{Bi}, the Beer's Law constant for the basic form of the indicator, measure the buffer solution, and then redetermine E_{Bi}. To determine E_{Bi}, a solution containing the indicator at concentration M_{DNP}, and enough base to ensure that the indicator be in the basic form, was diluted with a solution of base; it was found that, within the experimental error, the extinction was directly proportional to F, the fraction of the original concentration of indicator,

$$E = \log G_0 - \log G = E_{Bi}F$$

and E_{Bi} was taken as the average for the set. In computing the indicator ratio [Bi]/[Ai] in the buffer solutions the mean of the initial and final values of E_{Bi} was employed.

With the Rubicon filter No. 440, or 440 plus 4302, there was negligible absorption of light by the acid form of the indicator, but this was no longer true with No. 400 and 420, and the Beer's Law constants E_{Ai} for the acid forms of the dinitrophenols were accordingly measured with the latter filters. The indicator ratio was computed by means of the equation

$$[Bi]/[Ai] = \{E - E_{Ai}\}/\{E_{Bi} - E\}.$$

Most of the measurements were made with Filter No. 440 or 440 plus 4302.

During the course of the colorimetric runs no attempt was made to regulate the temperature, which ranged from 23.0° to 30.3°C. It was believed that while K_{AiB} would undoubtedly vary with the temperature, the temperature coefficient would be about the same for the parent and the substituted acid, and the ratio $K_{A_xB_0}$ little affected. This proved to be the case. For example, for triphenylacetic acid in methanol, where the range in temperature was greatest, the results

$\log K_{A_xB_0}$	0.313	0.339	0.305	0.315
Temp, °C	30.3	29.6	24.5	23.3

show that any effect of change in temperature lies within the experimental error of the measurements.

A typical colorimetric experiment is shown in Table II. The buffer solutions were made up by partial neutralization of acid by lithium ethylate to have a buffer ratio of 5.000. In determining E_{Bi} three dilutions of the original solution were made, and E_{Bi} is the average of values obtained at $F = 1.0$, 0.7, 0.5, and 0.3, respectively. The values of K_{AiB} are listed in the order in which they were determined. It will be seen that there is no trend in $K_{A_xB_0}$ with change in ionic strength, and consequently the average value may be taken as the thermodynamic equilibrium constant.

The colorimetric and electrometric determinations are summarized in Table III. The electrometric determinations were all obtained with a buffer ratio of 1/1 for both parent and substituted acid. In the colorimetric determinations, on the other hand, the buffer ratio was sometimes varied, e.g., the four

TABLE II. *Typical colorimetric determination of* $K_{A_xB_0}$

Parent acid, HAc — Solvent, C_2H_5OH
Substituted acid, HφAc — Avg temp, 29.0°C
2,5-Dinitrophenol, $5.0 \times 10^{-5}M$ — Filter No. 440
Buffer ratios, $[A_0]/[B_0] = 5/1$; $[A_x]/[B_x] = 5/1$
E_{Bi} at start, 0.1940 ± 0.9%; at end, 0.1894 ± 0.8%

Buffer	Ionic strength	$\frac{[Bi]}{[Bi]+[Ai]}$	K_{AiB_0}	K_{AiB_x}	$\log K_{A_xB_0}$
$A_0 - B_0$	0.020	0.5921	7.26		
$A_x - B_x$	0.020	0.4538		4.16	0.242
$A_0 - B_0$	0.015	0.5895	7.18		
$A_x - B_x$	0.015	0.4465		4.04	.250
$A_0 - B_0$	0.010	0.5952	7.35		
$A_x - B_x$	0.010	0.4507		4.10	.253
$A_0 - B_0$	0.005	0.5921	7.26		
$A_x - B_x$	0.005	0.4502		4.10	.248
			Avg 7.26 ± 0.6%	4.10 ±0.7%	0.248 ± 0.003

values tabulated for diphenylacetic acid in ethanol were obtained with the following pairs of values of $[A_0]/[B_0]$ and $[A_x]/[B_x]$:

4/1, 1/1; 5/1, 3/1; 5/1, 3/1; 5/1, 3/1.

The stoichiometric buffer ratio was corrected when necessary for the dissociation of the acid.

Solubility Measurements

It will be observed that no value of $\log K_{A_xB_0}$ is given in Table III for di- or triphenylacetic acid in water. For diphenylacetic, $K_{A_xB_0}$ may be computed from known values of $K_{H\phi_2Ac}$ and K_{HAc}, but for triphenylacetic the very slight solubility of the acid in water has hitherto prevented determination of the dissociation constant.

To obtain the dissociation constant of triphenylacetic acid in water we resorted to the solubility

method of Löwenherz (12a, 13). This calls for the dissolution of a sparingly soluble acid in the solution of a base of appropriate strength, whereupon acid is converted to its conjugate base, and more dissolves.

TABLE III. *Summary of colorimetric and electrometric determinations of* $K_{A_xB_0}$

Solvent	$\log K_{A_xB_0}$		
	Color.	emf*	Avg
Phenylacetic acid			
Water	0.455	0.448	
	0.415		
	0.435 Avg		0.442
Methanol	0.243	0.250	
	0.245	0.257	
	0.244 Avg	0.253 Avg	0.249
Ethanol	0.248	0.237	
	0.234	0.231	
	0.241 Avg	0.241	
		0.231	
		0.235 Avg	0.238
Diphenylacetic acid			
Methanol	0.398	0.411	
	0.381	0.411	
	0.379	0.411 Avg	
	0.386 Avg		0.395
Ethanol	0.356	0.384	
	0.347	0.346	
	0.353	0.380	
	0.351	0.384	
	0.352 Avg	0.373 Avg	0.363
Triphenylacetic acid			
Methanol	0.313	0.324	
	0.339	0.324	
	0.305	0.324 Avg	
	0.315		
	0.318 Avg		0.321
Ethanol	0.225	0.242	
	0.235	0.235	
	0.233	0.245	
	0.231 Avg	0.241 Avg	0.236

* Temp, 25°C.

We used, as the basic solution, a solution of sodium cacodylate. When equilibrium is established,

$$H\phi_3Ac + Cac^- \rightleftharpoons \phi_3Ac^- + HCac \qquad (XI)$$

$$\frac{K_{H\phi_3Ac}}{K_{HCac}} = \frac{[\phi_3Ac^-][HCac]}{[H\phi_3Ac]_{satd}\,[Cac^-]} = \frac{Y^2}{[H\phi_3Ac]_{satd}\,(C - Y)} \qquad (XII)$$

where $[H\phi_3Ac]_{satd}$ is the solubility of the molecular acid. The other symbols will be defined later. The assumption underlying Löwenherz's method is that the concentration of molecular acid in the saturated solution is the same in water as in dilute solutions of strong electrolytes. Usually the activity coefficients of nonelectrolytes do not differ from unity by more than a few per cent in dilute salt solutions, e.g., the activity coefficient of molecular benzoic acid in 0.1*M* potassium chloride solution at 25°C is 1.04 (14) [cf. also Osol and Kilpatrick (15)]. It will be seen shortly that owing to the difficulty of determining $[H\phi_3Ac]_{satd}$ the assumption is certainly sufficiently good for present purposes.

It proved impractically slow to establish equilibrium starting with solid triphenylacetic acid and a solution of sodium cacodylate, so a sample of acid was dissolved in an excess of sodium hydroxide solution, the solution was warmed to 60–85°C, and into it was run an amount of cacodylic acid solution equivalent to the sodium hydroxide. On cooling to 25°C crystals of triphenylacetic acid formed. They were filtered off. Then to an aliquot of the filtrate hydrochloric acid was added to make the resulting solution 0.1*M*, whereupon triphenylacetic acid equivalent to the triphenylacetate precipitated, and was filtered off, washed with water, dried in an oven at 60°C, and weighed. If crystallization of triphenylacetic acid did not set in after the solution had stood a week or two in the thermostat at 25°C, the solution was evaporated on a water bath under reduced pressure until crystals did form when the temperature was dropped to 25°C. Concentrations were computed in all cases on the basis of the weight of water in the vessel at the time of analysis. The results obtained are shown in the first and second columns of Table IV.

The dissociation constant of cacodylic acid in water at 25°C is 5.33×10^{-7} (16), from which it can be shown that dissociation of the cacodylic acid formed in reaction (XI) is negligible for the solutions of Table IV, so that it is permissible to take

$$[HCac] = [\phi_3Ac^-] = Y \quad \text{and} \quad [Cac^-] = C - Y.$$

The ratio $Y^2/(C - Y)$ then gives the product $[H\phi_3Ac]_{satd} \times \{K_{H\phi_3Ac}/K_{HCac}\}$ according to equation (XII). The values of the ratio listed in the last column of Table IV show no trend with increase in ionic strength, which means that unless there is a compensating change in $K_{H\phi_3Ac}/K_{HCac}$, which is unlikely, $[H\phi_3Ac]_{satd}$ is constant within the error of the measurements. As will be shown later, $[H\phi_3Ac]_{satd}$ is so small that a ten per cent change in it would have no effect on Y and $(C - Y)$.

The remaining step in the determination of $K_{H\phi_3Ac}$ is the measurement of the solubility of the molecular

acid. For this we employed the two methods which are illustrated below by means of a typical run.

Method I.—A 0.2536 g sample of triphenylacetic acid was dissolved in 50 ml of 0.02*M* sodium hydroxide and the resulting solution diluted with water to 100.0 ml. Then 2.00 ml of this solution was diluted to one liter, and there was added, over a period of five minutes, and with vigorous shaking, 3 ml of 12*M* hydrochloric acid solution, after which the flask was placed in the thermostat. An opalescent precipitate gradually appeared. The flask was kept in the thermostat, with occasional removal for shaking, for two hours after the appearance of the precipitate.

TABLE IV. *Equilibrium between triphenylacetic acid and cacodylate ion in water at 25°C*

$[H\phi_3Ac]_{satd.} \times \{K_{H\phi_3Ac}/K_{HCac}\} = Y^2/(C - Y)$

Stoichiometric molarity NaCac $C \times 10^3$	M/l $H\phi_3Ac$ Precipitated, $Y \times 10^3$	$\frac{Y^2}{C-Y} \times 10^4$
13.38	2.539	5.95
9.605	2.150	6.20
7.164	1.845	6.40
6.542	1.745	6.34
5.340	1.571	6.55
5.306	1.568	6.58
3.902	1.276	6.16
3.902	1.290	6.42
		Avg 6.32 ± 0.17

TABLE V. *Solubility of triphenylacetic acid*

Solvent, water; Temp, 25°C

$H\phi_3Ac$ taken, mg/l	M_{HCl} Method I	Solubility, mg/l	
		Method I	Method II
1.3	0.036	0.85	0.7
2.5	0.036	0.95	0.8
5.1	0.036	0.8	0.85
3.8	0.036	0.95	
5.7	0.036	1.0	0.95
1.4	0.036	0.85	0.75
4.3	0.036	0.85	
2.8	0.036	0.8	
1.5	0.024	0.85	
2.9	0.024	0.7	
4.4	0.036	0.8	
5.9	0.060	0.85	
		Avg 0.85 a.d. 6%	Avg 0.85 a.d. 10%

TABLE VI. *Acid strengths of the phenyl-substituted acetic acids at 25°C*

Solvent	$pK = -\log K$			
	HAc	$H\phi Ac$	$H\phi_2Ac$	$H\phi_3Ac$
Water	4.76[a]	4.32	3.94[c]	3.96[d]
Methanol	9.76[b]	9.51	9.36	9.44
Ethanol	10.44[b]	10.20	10.08	10.20

[a] MacInnes and Shedlovsky (2).
[b] Minnick and Kilpatrick (17).
[c] Dippy and Williams (3).
[d] Present investigation, by the solubility method.

At the end of this period the solution was filtered by suction through a crucible with a sintered glass bottom. The crucible, held in a handkerchief, was placed over the top of the flask, the combination was inverted, the crucible fitted into the holder in the suction flask, and the volumetric flask clamped to a ringstand. The height of the inverted flask was regulated to keep the self-filling crucible one-third full. The precipitate of triphenylacetic acid was washed with water until free of chloride, dried in an oven at 60°C, weighed, and rewashed and dried to constant weight. The constant weight of crucible plus precipitate was 10.2670 g after washing with 50 + 30 + 30 + 30 ml of water. Since the weight of the empty crucible was 10.2627 g, and since the solution was made up to contain 51 mg of acid in 1.00 liter, there remained in solution 0.0051 − 0.0043 = 0.0008 g.

The precipitate in the crucible was next extracted with warm benzene. After washing with 30 + 30 ml of benzene the weight of the crucible was constant at 10.2627 g. The acid extracted therefore weighed 0.0043 g and the solubility was again 0.0051 − 0.0043 = 0.0008 g.

Method II.—The filtrate obtained in the experiment described above, viz., one liter of saturated solution, was evaporated to dryness in a 200-ml quartz beaker. The residue was treated with a few drops of 0.02*M* sodium hydroxide solution, washed with water into a crucible, and filtered. The final volume of the filtrate plus washings was 15–20 ml. The triphenylacetic acid in the filtrate was precipitated by the addition of 5 ml of 12*M* hydrochloric acid, and the precipitate was transferred to a suction crucible which had previously been weighed. The precipitate was washed and dried to constant weight, as before. The constant weight of crucible plus precipitate was 11.8934 g and the weight of the empty crucible 11.8925 g. Hence there was obtained 0.0009 g of acid from a liter of the saturated solution. The precipitate in the crucible was next extracted with warm benzene, as before; the amount extracted was 0.0008 g. The average solubility by Method II was therefore 0.00085 g/l.

The results obtained are listed in Table V. The hydrochloric acid concentration given in the second column is that of the solution in which the precipitate of triphenylacetic acid formed, in Method I. When the solubility is given to two decimal places, in column 3 or 4, it is due to the fact that the figure

recorded is the average of the values without and with extraction of the precipitate by benzene.

According to the data of Table V, the first approximation to the solubility of molecular triphenylacetic acid is $0.00085/288 = 3.0 \times 10^{-6}$ mole/l, and computing a first value of $K_{H\phi_3Ac}$ from equation (XII) one obtains 1.1×10^{-4}. However, since less than one per cent of the acid would be present as ions in the hydrochloric acid solutions of Table V—which is much less than the error of the measurements—these may be accepted as the final values.

Discussion

In Table VI are shown the values of pK for acetic acid and the phenyl-substituted acetic acids, in water, methanol, and ethanol. The pK's for the substituted acids were computed, with two exceptions, from K_{HAc} as given in the second column of Table VI and log $K_{A_xB_0}$ as given in the last column of Table III.

The dissociation constants themselves are shown in Fig. 1, plotted as functions of $(n - 1)$, where n is the number of resonance forms in the anion (6). Reading from left to right, the four points on each curve represent acetic, mono-, di-, and triphenylacetic acid, respectively. It is clear that the relationship proposed by Jenkins fails for triphenylacetic acid in water, and that it fails for both di- and triphenylacetic in the alcohols. The fact that tri- is no stronger than diphenylacetic in water, and is definitely weaker than diphenylacetic in the alcohols, is contrary to the predictions of equations (I), (II), and (IV) also.

It may be of interest to point out that trichloroacetic acid and trimethylacetic acid do not exhibit the anomalous behavior of triphenylacetic. The fit of the data for the chloroacetic acids to the empirical equations is complicated by the fact that there is no reliable value of the dissociation constant of trichloroacetic acid in water; however, Baughan (7) has pointed out that in methanol there is good agreement between the observed value and that calculated by equation (IV). Similarly, Branch and Calvin (5) list for the dissociation constant of trimethylacetic acid in water, as calculated by equation (II), a value close to that observed.

In Fig. 2, log $K_{A_xB_0}$ is plotted against the reciprocal of the dielectric constant of the solvent to test the Wynne-Jones (18) equation

$$\ln K_{A_xB_0} = \ln K_{a_xb_0} + \frac{e^2(2Z_A - 1)}{2kT}\left[\frac{r_{A_0} - r_{A_x}}{r_{A_0}r_{A_x}}\right]\left(\frac{1}{D}\right)$$

where $K_{a_xb_0}$ is the limiting value of $K_{A_xB_0}$ for $D = \infty$, Z_A is the charge on the acid, and r_{A_0} and r_{A_x} are the effective radii of the acids. A linear relationship between log $K_{A_xB_0}$ and $1/D$ is not observed in the present case. For each of the phenyl-substituted acids $K_{A_xB_0}$ in water is considerably larger than the value predicted by extrapolation of the line through the points in methanol and ethanol.

The data of Table VI cannot be explained on the basis of the Kirkwood-Westheimer theory, for according to equations (VI) and (VII) a lowering of the dielectric constant of the solvent should result in a decrease in D_R and a consequent increase in the strength of the substituted acid. A decrease in $K_{A_xB_0}$ is, however, observed in every case. This means that if the position of the point dipole in the molecule of the substituted acid remains unchanged with change of solvent, it is necessary to assume a considerable decrease in the radius of the molecular cavity on going from water to methanol or ethanol.

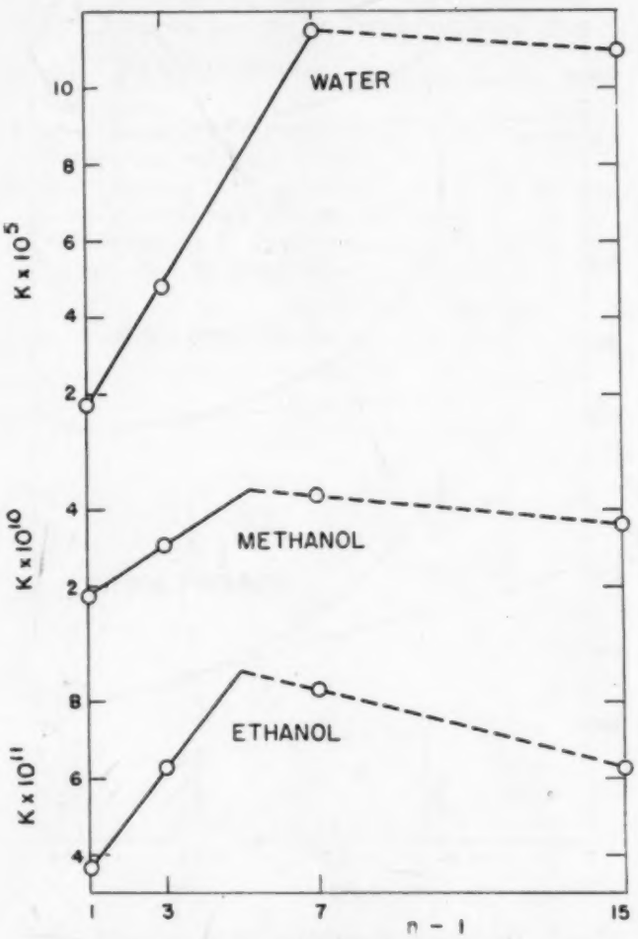

Fig. 1. The Jenkins relationship for the phenyl-substituted acetic acids.

It does not appear fruitful to apply Brown's (19, 20) concept of bond strains to the phenyl-substituted acetic acids, because any strain resulting from introduction of phenyl groups into the molecule would affect the bond between the alpha carbon and the carboxyl carbon, not the oxygen-hydrogen bond,

so the same strain should operate in the molecule and in the anion. Consideration of the geometry of the molecule of a phenyl-substituted acetic acid shows, however, that there can be interference between a carboxyl oxygen and hydrogen attached to an ortho carbon atom, which might cause the oxygen to move closer to the second oxygen atom of the carboxyl group. If form II below makes a significant contribution to the resonance energy, displacement of the oxygen atoms toward each other, with introduction of successive phenyl groups, would be acid-weakening. The contribution of II is however expected to be small (5).

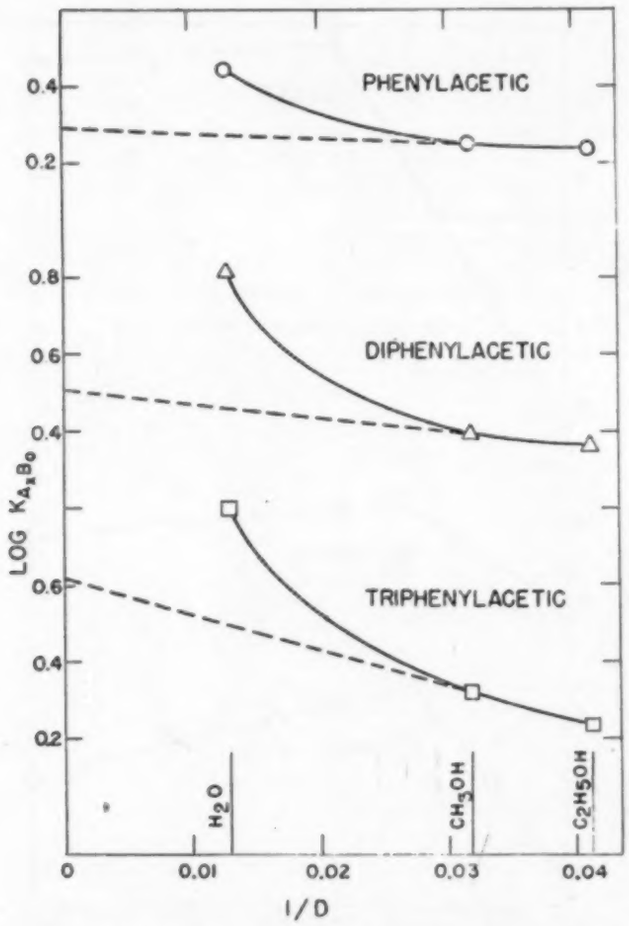

FIG. 2. The relative strengths of the phenyl-substituted acetic acids.

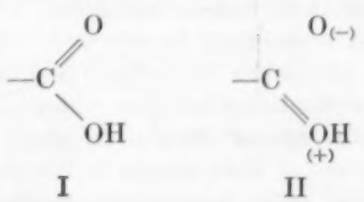

I II

It might be thought that the failure of the third phenyl group to bring about an increase in acid strength was due to dimer formation through hydrogen bonding:

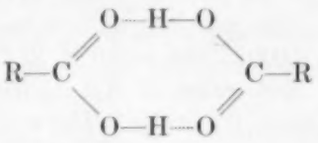

In the dimer of triphenylacetic acid the bonds would be surrounded by a barrier of six bulky phenyl groups, which would tend to prevent the contact with solvent molecules which is necessary for ionization. If appreciable dimerization occurred with these acids, however, it would have become evident in the colorimetric experiments in which the concentration of acid in the buffer solution was varied. Assuming that only the monomer ionizes (21), and introducing the association constant L

$$2\ HA \rightleftharpoons H_2A_2$$

$$[H_2A_2] = L[HA]^2$$

and setting the stoichiometric concentration of buffer acid equal to a, and that of buffer base to b, one has for the apparent classical ionization constant

$$K = [H^+]\{b + [H^+]\}/\{a - [H^+]\}$$

and for the true constant

$$K' = [H^+]\{b + [H^+]\}/\{a - [H^+] - 2L[HA]^2\}.$$

For $L = 1$, the ratio K'/K changes from 1.17 at $a = 0.1M$ to 1.30 at $a = 0.2$, and for larger L's, doubling a causes a pronounced increase in the ratio at lower concentrations. Change in K'/K would cause a corresponding change in the relative strength computed from the apparent rather than the true ionization constant. No trend in $K_{A_xB_0}$ or in $K_{A/B}$ was found in the colorimetric experiments upon reducing the acid concentration, however.

The decrease in solubility with increase in the number of phenyl groups in the acid is shown below for water as solvent, at a temperature of 25°C.

Acid	*Solubility (moles/l)*
$H\phi Ac$	0.131
$H\phi_2Ac$	0.00060
$H\phi_3Ac$	0.000021

The solubilities of the first two are from The International Critical Tables; that of the third is calculated from $K_{H\phi_3Ac}$ and $[H\phi_3Ac]_{satd.}$ The same order was found in the alcohols. The decrease in solubility suggests that perhaps extent of solvation is an important factor here. If the solvation of the anion is much more extensive, owing to its charge, than that of the molecular acid, and if the extent of

solvation decreases with introduction of successive phenyl groups, in the reaction

$$H\phi_3Ac + \phi_2Ac^- \rightleftharpoons H\phi_2Ac + \phi_2Ac^-$$

the right-to-left process will be favored, by solvation, over the left-to-right.

Any discussion of this paper will appear in a Discussion Section, to be published in the December 1953 issue of the JOURNAL.

REFERENCES

1. C. G. DERICK, *J. Am. Chem. Soc.*, **33,** 1152 (1911).
2. D. A. MACINNES AND T. SHEDLOVSKY, *J. Am. Chem. Soc.*, **54,** 1429 (1932).
3. J. F. J. DIPPY AND F. R. WILLIAMS, *J. Chem. Soc.*, **1934,** 161.
4. G. H. JEFFERY AND A. I. VOGEL, *J. Chem. Soc.*, **1934,** 166.
5. G. E. K. BRANCH AND M. CALVIN, "The Theory of Organic Chemistry," Ch. VI, Prentice-Hall, Inc., New York (1941).
6. H. O. JENKINS, *Nature*, **145,** 149 (1940); **145,** 625 (1940); *J. Chem. Soc.*, **1940,** 1447.
7. E. C. BAUGHAN, *Nature*, **146,** 461 (1940).
8. N. BJERRUM, *Z. physik. Chem.*, **106,** 219 (1923).
9. A. EUCKEN, *A. angew. Chem.*, **45,** 203 (1932).
10. J. G. KIRKWOOD AND F. H. WESTHEIMER, *J. Chem. Phys.*, **6,** 506 (1938).
11. H. LUND AND J. BJERRUM, *Ber.*, **64B,** 210 (1931).
12. J. H. ELLIOTT AND M. KILPATRICK, *J. Phys. Chem.*, **45,** 472 (1941).

12a. R. LÖWENHERZ, *Z. physik. Chem.*, **25,** 394 (1898).

13. K. J. PEDERSEN, *Kgl. Danske Videnskab. Selskab. Mat.-fys. Medd.*, **14,** No. 9 (1937).
14. E. F. CHASE AND M. KILPATRICK, *J. Am. Chem. Soc.*, **53,** 2589 (1931).
15. A. OSOL AND M. KILPATRICK, *J. Am. Chem. Soc.*, **55,** 4430 (1933); **55,** 4440 (1933).
16. M. L. KILPATRICK, *J. Am. Chem. Soc.*, **71,** 2607 (1949).
17. L. J. MINNICK AND M. KILPATRICK, *J. Phys. Chem.*, **43,** 259 (1939).
18. W. F. K. WYNNE-JONES, *Proc. Roy. Soc. London*, **A140,** 440 (1933).
19. H. C. BROWN, H. I. SCHLESINGER, AND Z. CARDON, *J. Am. Chem. Soc.*, **64,** 325 (1942).
20. H. C. BROWN, H. BARTHOLOMAY, AND H. B. TAYLOR, JR., *J. Am. Chem. Soc.*, **66,** 435 (1944).
21. A. KATCHOLSKY, H. EISENBERG, AND S. LIFSON, *J. Am. Chem. Soc.*, **73,** 5889 (1951).

The Capacity of Polarized Platinum Electrodes in Hydrochloric Acid[1]

W. D. Robertson[2]

Hammond Metallurgical Laboratory, Yale University, New Haven, Connecticut

ABSTRACT

Electrode capacity of platinum electrodes was measured in hydrochloric acid by an impedance bridge. Capacity was determined as a function of polarizing voltage, concentration, and frequency. It appears that electrode capacity cannot be interpreted exactly in terms of a simple equivalent circuit. Capacity, calculated as a series circuit, goes through a minimum at 20 μf/cm^2 and +0.75 volt on the *N* calomel scale. Comparison of platinum with mercury at the minima indicates that the difference in potential, 1.85 volts, corresponds to the contact potential difference.

Introduction

In general, the concentration of ions near a metal surface immersed in an aqueous electrolyte is different from that in the homogeneous volume of electrolyte at some distance from the surface (1). Since conditions in the immediate vicinity of a surface may be presumed to control reaction rates, a detailed understanding of the mechanism of heterogeneous kinetics requires investigation of the ionic atmosphere near a surface with respect to the activity of more or less close-packed ions and their association with metallic surface atoms (ions).

The analytical methods employed must be such that the prevailing steady state is not disturbed. Furthermore, the measurement of the small excess surface concentration, and its distribution in space, requires sensitivity beyond the range of conventional techniques. Fortunately there are indirect electrical methods that conform to the preceding conditions; but extensive theoretical and experimental development is necessary before they can be directly applied to heterogeneous reaction kinetics at a solid metal electrode.

A metal surface in contact with an electrolyte is, in effect, a condenser in which the charge consists of electrons in the metallic phase and more or less hydrated ions in the solution phase. The electron charge is probably located in a plane parallel with the metal interface and very close to it, possibly even extending slightly beyond it under certain conditions; the ionic charges are variously distributed according to type and external polarization but, in general, there will be a layer of adsorbed ions at a distance equal to the effective ionic radius and a diffuse ionic atmosphere in which ions of one sign predominate. The excess charge in the diffuse layer decreases rapidly with distance and the half thickness is usually less than 100 Å.

It is possible, in principle, to measure the capacity of this condenser and thereby to investigate the constitution of the interphase boundary with respect to magnitude and distribution of charge. The most extensive investigations of this kind have been made on mercury by Grahame and by Frumkin and the theoretical and experimental work has been reviewed by Grahame (2). Ershler and coworkers (3–5) have also investigated the electrode capacity of platinum electrodes in connection with the mechanism of hydrogen overvoltage and for the purpose of comparison with previous work on mercury. However, the specific values obtained for platinum are uncertain because the area was never well defined and the effect of frequency, when it was investigated, was found to be large; also, unlike mercury for which electrode capacity may be derived from surface tension (electrocapillary) measurements, there is no independent method of measuring electrode capacity of solid metals and consequently no direct method of verifying the results, other than internal self-consistency and reproducibility.

The present work is primarily concerned with the determination, by an impedance bridge method, of the specific electrode capacity of platinum in hydrochloric acid as a function of applied polarizing potential, concentration, and frequency of the small component of alternating current superimposed on the direct current polarization. Additional experimental variables and techniques are also considered in some detail.

Apparatus

The electrode capacity of solid metals may be measured either by direct current methods (6, 7) in which charge and associated potential change are

[1] Manuscript received August 7, 1952. This paper was prepared for delivery before the Philadelphia Meeting, May 4 to 8, 1952.

[2] The experimental work reported was done while the author was Research Associate, Institute for the Study of Metals, University of Chicago.

determined, or by the use of an alternating current bridge. The most versatile method employs an appropriately designed impedance bridge with which the differential capacity, dq/dE, may be measured over a range of frequencies and applied polarizing voltage. The principal modification from conventional bridge circuits is the use of a low alternating probe voltage of less than 10 millivolts, which requires large amplification in the detector circuit. Except for amplifier and filter, the apparatus employed, Fig. 1, is similar to that developed by Grahame for measurements on mercury (8). It consists of a variable frequency audio oscillator, a potentiometer input voltage control (General Radio Microvolter), and a shielded bridge transformer feeding a series resistance-capacitance bridge assembled with precision decade resistors and condensers, all appropriately shielded and grounded at a single point. The detector circuit consists of a high gain, tuned amplifier, a variable frequency filter, and oscilloscope null indicator.

Considerable care is required in design and assembly of bridge components to eliminate extraneous capacity, which introduces error, and to eliminate interference which reduces sensitivity, particularly at low frequencies. Interference was essentially eliminated by complete shielding of all components and connections and by employing battery-powered units in the output circuit as well as a tuned amplifier and filter. The operation of the assembled bridge was evaluated by measuring high quality calibrated mica condensers and noninductive resistors in various combinations, both with respect to magnitude and frequency dependence; precision was developed to better than one per cent in measuring capacity, in the range in question, and extraneous frequency dependence was entirely eliminated.

The cell containing the platinum electrode and counter electrode constitutes one arm of the bridge, the unknown impedance. Since electrode capacity is a function of potential, it is necessary to measure this quantity and to provide means of varying it from an external battery. The auxiliary polarizing circuit consists of a potentiometer with which the electrode potential is varied with respect to a normal calomel cell in the same solution and an electrometer amplifier in conjunction with a second precision potentiometer that was used to measure the electrode potential. Since both alternating and direct currents are involved, a large inductance was placed in the direct current circuit and condensers were appropriately distributed in the bridge circuit to confine alternating and direct currents to their respective parts of the apparatus.

The all glass cell, Fig. 2, was designed so that it could be readily evacuated and the electrolyte freed of air in a separate container before coming in contact with the electrode surface; subsequently the cell and electrolyte were saturated with hydrogen, unless other atmospheres are specifically indicated. It is important to eliminate all greased joints in contact with the electrolyte since it has been demonstrated (9) that previous erroneous results with mercury have resulted from grease contamination. Connection from the cell to the reference electrode is, therefore, made through an ungreased stopcock, and the joint between the electrolyte reservoir and the cell was fitted with an inner tube through which the

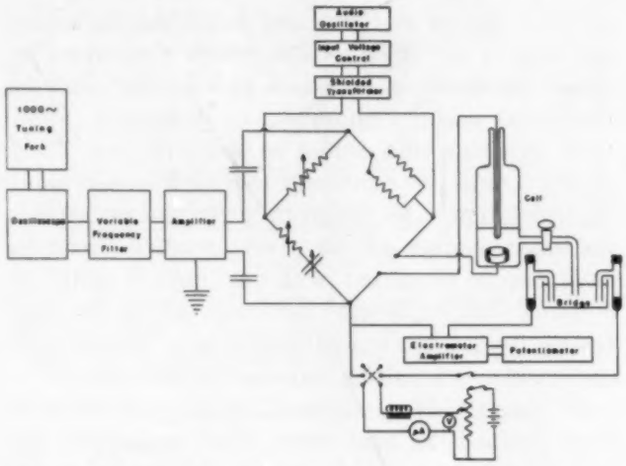

FIG. 1. Impedance bridge and associated electrical circuit employed to measure differential capacity of platinum electrodes.

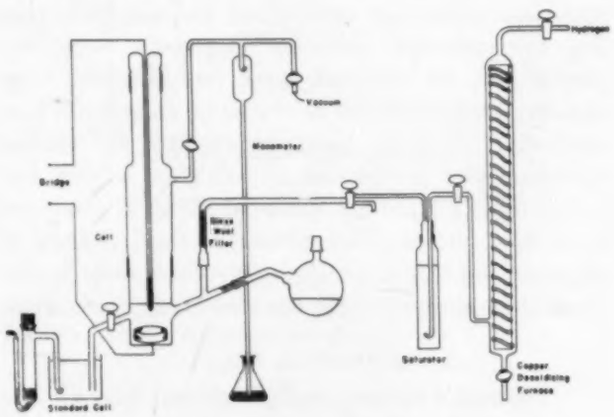

FIG. 2. Cell and purification train used for electrode capacity determination.

electrolyte passed, out of contact with the greased joint.

The counter electrode required for the impedance measurement is a platinized platinum ring of large area concentric with the test electrode. The error introduced by the capacity of the counter electrode in series with the surface whose capacity is to be measured can be ignored because its impedance is negligible in comparison with the small test electrode.

To make precise absolute measurements of electrode capacity it is necessary to know the area of the

electrode surface; it must be small since the specific capacity is very large (microfarads) and its impedance is correspondingly small. These requirements were met by sealing small platinum wires of different diameters through the closed end of soft glass cylinders. A well-defined cross-sectional area of wire was obtained by grinding and polishing the bottom of the glass cylinder until the platinum wire and glass surface were in one optically flat plane and the platinum was free of scratches as observed by metallographic microscope. The geometric area of exposed platinum was obtained by photographing the polished surface at 100× and measuring the magnified area of the cross section, which was varied between the limits of 0.15 and 13.8 × 10^{-3} cm^2. An additional useful technique was developed, applicable to metals that cannot be sealed in glass. While organics must be rigorously excluded it was found that platinum wires sealed in lucite and polished in the same manner as the glass-mounted electrodes gave results consistent with platinum in glass indicating that lucite does not contaminate the electrolyte (hydrochloric acid) and it may, therefore, be employed as a mounting material for other metals.

All reagents were recrystallized in Pyrex and acids were distilled, at least once. Glass containers and apparatus were steamed over alkaline permanganate for prolonged periods. Hydrogen and nitrogen, used for saturating the electrolyte, were deoxidized by passing over hot copper. After measurement with plane electrodes had established the specific capacity, hemispherical platinum electrodes were employed and the electrode area was obtained from capacity measurements in the same solution. These electrodes are very easily constructed by sealing platinum wire in the end of soft glass tubing and fusing the wire until a spherical shape is produced by surface tension. The removal of the last trace of adsorbed impurities on the electrode surface is discussed in connection with the effects of polarization.

Experimental Results

Electrode Capacity in Hydrochloric Acid as a Function of Potential

In using an impedance bridge to measure capacity in a network, either the distribution of circuit elements—resistors, condensers, and inductance—is known, or the equivalent circuit must be synthesized from the frequency dependence. Electrode capacity is in the latter category insofar as the equivalent circuit, if it exists, is unknown. In the simplest case of a symmetrical bridge in which the distribution of unknown circuit elements is the same as that in the opposite and known arm of the bridge, the bridge balance point will be independent of frequency; otherwise, it will be some function of frequency depending on the number and distribution of elements in the unknown network whose impedance is balanced against some known but different combination of circuit elements. For the present purpose of describing the general characteristics of electrode capacity it will be assumed that the electrode network can be represented by a simple series resistance and capacitance and the comparatively small, although important, effect of frequency will be considered separately.

The capacity of polished platinum electrodes in *1N* hydrochloric acid, calculated as a series resistance and capacitance at 1000 cps, is shown in Fig. 3. The form of the curve and magnitude of values are

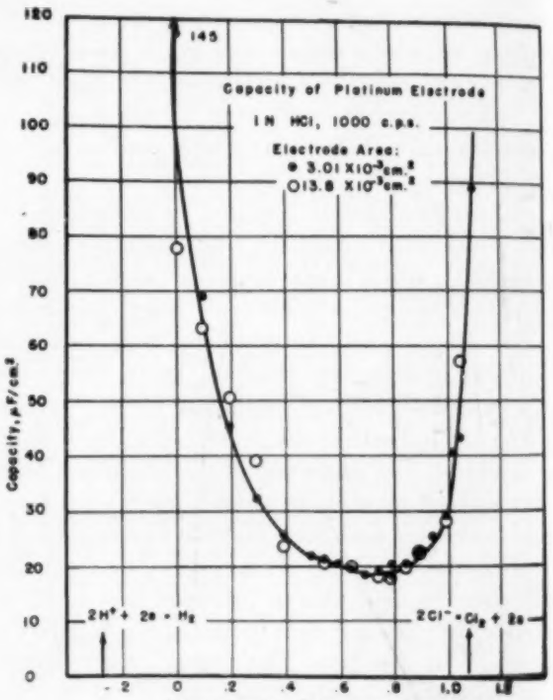

FIG. 3. Differential capacity of two polished platinum electrodes of different area in normal hydrochloric acid as a function of applied polarization voltage with respect to the normal calomel electrode.

similar to those obtained by Ershler and Proskurnin (3) and Dolin and Ershler (5), but because the area of their electrodes is uncertain, the present values are believed to be more nearly of absolute significance. This is further substantiated by measurements of capacity at the minimum with respect to potential, employing polished electrodes of different apparent areas varying by a factor of one hundred (Fig. 4). It is evident that electrode capacity is directly proportional to measured apparent area and the fact that the line passes through zero indicates that the polished surface approximates a true plane, within the limits of the technique, to detect surface irregularities. Obviously, also, the capacity is a

specific property of the surface depending only on its extent in a given solution at a given polarizing voltage.

Reproducibility is indicated by two sets of values in Fig. 3, obtained at different periods in the development of the method and employing different electrodes. As a result of repeated measurements it appears that the characteristic value of electrode capacity at the minimum in hydrochloric acid is 19 ± 1 $\mu f/cm^2$, which occurs at a potential of 0.75 on the N calomel scale.

Change of Electrode Capacity in Time

The results indicated in the various figures represent a steady state established in time and the period required to change the constitution of the double layer, associated with a given polarizing voltage, to some other state is shown in Fig. 5. It appears that a finite time is required for the process which involves diffusion of ions into and out of the double layer, orientation at the surface, and possibly saturation of the metal with hydrogen. It is interesting that the course of events is apparently different depending on whether the approach is through the minimum or only up to the minimum of electrode capacity. For example, in going from 0.45 volt to 0.75 volt the capacity decreases rapidly and continuously to the lower value associated with the minimum; however, in going past the minimum to 0.85 volt the capacity first decreases and then increases to the characteristic value; an inverse curve is followed in returning to 0.45 volt. A detailed explanation of the preceding sequence of effects resulting from a change in polarizing voltage cannot be deduced from the available experimental data. It is always possible in this work that trace impurities are responsible for otherwise unexplained effects; alternatively, it has been suggested that the slow process may result from the necessity of establishing equilibrium with respect to hydrogen in the metallic phase. The latter explanation is at least consistent with the fact that when a steady state is reached, at or near minimum capacity, it is stable in time over periods of hours and only momentarily altered by vibration, provided the cell and everything associated with it is absolutely clean; otherwise, incorrect and unstable values are obtained.

The possibility of changing the double layer constitution by altering the polarizing potential was employed as a method of removing from the metal surface the last trace of adsorbed impurities which cannot be eliminated by any conventional technique; indeed, it is perhaps the only possible method for achieving the required clean surface. In practice, the electrode was cleaned in nitric acid, rinsed repeatedly in water and in the electrolyte, and finally polarized successively between the limits of 0.0 and 1.0 volt on the N calomel scale before measurements were taken. The final criterion of good operating conditions was stability in time at the capacity minimum. Again the technique differs from that for mercury where the dropping electrode may be employed and the surface constantly renewed in a period short with respect to diffusion of adsorbable impurities.

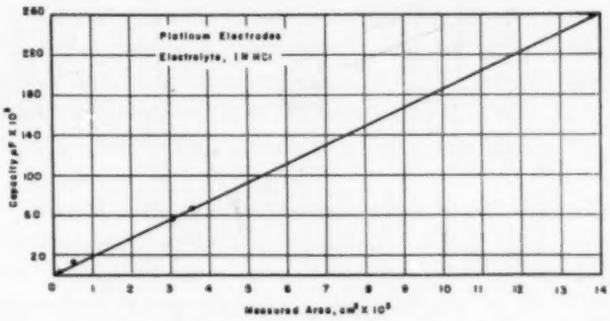

FIG. 4. Differential electrode capacity of polished platinum in normal hydrochloric acid at +0.75 volt with respect to normal calomel as a function of electrode area.

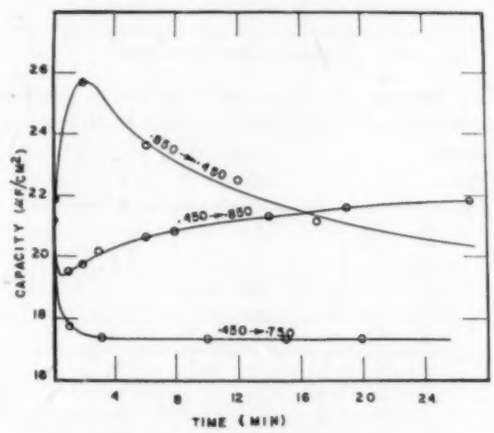

FIG. 5. Differential electrode capacity of platinum in normal hydrochloric acid as a function of time after changing the applied polarizing voltage.

Effects of Oxygen, Hydrogen, and Nitrogen

The effect of saturating the electrolyte with different gases, oxygen, nitrogen, and hydrogen (Fig. 6), is confined to the cathodic branch of the capacity curve and there is no significant effect on the capacity minimum, which constitutes further evidence that this point is a characteristic of the electrolyte.

Concentration Dependence of Electrode Capacity

The concentration dependence of electrode capacity is shown in Fig. 7 for hydrochloric acid from $1N$ to 0.0 IN. It appears that the effects of changing concentration are not symmetrical with respect to

polarization and that a plateau occurs on the anodic branch of the capacity curves for the lower concentrations which is absent at *IN*, at least within the indicated polarization range. The capacity minimum is shifted approximately 0.2 volt in a negative

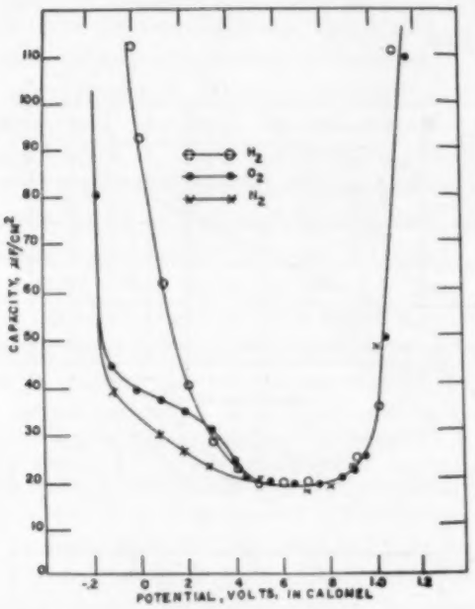

FIG. 6. Differential electrode capacity of platinum in normal hydrochloric acid saturated with hydrogen, oxygen, and nitrogen.

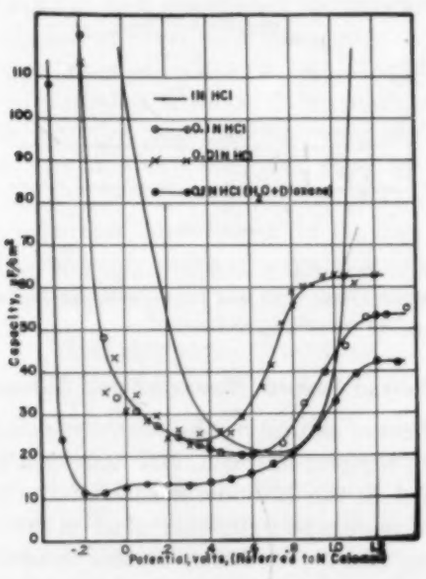

FIG. 7. Differential electrode capacity of platinum in hydrochloric acid as a function of concentration and in hydrochloric acid containing 50 per cent water and 1-4 dioxane as solvent.

direction for each tenfold dilution and is slightly raised in value.

Also shown in Fig. 7 is the capacity curve for 0.0 *IN* HCl made up with 50 per cent water and 1-4 dioxane in which the average dielectric constant of the solvent is 35. While, in general, the electrostatic capacity is directly proportional to the dielectric constant, in the present case it is probable that dioxane molecules are preferentially adsorbed at the platinum surface and the effect of dielectric constant of the solvent is not directly indicated by the curves.

Capacity and Frequency Dependence

Previous measurements of electrode capacity employing alternating current have either been made at constant frequency or, when the effect of frequency was investigated, it was found to be large (5) and, consequently, preceding measurements at constant frequency lose much of their significance. The present work was undertaken partly to determine whether or not the double layer could be represented by a simple electrical analogue deduced from the frequency dependence of electrode impedance and,

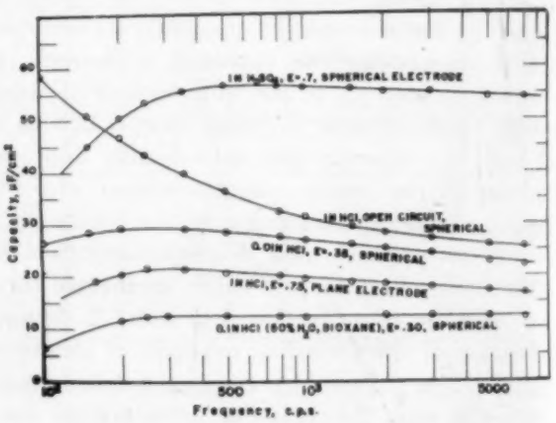
1N H₂SO₄, E°=.7, SPHERICAL ELECTRODE
1N HCl, OPEN CIRCUIT, SPHERICAL
0.01N HCl, E°=.38, SPHERICAL
1N HCl, E°=.75, PLANE ELECTRODE
0.1N HCl (50% H₂O, DIOXANE), E°=.30, SPHERICAL
Capacity, μF/cm²
Frequency, c.p.s.

FIG. 8. Differential electrode capacity of platinum calculated as a series resistance and capacitance, as a function of frequency, polarization, and electrolyte.

in any case, the work would be incomplete without an investigation of the effect of frequency.

It is necessary to consider the following factors, assuming that the bridge itself is not contributing frequency effects which, in the present case, were exhaustively investigated and eliminated: (*a*) the shape of the electrode; (*b*) the concentration of the electrolyte; (*c*) the type of electrolyte; (*d*) the presence of adsorbed impurities; and (*e*) the polarization voltage. Fig. 8 presents a summary of values covering the various cases, calculated as a series R-C circuit and plotted as a function of frequency. Fig. 9, on a greatly expanded scale, shows the different results obtained by assuming parallel or series networks to represent the measured electrode impedance, given in Table I.

It is evident from Fig. 8 that the variation with frequency is small except in the case of the unpolarized electrode and in sulfuric acid, and of the

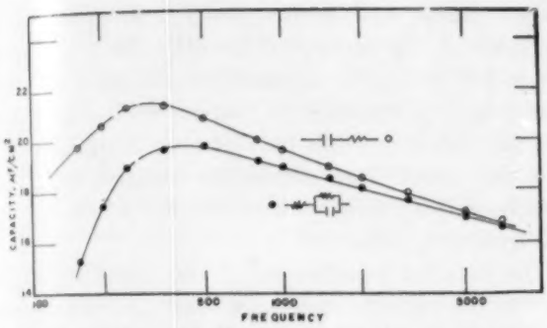

FIG. 9. Differential electrode capacity of platinum in normal hydrochloric acid calculated as a series and a parallel network, as a function of frequency.

TABLE I. *Impedance data for a plane platinum electrode in 1N HCl at 0.75 volt external polarization, referred to N calomel*

Frequency	C_S	R_S	R_1	R_2	Series Circuit		Parallel Circuit	
					R_x	C_x	R_x	C_x
cps	*μf*	*ohms*	*ohms*	*ohms*	*ohms* × 10^{-3}	*μf/cm²*	*ohms* × 10^{-4}	*μf/cm²*
7000	0.05	60	229	1000	0.262	16.8	1.6	16.7
5000	0.05	84	233	1000	0.362	17.1	2.2	16.9
3000	0.05	151	243	1000	0.622	17.9	3.0	17.6
2000	0.05	244	252	1000	0.970	18.5	4.3	18.1
1500	0.05	351	258	1000	1.360	18.9	5.1	18.5
1000	0.05	600	267	1000	2.250	19.6	6.2	18.9
800	0.05	800	272	1000	2.940	20.0	7.7	19.2
500	0.05	1500	284	1000	5.270	20.9	10.0	19.8
350	0.05	2600	290	1000	9.000	21.3	12.0	19.7
250	0.05	4400	290	1000	15.200	21.3	15.0	19.0
200	0.05	6600	280	1000	23.600	20.6	15.9	17.5
160	0.05	1100	270	1000	40.700	19.8	17.0	15.3

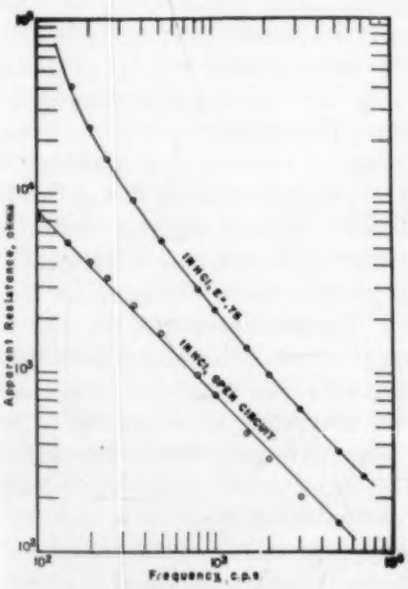

FIG. 10. Apparent electrode resistance as a function of frequency for an unpolarized electrode and for +0.75 volt polarization in normal hydrochloric acid.

same magnitude as the general reproducibility which justifies the procedure of reporting results at constant frequency and assuming a series network for the purpose of obtaining capacity at 1000 cps. However, the frequency dependence is perfectly reproducible and in any one series of measurements, taken as a function of frequency, the curves are invariably as shown. The frequency effects appear to be properties of the electrolyte and polarization voltage and to be independent of electrode geometry. Both plane and hemispherical electrodes show the presence of a flat maximum between 250–350 cps; in sulfuric acid the maximum occurs at 500–600 cps and in hydrochloric acid containing dioxane the capacity rises to a constant value at 300 cps. On the other hand, the capacity of an unpolarized spherical electrode is an entirely different function and is, in fact, inversely proportional to the square root of the frequency.

The apparent resistance of different electrodes is shown as a function of frequency in Fig. 10 for the two principal cases of an electrode polarized to the potential of the capacity minimum and an unpolarized electrode. The resistance is large and dependent on frequency; in the latter case it is inversely proportional to the frequency. The specific resistivity depends on electrode area, as shown in Table II.

TABLE II. *Dependence of electrode resistance at the capacity minimum on electrode area*

Area	Apparent resistance	Resistance × area
cm² × 10^3	*ohms*	*ohms cm²*
0.13	12500	1.63
0.50	2270	1.14
3.02	660	1.98
13.8	104	1.44

The accurate determination of resistance with the present apparatus designed for capacity measurements is not possible and the very small electrodes required for the latter purpose further reduce precision; however, as a first approximation, the resistance area product (Table II) indicates that resistance is proportional to area, showing that it is a property of the electrode-electrolyte interface.

Discussion

Lacking independent means of measurement and thermodynamic or kinetic development of theory, extensive interpretation of the differential capacity of polarized platinum and other solid metal electrodes is probably not warranted until more data are available with respect to ionic type and concentration. It is, however, evident that reproducible results may be obtained with some precision, and the technique offers possibilities for development as a means of investigating the properties of metal interfaces in contact with ionic solutions.

The general characteristics of electrode capacity with respect to potential differ from those obtained

with mercury. For example, the maxima and minima that occur on most mercury capacity curves at potentials near the electrocapillary maximum are absent, at least within the range of polarization permitted with platinum.

One of the most significant features of the differential capacity curves of platinum is the minimum with respect to potential that corresponds to the minimum on mercury curves at potentials cathodic to the electrocapillary maximum. In the latter case a common minimum is reached with most ion types (10); it is slightly dependent on concentration, varying from about 16 to 12 $\mu f/cm^2$ at potentials from -1.1 to -1.3 volts relative to the normal calomel electrode as concentration decreases from 1 to 0.001 M. The minima observed with platinum in hydrochloric acid, Fig. 7, occur at about 20 $\mu f/cm^2$ and potential from $+0.75$ to $+0.35$ on the same scale. The direction of potential shift with concentration is the same in both cases, but the capacity of mercury decreases with increasing concentration while that of platinum appears to increase slightly.

It is interesting to observe, although its significance is not certain at present, that the difference of potential between platinum and mercury at comparable capacity minima is approximately 1.85 volts which corresponds to the contact difference of potential between platinum and mercury, for which the work functions are taken as 6.3 and 4.5 volts, respectively (11). For this comparison to be valid it is necessary that the potential drop across the mercury and platinum solution interfaces be the same, and in the present case this is assumed to occur at the potentials of the respective capacity minima; alternatively, the minima represent corresponding states of the double layer which are comparable. It should be stated that there is no implication here of zero potential between metal and electrolyte. Obviously, accuracy is not great in the preceding comparison and, furthermore, the shift in potential with respect to concentration is somewhat less for mercury than for platinum; but, since the thermionic and photoelectric potentials of platinum differ by about 1 volt (12), the comparison is at least as good as the physical data and perhaps considerably better.[3]

The decrease in capacity as the mercury curves approach a minimum at potentials more cathodic than the electricapillary maximum has been attributed (10) to the repulsion of preferentially adsorbed anions and, consequently, the approach to the minimum is controlled by the type of anion. It is probable that the asymmetric character of platinum capacity curves with respect to the hydrogen and chlorine potentials may also be ascribed to the different properties, principally relative size, hydration and bonding with platinum, of the chloride and hydrogen ions.

The detailed significance of the quantity 20 $\mu f/cm^{-2}$ at the capacity minimum is not yet clear except that it is a true property of the surface insofar as it is proportional to surface area. At this point also the small currents (less than 1 μa) passing at potentials more or less negative than the potential of the minimum go to zero, possibly indicating that both hydrogen ions and chloride ions are equally dispersed in the diffuse double layer and neither ion contributes or accepts charge from the electrode. If the latter conclusion is valid it may indicate that the magnitude of the capacity minimum is primarily a property of the solvent.

In this connection the effect of introducing a comparatively large organic molecule, 1-4 dioxane, thereby reducing the average dielectric constant of the solvent from 78 to 35 was investigated and the result is shown in Fig. 7. The capacity minimum now extends over a large potential range and the specific capacity is decreased, particularly at cathodic potentials. At anodic potentials it appears that chloride ions are still determining the properties of the double layer with respect to potential although the capacity is lowered by the presence of dioxane; at potentials more negative than $+0.55$ volt, the minimum in the absence of dioxane, the capacity is continuously reduced by the increasing number of dioxane molecules moving into the region of high field strength at the surface until either dioxane is reduced, leading to a rapid rise in capacity (pseudocapacity) or hydrated hydrogen ions displace dioxane molecules at a potential which is more negative by 0.75 volt than the corresponding case of pure water as the solvent. The widening of the range of potential at the capacity minimum is thus associated with the adsorption and polarizing properties of the molecules in question.

The apparent series resistance at potentials near the capacity minimum, shown in Fig. 10, is several orders of magnitude greater than the resistance calculated (14) from electrode geometry and the resistivity of the electrolyte; it is not significantly dependent on potential or on the presence of dioxane but is approximately proportional to electrode area. It appears that this resistance is a property of the polarized electrode and not of impurities, a conclusion that is substantiated by the general reproducibility and constancy in time of the associated capacity.

It is important to examine the effect of frequency

[3] When this paper was submitted for publication the author's attention was called to two recently translated Russian papers (15, 16), which were previously unknown to him. The work of Borisova, Ershler, and Frumkin shows that the above conclusion regarding the contact potential also applies to lead, cadmium, and thallium in a variety of electrolytes and, consequently, there appears to be little doubt of its general validity.

on the impedance of the double layer because additional tools are required to interpret the capacity data in chemical terms. The measurements themselves are unambiguous insofar as impedance is concerned; ambiguity enters when one attempts to synthesize a model circuit of simple elements which has the same frequency response and which might, therefore, be presumed to represent conditions at the electrode.

It is obvious that the simple series and parallel networks (Fig. 9) either do not represent the equivalent network of the electrode surface or the capacity of the double layer is a function of frequency. With respect to the former possibility, numerous simple networks involving capacity, inductance, and resistance have been assumed and compared with the impedance data but none has been found that yields a capacity independent of frequency; unquestionably a complex network could be devised whose frequency dependence would approximate that actually found, but such a complex network would be relatively useless as a model of the double layer and the empirical solution would contribute nothing to an understanding of the conditions at the electrode surface. On the other hand, when the constitution of the double layer is considered with respect to diffusion, the presence of three charge carriers (two of which, the ions, are polarizable to different degrees), and the inhomogeneous field at the metal surface, it is possible that the apparent double layer capacity may be dependent on frequency. Furthermore, the frequency of dependence will be determined by the applied polarization; as indicated in Fig. 8, the capacity is inversely proportional to the square root of frequency for the unpolarized electrode, in accordance with the determinations of electrode capacity made in connection with conductance measurements (13).

The apparent capacity maximum of the polarized electrode with respect to frequency might be interpreted in terms of a relaxation phenomena, but the low frequency certainly precludes relaxation associated with the homogeneous ionic atmosphere which occurs in the megacycle range. However, the properties of ions associated with a solid metal interface are not necessarily similar in response to a changing field as the properties of the relatively free ionic charges in solution. There is a minimum distance of approach toward the surface defined by the compressibility of the ion and its associated hydration; movement parallel to and away from the interface will also be restricted by bonding or adsorption forces. All these factors will tend to increase the time of rotation and orientation at the solid surface.

Emphasis is placed on the frequency dependence because it is thought that extraneous factors like electrode shape and contamination have been excluded or evaluated and the frequency dependence remains as a property of the ions in an alternating field at a solid surface. Further experimental work, preferably as a function of temperature, is necessary to evaluate the electrode properties in terms of a rate process and until the data are available more definite conclusions are withheld. It may be concluded from the preceding work, in accordance with recent theoretical considerations (17), that the best approach is not that of attempting to synthesize equivalent circuits to represent the double layer, but a detailed analysis of the electrode impedance as a function of frequency, ion type, and temperature. For any particular combination of conditions an equivalent network may be devised to match electrode impedance, but generality is lost in the process if analysis is confined to a determination of the equivalent circuit.

Acknowledgment

This work was conducted while the author was associated with The Institute for the Study of Metals, University of Chicago, and was partially supported by Army Air Force Contract Number AF33(038)-6534. The author is indebted to many colleagues for suggestions and assistance in apparatus design, particularly Dr. John Garrison.

Any discussion of this paper will appear in a Discussion Section, to be published in the December 1953 issue of the Journal.

REFERENCES

1. N. K. Adam, *"The Physics and Chemistry of Surfaces,"* Oxford University Press, Oxford, England (1941).
2. D. C. Grahame, *Chem. Revs.*, **41**, 441 (1947).
3. B. Ershler and M. Proskurnin, *Acta Physicochim. U.R.S.S.*, **6**, 195 (1937).
4. B. Ershler, *Acta Physicochim. U.R.S.S.*, **7**, 327 (1937).
5. P. Dolin and B. Ershler, *Acta Physicochim. U.R.S.S.*, **13**, 747 (1940).
6. F. P. Bowden and E. K. Rideal, *Proc. Roy. Soc., London*, **120**, 59 (1928).
7. F. P. Bowden and K. E. W. Grew, *Discussions, Faraday Soc.*, **1**, 91 (1947).
8. D. C. Grahame, *J. Am. Chem. Soc.*, **68**, 301 (1946).
9. M. Proskurnin and A. Frumkin, *Acta Physicochim. U.R.S.S.*, **4**, 825 (1936).
10. D. C. Grahame, Tech. Rept. #6 to Office of Naval Research, May 25, 1951.
11. J. A. Becker, *Revs. Mod. Phys.*, **7**, 123 (1935).
12. C. Herring, *Revs. Mod. Phys.*, **21**, 185 (1949).
13. G. Jones and S. M. Christian, *J. Am. Chem. Soc.*, **57**, 272 (1935).
14. J. Jeans, "Mathematical Theory of Electricity and Magnetism," p. 352, Cambridge University Press, Cambridge, England (1948).
15. T. Borisova, B. Ershler, and A. Frumkin, *J. Phys. Chem. U.S.S.R.*, **22**, 925 (1948).
16. T. Borisova and B. Ershler, *J. Phys. Chem. U.S.S.R.*, **24**, 337 (1950).
17. D. C. Grahame, Technical Report #8 to The Office of Naval Research, June 1952.

"The enthusiastic response of our employees . . ."

ALDEN G. ROACH
President, Columbia-Geneva Steel Division and Consolidated Western Steel Division, United States Steel Corporation

"It is most gratifying to me that the employees of the Columbia-Geneva Steel Division and the Consolidated Western Steel Division of United States Steel Corporation have accorded meaning to their belief that the security of our nation rests upon our cooperative effort. The enthusiastic response of our employees made me doubly glad we conducted a person-to-person canvass for the Payroll Savings Plan for U. S. Defense Bonds."

The experience of Columbia-Geneva and Consolidated Western Divisions of United States Steel Corporation is not an isolated one.

Since January 1, 1951, hundreds and hundreds of companies have conducted person-to-person canvasses of their plants and offices. In every instance, employee participation in the Payroll Savings Plan has increased—sometimes from a low figure—to 60, 70, 80%. In a number of plants, participation passed the 90% mark.

The explanation is simple.

Employees *want* to provide for their future security.

Given an opportunity to enroll in the Payroll Savings Plan they respond immediately—as evidenced by the fact that more than 2,000,000 men and women have joined the Payroll Savings Plan since January 1, 1951.

The monthly take-home savings of the 7,500,000 now in the Payroll Savings Plan totals $150,000,000 per month—and growing rapidly.

As a step toward *your* personal security, and the security of your associates, bring this page to the attention of your top executive. Tell him that—

- a person-to-person canvass of your plant can be conducted without pressure, prize awards or other stimulation. (In many plants, employee organizations have undertaken the actual distribution of Payroll Savings Application Blanks.)
- The Savings Bond Division, U. S. Treasury Department, Suite 700, Washington Building, Washington, D. C., will gladly help your company with suggestions, posters, envelope stuffers and other aids.

The U.S. Government does not pay for this advertisement. It is donated by this publication in cooperation with the Advertising Council and the Magazine Publishers of America.

Journal of The Electrochemical Society
235 West 102 Street, New York, N. Y.